Defining the development of gp120-gp41 interface directed broadly neutralizing antibodies in HIV-1 infection

Vincent Nkosinathi Hlatshwayo

A Thesis submitted to the Faculty of Health Sciences, University of the Witwatersrand, Johannesburg, in fulfilment of the requirements for the degree of Doctor of Philosophy (PhD).

Johannesburg, 2023.

DECLARATION

I, Vincent Nkosinathi Hlatshwayo (551762), am a student registered for the degree of PhD in the academic year 2023. I hereby declare the following:

I am aware that plagiarism (the use of someone else's work without their permission and/or without acknowledging the original source) is wrong.

I confirm that the work submitted for assessment for the above degree is my own unaided work except where explicitly indicated otherwise and acknowledged. I have not submitted this work before for any other degree or examination at this or any other University.

Signature  02 June 2023

The financial assistance of the National Research Foundation (NRF) and WITS PMA towards this research is hereby acknowledged. Opinions expressed and conclusions arrived at, are those of the author and not necessarily to be attributed to the NRF or Wits PMA.

DEDICATION

For my son Zawadi. My wish for you is to keep searching for knowledge and use that knowledge to benefit those closer to you!

For my wife Vicky. Without your support I doubt I would have reached this far.

For my mom, thank you for always supporting my dreams and for being my number one cheerleader

Output from this thesis: presentations and publications

1. Vincent N. Hlatshwayo, Constantinos K. Wibmer, Cathrine Scheepers, Dale Kitchin, Sharon V. Madzorera, Daniel J. Sheward, Nigel J. Garrett, Salim S Abdool Karim, Carolyn Williamson, Lynn Morris and Penny L. Moore. Characterization of the viruses that shaped the evolution of a broadly neutralizing antibody targeting the gp120-gp41 interface of the HIV-1 envelope. 24th International Bioinformatics Workshop on Virus Evolution and Molecular Epidemiology (VEME) & Croucher Summer Course: Computational Genomics of Viral Evolution and Epidemiology. The University of Hong Kong, Hong Kong, August, 2019. (Poster Presentation). Won the best poster presentation

2. Vincent N. Hlatshwayo, Constantinos K. Wibmer, Cathrine Scheepers, Dale Kitchin, Sharon V. Madzorera, Daniel J. Sheward, Nigel J. Garrett, Salim S Abdool Karim, Carolyn Williamson, Lynn Morris and Penny L. Moore. Characterization of the viruses that shaped the evolution of a broadly neutralizing antibody targeting the gp120-gp41 interface of the HIV-1 envelope. Infectious Diseases of Africa (IDA). River club, CAPE TOWN, October, 2019. (Poster Presentation), Invited Faculty Member (based on previous year IDA performance)

3. Vincent N. Hlatshwayo, Constantinos K. Wibmer, Cathrine Scheepers, Dale Kitchin, Nigel J. Garrett, Salim S Abdool Karim, Lynn Morris, Penny L. Moore. Tracing the evolution of a broadly neutralizing antibody targeting the gp120-gp41 interface of the HIV-1 envelope. South African Immunology Society (SAIS). Aha

Gateway, Durban, July, 2019. (Oral Presentation). Won the second-best oral presentation

4. Vincent N. Hlatshwayo, Constantinos K. Wibmer, Cathrine Scheepers, Dale Kitchin, Sharon V. Madzorera, Daniel J. Sheward, Nigel J. Garrett, Salim S Abdool Karim, Carolyn Williamson, Lynn Morris and Penny L. Moore. Characterization of the viruses that shaped the evolution of a broadly neutralizing antibody targeting the gp120-gp41 interface of the HIV-1 envelope. Infectious Diseases of Africa (IDA). River club, Cape Town, November, 2018. (Oral Presentation). Won the best poster presentation

Abstract

A prophylactic HIV-1 vaccine will likely need to elicit broadly neutralizing antibodies (bNAbs) against conserved HIV-1 envelope epitopes such as the gp120-gp41 interface which includes the FP. The isolation of gp120-gp41 interface-, and FP-directed bNAbs from chronically HIV-infected donors has made this epitope an appealing vaccine target. Moreover, promising preclinical immunogenicity animal studies have shown the possibility of eliciting such responses in animals. However, little is known about the population prevalence or kinetics of gp120-gp41 interface responses, including FP-directed responses. Lastly, few FP-directed antibodies have been isolated from people living with HIV (PLWH), limiting our understanding of common developmental pathways that can be explored for vaccine purposes.

Here, we first assessed the prevalence of bNAbs in participants previously enrolled in the CAPRISA 004 Tenofovir gel trial (CAP004). We show that in this cohort, only 12% of individuals developed breadth at three years post-infection, and that high viral load and low CD4 count were associated with bNAb development, as previously reported. ELISA screening showed that only 13% of individuals developed FP-directed responses at three years post-infection. Of the 13% (n=9), only two donors had broad plasma responses, including donor CAP312, whose plasma exhibited 64% neutralization breadth at three years post-infection. In CAP312, FP binding and heterologous neutralization against a multi-clade 22 virus panel appeared simultaneously, within one year (~ 50 weeks post-infection). Taken together, our findings suggest that gp120-gp41 interface- and FP-directed responses are infrequently elicited during infection.

As few FP-specific bNAbs have been isolated to date, little is known about their shared features that could be exploited for eliciting FP-specific bNAbs by vaccination. We next isolated three FP-specific mAbs from donor CAP312 at three years post-infection; AIRU-F8, AIRU-G9 and AIRU-G4 with 64, 45 and 5% breadth, respectively. We showed that our mAbs, and previously isolated bNAbs PGT151 and ACS202 share gene usage and have a similar unusually long CDRH3, as a result of a conserved motif inherited from the germline *IGHJ6*02* gene. Furthermore, we showed that CAP312 mAbs have even longer CDRH3s compared to PGT151 and ACS202 despite this shared motif. We also showed, using point mutants and glycan mutants that our FP-specific mAbs have a unique neutralization profile compared to published mAbs. Overall, these results suggest that FP-specific mAbs share structural and genetic features that could be explored further for lineage vaccine development.

Lastly, we delineated the ontogeny of the gp120-gp41 interface-directed nAb CAP248-2B by tracing the evolutionary pathways utilising longitudinal samples from 11-281 weeks post-infection (wpi). CAP248-2B interacts with the HIV-1 Env trimer through a long light chain CDRL3 that inserts into the viral membrane, and a heavy chain CDRH1 ^{32}ED^{33} motif that interacts with gp41. We showed that the unusually long light chain CDRL3 and the heavy chain ^{32}ED^{33} motif are functionally redundant against heterologous viruses. We also showed that affinity maturation mutations in this lineage selected a lineage with limited heterologous neutralization breadth.

In summary, these findings support further research into gp120-gp41- and FP-specific responses in multiple cohorts. Furthermore, future studies should aim to elucidate

mechanisms governing the development of these responses so that productive developmental pathways can be identified and exploited for vaccine design.

Acknowledgement

I would like to express my absolute appreciation and gratitude to my supervisors aka LAB MOTHERS; Professor. Penelope “Penny” Linda Moore and Dr Cathrine Scheepers for their intellectual input, support, and encouragement provided throughout the duration of this project. To Prof. Moore, thank you for your support beyond academic work, you have availed yourself and made sure that you support us as students in any way possible. To my co-supervisor Dr Catherine Scheepers, I am truly grateful for your assistance which has been pivotal to the completion of this project and giving a constructive critique. I do not have enough words to express my heartfelt gratitude.

I would also like to express my heartfelt appreciation to the following people whose support was a necessary part of this work: Professor. Lynn. Morris for granting me access to your lab and always giving constructive criticism. To Dr Dale Kitchin (Malume), without your assistance I wouldn’t have managed to understand NGS. I am deeply grateful. Dr Bronwen Lambson, thank you for being patient and helping with molecular biology and always willing to help out with proofreading my documents.

I would also like to thank my colleagues at AIRU whom I have learned a lot and made friends and family. The constructive conversations, support, great times we shared and trainings has made my experience in this unit very pleasant.

I would like to thank my family and friends (Nathi, Mlu and Brian) for their support.

Last, but not least, I thank **God** for giving me wisdom and a great deal of strength to persevere.

Table of contents

List of Figures

Chapter 1

Chapter 2

Chapter 3

List of Tables

List of abbreviations

AIDS	Acquired Immunodeficiency Syndrome
bNAb	Broadly neutralizing antibody
CA	Capsid protein
CAPRISA	Centre for the AIDS Program of Research in South Africa
C1, C2, C3, C4, C5	Conserved gp120 regions 1 to 5
CCR1, 2b, 3, 5, 8, 9	Chemokine (C-C motif) receptor 1, 2b, 3, 5, 8, 9
CD4	Cluster of differentiation 4
CD4bs	CD4 binding site
CDR	Complementarity determining region
CRF01	Circulating Recombinant Form 01
CT	Cytoplasmic tail of gp41
CXCR1, 4, 6	chemokine (C-X-C motif) receptor 1, 4, 6
D gene	Diversity gene
DC-SIGN	Dendritic cell-specific intracellular adhesion molecule-3-grabbing non-integrin

dUTPase	Deoxyuridine triphosphatase
Env	Envelope glycoprotein
Fab	Antigen binding antibody fragment
Fc	Crystallisable antibody fragment
FP	Fusion peptide
FPPR	Fusion peptide proximal region
FWR	Framework region
Gag	Group-specific antigen
gp160, gp120, gp41	glycoprotein 160 kDa, 120 kDa, 41 kDa
HIV-1, HIV-2	Human Immunodeficiency Virus type-1, -2
IC50	50% inhibitory concentration
ID50	50% inhibitory dilution
ID	Inner Domain
IgG	Immunoglobulin G
IN	Integrase
J gene	Joining gene

MA	Matrix protein
mAb	Monoclonal antibody
MPER	Membrane proximal external region
Nef	Negative factor
NC	Nucleocapsid protein
OD	Outer Domain
PBMCs	Peripheral blood mononuclear cells
PLWH	People living with HIV/AIDS
Pol	Polymerase
PR	Protease
Rev	Regulator of expression of viral proteins
RT	Reverse Transcriptase
RNA	Ribonucleic acid
SHIV	Chimeric Simian/Human Immunodeficiency Virus
SIV	Simian Immunodeficiency Virus
SU	Surface Unit

Tat	Trans-activator
TM	Transmembrane Region of gp41
UNAIDS	United Nations programme on HIV/AIDS
V1, V2, V3, V4, V5	Gp120 Variable loop regions 1 to 5
VH gene	Heavy chain variable gene
Vif	Viral infectivity factor
Vκ gene	Kappa light chain variable gene
Vλ gene	Lambda light chain variable gene
Vpr	Viral protein R
Vpu	Viral protein unique

Amino acids

Amino Acid	Three-Letter code	One-Letter code
Alanine	Ala	A
Arginine	Arg	R
Asparagine	Asn	N
Aspartic acid	Asp	D
Cysteine	Cys	C
Glutamic acid	Glu	E
Glutamine	Gln	Q
Glycine	Gly	G
Histidine	His	H
Isoleucine	Ile	I
Leucine	Leu	L
Lysine	Lys	K
Methionine	Met	M
Phenylalanine	Phe	F

Proline	Pro	P
Serine	Ser	S
Threonine	Thr	T
Tryptophan	Trp	W
Tyrosine	Tyr	Y
Valine	Val	V

Nucleotides

A	Adenine	H A, C, or T
C	Cytosine	R A or G
G	Guanine	S G or C
T	Thymine	W A or T
U	Uracil	Y C or T

Chapter 1

Introduction

1.1 HIV pandemic: background and epidemiology

In the 1980s, an unknown disease was presenting a public health problem among men who have sex with men (MSM) in the USA, with patients presenting with Kaposi sarcoma and a rare form of lung infection called "*Pneumocystis carinii pneumonia* (PCP)" (Masur et al., 1981). The disease was later named acquired immunodeficiency syndrome (AIDS). The causative agent of AIDS was identified by laboratories in the USA and France independently as Human T- cell leukaemia virus (HTLV-III), Lymphadenopathy associated virus (LAV), and subsequently Human Immunodeficiency Virus (HIV) in 1984 (Barre-Sinoussi et al., 1983).

HIV/AIDS is a zoonotic disease caused by two types of viruses: HIV-1 and HIV-2 (Tortora et al., 2010). HIV-1 accounts for the majority of infections worldwide and is related to Simian Immunodeficiency Virus (SIVcpz) infecting chimpanzees in Central Africa (Maartens, et al., 2014; Tortora et al., 2010). Conversely, HIV-2 is a less virulent strain mainly found in the West African region and is related to the Simian Immunodeficiency Virus (SIVsmm) infecting sooty mangabey monkeys in West Africa (Maartens, et al., 2014; Tortora et al., 2010). Both viral infections cause AIDS, however, HIV-2 infection progresses to AIDS at a slower rate compared to HIV-1 infection (Sharp and Hahn, 2011). It is believed that cross-species transmission from

other primates into humans probably occurred by blood contamination through hunting and handling of bushmeat (Lever, 2009; Sharp and Hahn, 2011).

Three separate transmission events from chimpanzees have led to the classification of HIV-1 into three distinctive groups named M (main), N (non-M or O) and O (outlier) (Sharp and Hahn, 2011; Tortora et al., 2010). Another group called P was identified and shown to be closely related to the simian immunodeficiency virus infecting gorillas (SIVgor) and it is believed that it most likely arose from an independent gorilla to human transmission (Sauter et al., 2011; Sharp and Hahn, 2011). Similar to HIV-2, the HIV-1 groups N, O, and P are limited to West African countries (Sharp and Hahn, 2011). Group M is made up of nine clades: A, B, C, D, F, G, H, J, and K and recombinant viruses of these clades (Sharp and Hahn, 2011; Hemelaar et al., 2011; Bbosa et al., 2019). From this group, HIV-1 clade C is responsible for 50% of cases of HIV-1 infections worldwide and is predominantly found in southern Africa and India (Hemelaar et al., 2011; Bbosa et al., 2019). Different clades are dominant in varied geographic locations worldwide: clade B is predominantly found in the Americas, Western Europe and Australia. Clade A is dominant in east Africa, eastern Europe and central Asia (Hemelaar et al., 2011; Bbosa et al., 2019).

It has been four decades since the identification of the Human Immunodeficiency Virus (HIV) in 1983, as a causative agent of AIDS (Barre-Sinoussi et al., 1983). Since the discovery of HIV, approximately 84.2 million people have been infected and 40.1 million people have died (Barré-Sinoussi et al., 1983; UNAIDS, 2021). Eastern and southern Africa remain the most affected regions, accounting for approximately 54%

(20.6 million) of people living with HIV/AIDS (PLWH) globally (UNAIDS, 2021) (**Fig. 1**). Within this region, South Africa (SA) has the highest HIV burden, with an estimated 8.23 million people living with HIV at the end of 2021 (Johnson et al., 2022).

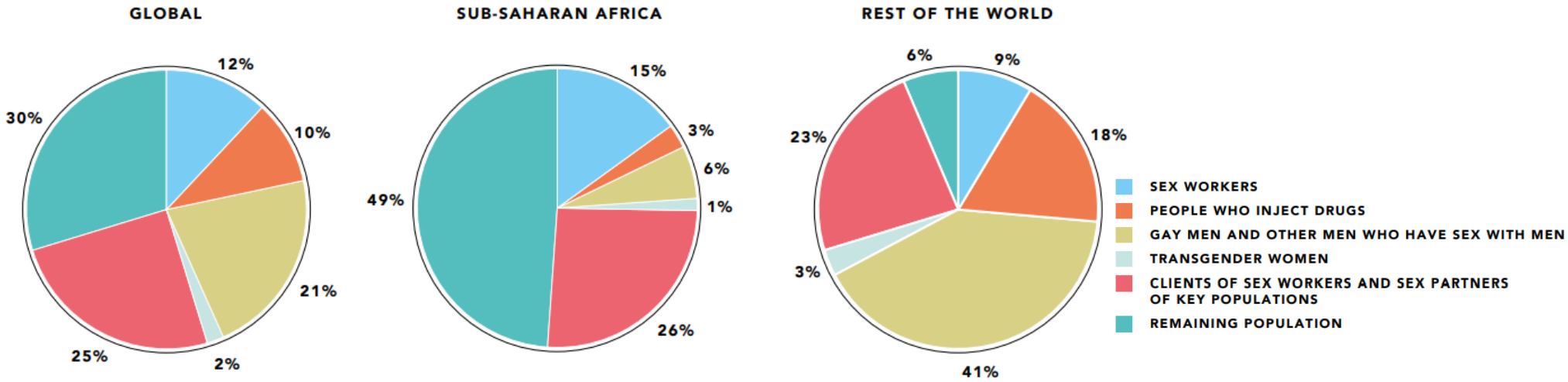

Adults and children estimated to be living with HIV | 2021

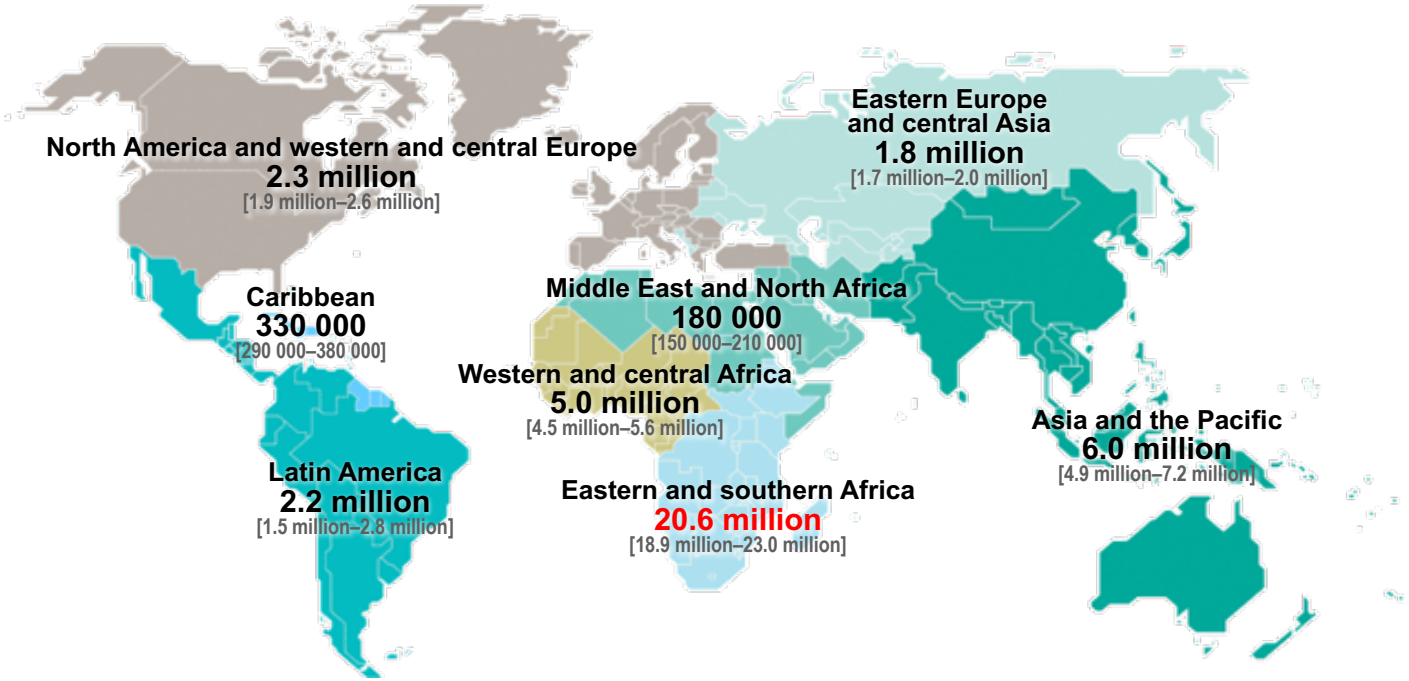

Total: 38.4 million [33.9 million–43.8 million]

Figure 1: Current HIV-1 new infections and prevalence of PLWH. (A) Pie charts showing percentage distribution of new HIV infections globally, sub-Saharan Africa and rest of the world excluding sub-Saharan Africa stratified according to risk populations. (B) World map showing the eight regions that are recognised by the UNAIDS. Eastern and Southern Africa statistics are highlighted in red as it shows the high burden of HIV/AIDS compared to the other regions. Colour of the map indicates the eight different regions that are recognised by the UNAIDS. PLWH: people living with HIV/AIDS. Graphic taken from UNAIDS aidsinfo fact sheet website (https://aidsinfo.unaids.org/)

The spread of HIV and new infections globally and in the sub-Saharan region is influenced, among other factors, by clients of sex workers (25%) followed by MSM (21%), sex workers (12%) and people who inject drugs (10%) (**Fig. 1**) (UNAIDS, 2021). Women in the sub-Saharan region are disproportionately affected by the HIV epidemic, accounting for 63% of new infections in 2021 (UNAIDS, 2021). Six in seven new infections were among adolescent girls aged 15-19 in 2021 (UNAIDS, 2021). In South Africa, HIV prevalence was recorded as 13.7% in 2021, with the KwaZulu Natal (KZN) province being the epicentre of the epidemic. This province recorded an exceptionally high HIV prevalence of 27.9%, and young women between the ages of 15-19 having a prevalence of 22% (Deeks et al., 2015; Kharsany et al., 2018). Socio-economic, behavioural, cultural factors, high incidence of vaginal bacteriosis and inflammation have increased the transmission of HIV among this population (Abdool Karim et al., 2017; Kharsany et al., 2018; Barnabas et al., 2018). Overall, despite great access and roll-out of the ART program in South Africa and globally to treat and to virally suppress HIV infected individuals so that they do not transmit and infect more people, HIV continues to present a challenge to public health as observed by the high

numbers of new infections. Thus, a more effective intervention such as a vaccine which has proven to eradicate diseases in the past, is urgently needed to deal with this epidemic.

1.2 HIV pathogenesis

There are three stages of HIV infection: eclipse phase, acute phase and chronic phase (**Fig. 2**). Following infection, during the eclipse phase, HIV replicates exponentially, establishes latent reservoirs, systematically spreads via lymphoid nodes and destroys gut-associated lymphoid tissue (Deeks et al., 2015). During the acute phase, anti-HIV antibodies are detectable, HIV has replicated exponentially and viral load is at its peak with 10^6-10^7 copies per ml of blood. There is hyper immune activation and hyper-inflammation resulting in flu-like symptoms (Deeks et al., 2015). Lastly, during chronic infection viral "set point" is achieved and replication is ongoing resulting in chronic inflammation. This is followed by CD^4 T-cell depletion through several mechanisms including apoptosis of uninfected bystander cells, direct viral killing of infected cells, and killing of infected CD4+ T cells by CD8+ cytotoxic white blood cells (Cos et al., 2002; Tortora et al., 2010). Years later, chronically infected individuals progress to the AIDS phase. However, the rate of progression to AIDS is dependent on the individual. Some individuals, termed "elite controllers" take several years, while others progress faster (Deeks et al., 2015). HIV/AIDS is defined as a multifactorial disease that gradually obliterates a person's immune system. White blood cells (especially T-lymphocytes) become deficient leading to observable clinical symptoms that are associated with immune deficiency such as: autoimmune inflammation and

susceptibility to opportunistic diseases (Barbaro and Klatt, 2002; Cos et al., 2002; Cos et al., 2004; Vermani and Garg, 2002; Deeks et al., 2015).

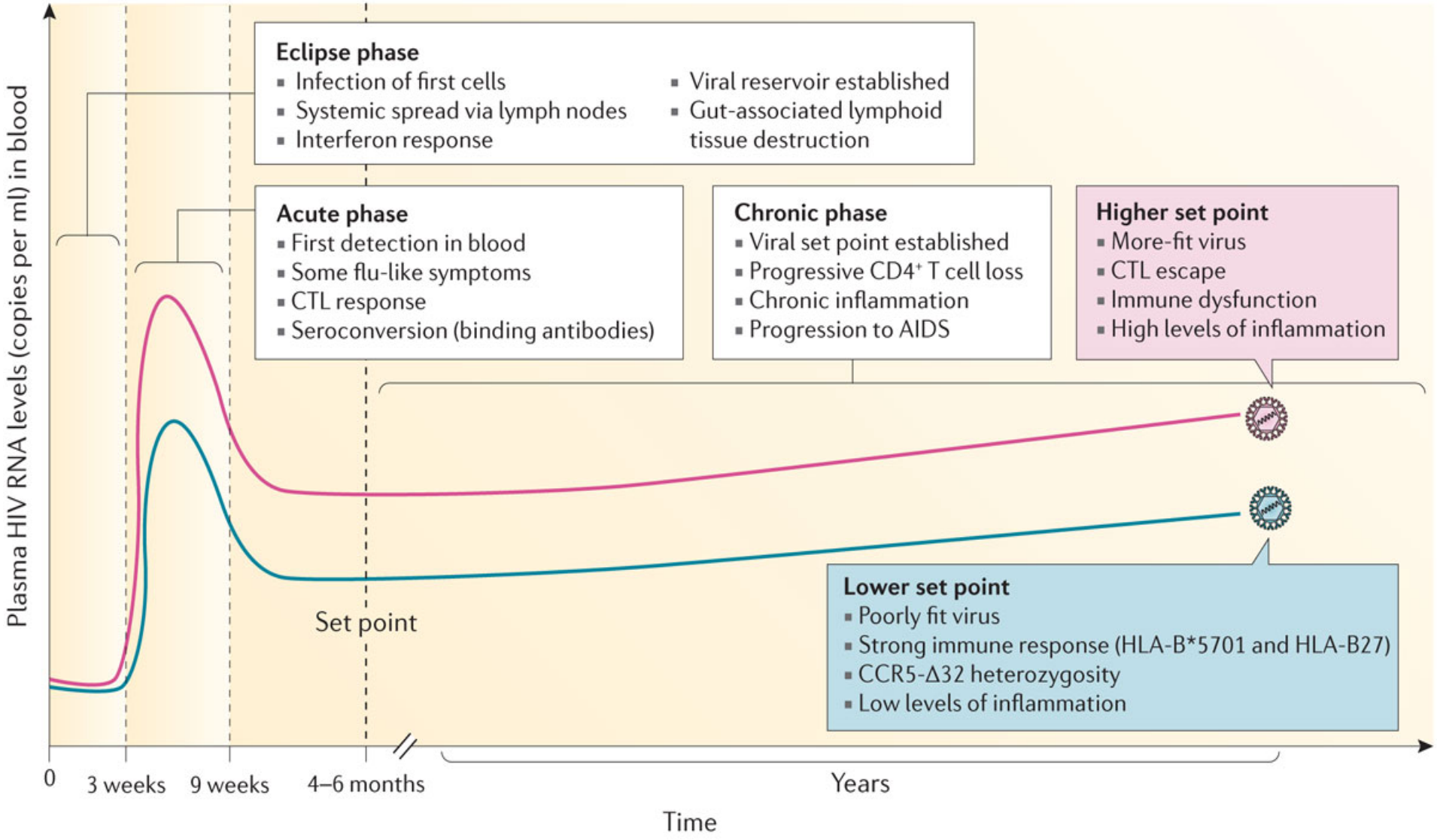
Eclipse phase
Infection of first cells
Systemic spread via lymph nodes
Interferon response
Viral reservoir established
Gut-associated lymphoid tissue destruction
Acute phase
First detection in blood
Some flu-like symptoms
CTL response
Seroconversion (binding antibodies)
Chronic phase
Viral set point established
Progressive CD4+ T cell loss
Chronic inflammation
Progression to AIDS
Higher set point
More-fit virus
CTL escape
Immune dysfunction
High levels of inflammation
Lower set point
Poorly fit virus
Strong immune response (HLA-B*5701 and HLA-B27)
CCR5-Δ32 heterozygosity
Low levels of inflammation
Set point
Plasma HIV RNA levels (copies per ml) in blood
0
3 weeks
9 weeks
4–6 months
Years
Time

Figure 2: Dynamics of HIV infection over time. HIV infection follows three phases: Eclipse, Acute and Chronic phases. Different events that happen during each phase are depicted in the figure. CTL, cytotoxic T lymphocyte; CCR5, CC-chemokine receptor 5; HLA, human leukocyte antigen (taken from Deeks et al., 2015).

1.2.1 The structure, genome and genetic diversity of HIV

HIV belongs to the Retroviridae family and the genus Lentivirus. Lentiviruses are characterized by a long incubation period and their ability to infect non-dividing cells (Sierra et al., 2005; Tortora et al., 2010). The virus has two identical 9.2 kb positive-sense, single-stranded RNA molecules. It uses virally encoded enzymes such as reverse transcriptase (RT) to synthesize a double-stranded DNA molecule that is inserted in the genome of infected cells (Sierra et al., 2005). The RNA molecules are composed of nine genes (*gag, pol, env, tat, rev, nef, vif, vpr* and *vpu*) which encode for proteins essential in the life-cycle, pathogenesis and structure of HIV (**Fig. 3A**) (Chinen and Shearer, 2002; Sierra et al., 2005). The first three genes encode the structural proteins and the remaining six genes encode regulatory proteins to promote viral transcription, mature virion release and/or viral pathogenesis (Chinen and Shearer, 2002; Sierra et al., 2005).

Infectious, mature HIV virions have a spherical shape of 100-120 nm in diameter (**Fig 3B**). The virus has a host derived lipid bilayer surrounding the core of the virus formed by p17 protein molecules (matrix proteins). Embedded into this lipid bilayer are viral-encoded trimeric gp120-gp41 proteins forming the envelope protein (Env). The RNA molecules are bound to p7 proteins forming a nucleocapsid. The genome together with three enzymes called reverse transcriptase (RT), integrase (IN) and protease

(PR) and the 6 accessory proteins: Vif, Tat, Vpu, Vpr, Nef, and Rev are enveloped by capsid proteins p24 to form a conical capsid (Sierra et al., 2005; Tortora et al., 2010; van Heuvel et al., 2022).

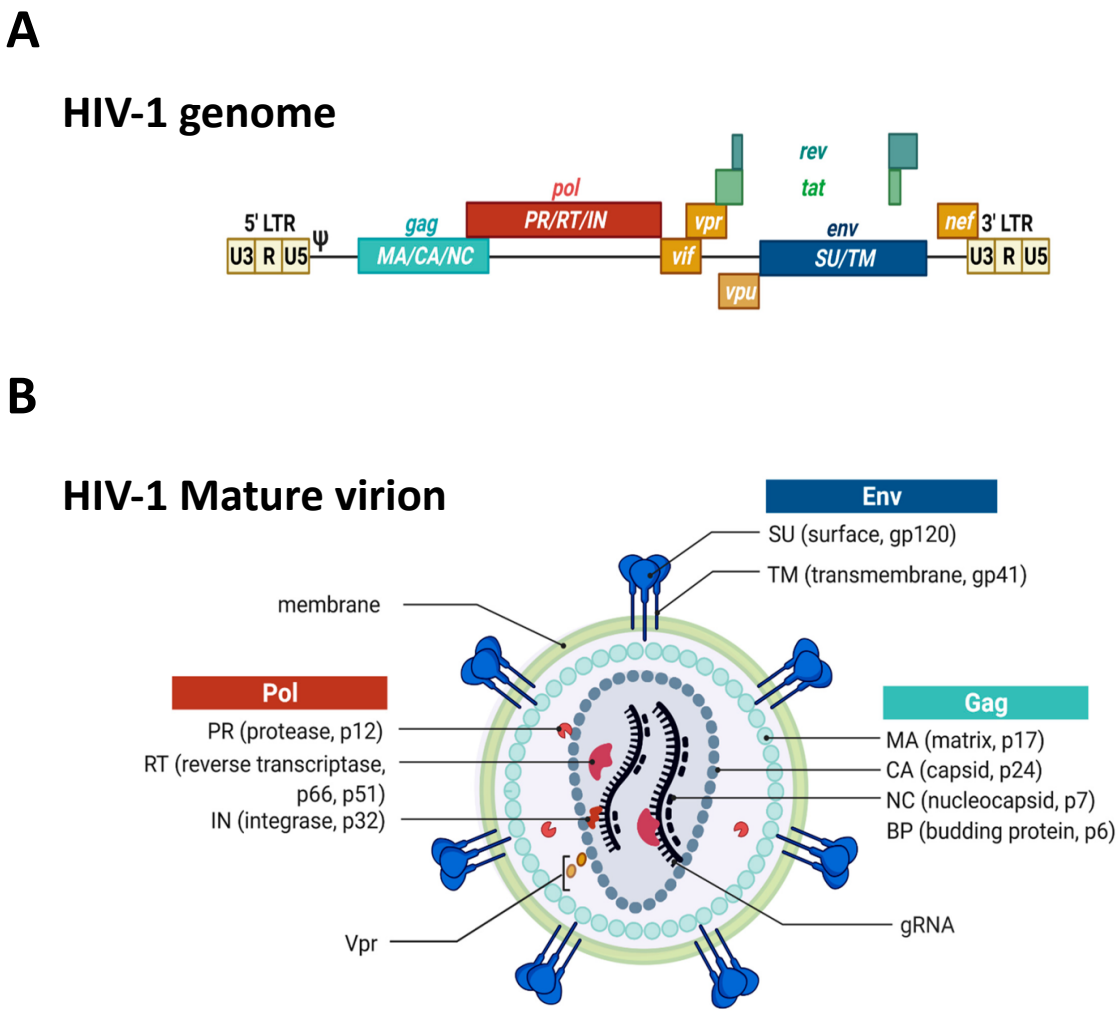

Figure 3: Schematic representation of the HIV-1 genome and virion. (A) Different genes that encode all of the HIV proteins are shown. The Long Terminal Repeats (LTR) highlighted in yellow, are located on both the 5' and 3' ends. LTRs are responsible for mediating HIV genome insertion into the host genome. Additionally, they serve as both promoter and

polyadenylation (Poly-AAA) signals at the 5' and 3' ends respectively. The genes encoding different proteins to form a fully mature virion are coloured green, red and blue for *gag*, *pol* and *env* respectively. Proteins encoded by these genes are abbreviated in the genes and full names are seen in panel B. Four accessory genes (*vpu, vpr, nef* and *vif*) are represented in orange. Two regulatory proteins (Tat and Rev) encoded by spliced introns are represented in dark green. (B) Structural representation of a mature, fully assembled HIV virion is shown with protein abbreviations explained. Additionally, the proteins derived from each gene are also shown. Surrounding the virion is a lipid bilayer (light green) which has Envelope proteins attached (blue). Underneath the lipid bi-layer is the matrix protein layer shown above as pale blue spheres. The two HIV RNA molecules are encased by the capsid protein. HIV enzymes are coloured red. Figure adapted from (van Heuvel et al., 2022)

1.2.3 HIV transmission

HIV-1 is predominantly transmitted sexually but can also be transmitted through infected bodily fluids such as blood. Approximately 80% of HIV-1 transmission events globally are because of heterosexual intercourse with an infected partner and infections are from a single HIV-1 variant called the transmitted/founder virus (T/F virus) (Derdeyn et al., 2004; Keele et al., 2008; Joseph et al., 2015). Chronically infected individuals have a diverse viral population, however they can only transmit a single T/F virus to initiate infection in the recipient partner (Keele et al., 2008; Joseph et al., 2015). However, it is worth noting that new emerging data suggest that this dogma no longer holds, because in serodiscordant studies it has been shown that infection is initiated by multiple viruses (Williamson et al, unpublished data). Following infection during the eclipse and acute phases in the recipient partner, the HIV-1 population is homogeneous and continues to multiply exponentially. However,

selection pressure such as antibody responses during the chronic phase trigger the evolution of the homogeneous population to be more heterogeneous resulting in quasispecies (**Fig. 4**) (Joseph et al., 2015). Quasispecies are a result of escape mutations against immune responses giving rise to various HIV-1 variants with different phenotypes such as high- or low- viral fitness, replication capacity and transmissibility (Joseph et al., 2015). As a result of viral diversity, the humoral/antibody response against HIV-1 is constantly evolving as well. The humoral response is typically directed to the Env protein of HIV-1 as it is easily accessible. However, the Env easily mutates to avoid antibody response. This then leads to an "arm's race" culminating in the development of strain-specific responses (in the majority of people) towards broadly neutralizing antibody (bNAb) responses (in few individuals) (Joseph et al., 2015) (see section 1.4 for more detail). During chronic infection, viral diversity is exponential. Moreover, the Env protein is also genetically diverse which presents a huge challenge for vaccine efforts focused on eliciting bNAb responses. Due to the Env diversity, the passive immunization strategy of using a single monoclonal antibody to prevent HIV acquisition will theoretically not succeed compared to using a cocktail of antibodies. Proof-of-principle studies to verify this hypothesis have been done (see section 1.3 for more detail) but more studies still need to be conducted to support or contradict recent findings.

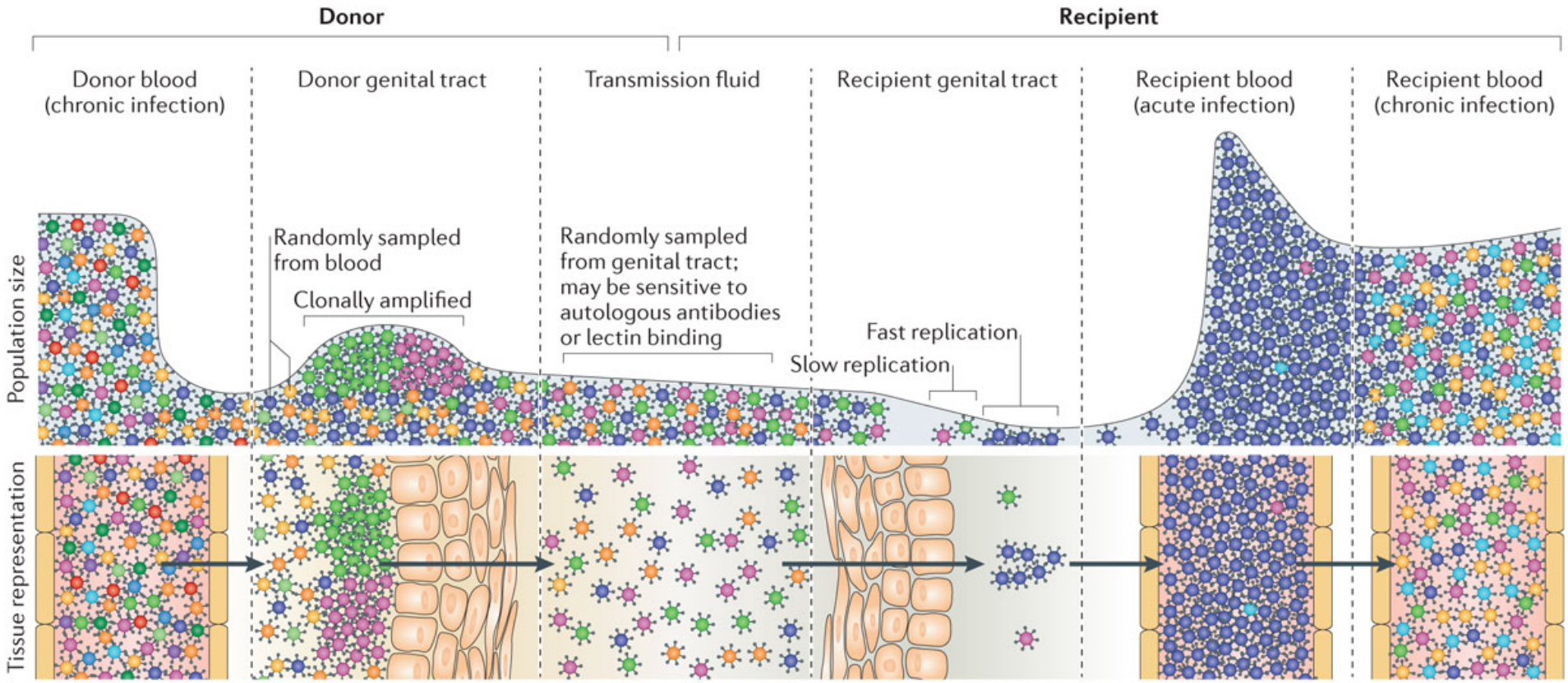
Donor
Recipient
Donor blood (chronic infection)
Donor genital tract
Transmission fluid
Recipient genital tract
Recipient blood (acute infection)
Recipient blood (chronic infection)
Population size
Randomly sampled from blood
Clonally amplified
Randomly sampled from genital tract; may be sensitive to autologous antibodies or lectin binding
Fast replication
Slow replication
Tissue representation

Figure 4: HIV-1 transmission and T/F evolution to generate viral quasispecies and Env diversity. Chronically infected individuals have diverse HIV-1 populations in their blood. During transmission from donor to recipient, several events take place that culminate in transmission of highly infectious virions able to initiate and propagate infection in the recipient individual. Genetic bottlenecks are observed from both the donor and recipient. In the donor at the mucosal barrier and in the transmission fluid (semen or cervicovaginal mucus), random selection of variants occurs. In the transmission fluid, the viral variants are further exposed to bottleneck sieving resulting in filtering out the majority of less fit viruses resulting in predominantly homogeneous viral population that will be transmitted to the recipient. Once in the recipient, homogeneous fast replicating viral variants soon become a heterogenous viral population. Figure adapted from Joseph et al., (2015).

1.3 Efforts to eradicate HIV/AIDS

As outlined above, South Africa (SA) has the highest HIV burden, with an estimated 8.23 million people living with HIV at the end of 2021 (Johnson et al., 2022). To address this important public health challenge, the South African government has greatly increased its antiretroviral therapy (ART) roll-out. However, despite the success of ART at reducing viral load and prolonging life-expectancy in PLWH, a search for a vaccine remains important given that 210,000 new infections occurred in 2021 in SA (UNAIDS, 2021). Parallel to using ART, there are several biomedical interventions and research approaches that are currently being pursued in order to eradicate HIV/AIDS in SA and globally. These include: pre-exposure prophylaxis (PrEP), post-exposure prophylaxis (PEP), circumcision, treatment as prevention (TasP), mother-to-child prevention (MTCT), microbicides (CAP004), and both passive

and active vaccination strategies. Currently, it is accepted that in order to eradicate HIV-1 a combination of the different biomedical interventions outlined below will need to be employed rather than just utilising only one intervention.

1.3.1 Pre-Exposure Prophylaxis (PrEP)

A combination of oral Tenofovir disoproxil fumarate and emtricitabine (TDF/FTC) that can be taken daily by HIV-negative individuals to prevent HIV infection. TDF/FTC has been well studied to show the protective ability of the PrEP strategy. In MSM and serodiscordant couples TDF/FTC has resulted in 86% and 76% HIV acquisition reduction respectively (McCormack et al., 2016; Baeten et al., 2012). Also, it has been shown that protection is concentration dependent (i.e. higher concentration of PrEP such as Tenofovir in the vagina correlates with protection) (Anderson et al., 2012; Kashuba et al., 2015). However, there are some conflicting studies that have reported either poor (Grant et al., 2010; Choopanya et al., 2013) or no efficacy of PrEP (van Damme et al., 2012; Marrazzo et al., 2015) in different population groups. These differences have been attributed to lack of adherence by individuals (Anderson et al., 2012).

1.3.2 Post-Exposure Prophylaxis (PEP)

A combination of oral Tenofovir + Lamivudine + Dolutegravir (TDF/3TC/DTG) or Tenofovir + Emtricitabine + Atazanavir + Lopinavir (TDF/FTC/ATV/LPV/r) for pregnant people taken daily following potential exposure to HIV to prevent infection. During the 1990s, Tsai *et al*., (1995) showed that immediate treatment with ART following SIV

exposure in Macaques prevented infection establishment. As a result, a case-control study in health care workers who were exposed to HIV and seroconverted proved that zidovudine was protective if administered early following exposure (Cardo *et al*., 1997). This then formed the basis for PEP in different countries. Thus, since 1996, only one case of occupationally acquired HIV has been reported (Kuhar et al., 2013), thus indicating the effectiveness of PEP strategy.

1.3.3 Circumcision

Circumcision has been shown in several studies to reduce the risk of HIV infection in men. Three independent clinical trials have shown a reduced risk of HIV acquisition by 50-60% in heterosexual relationships among circumcised males compared to uncircumcised males within the sub-Saharan region (Auvert et al., 2005; Gray et al., 2007; Bailey et al., 2007). Furthermore, circumcision has been shown to also reduce the risk of getting other sexually transmitted infections (Gray et al., 2007; Gray et al., 2009). However, for HIV positive males, no significant reduction in HIV transmission to HIV negative female partners has been observed (Wawer et al., 2009). Moreover, in MSM, there's insufficient data to conclude that circumcision offers any benefits in preventing HIV acquisition (Goodreau et al., 2014).

1.3.4 Treatment as prevention (TasP)

Involves providing antiretroviral therapy (ART) to HIV-positive individuals to suppress the virus to undetectable levels, which greatly reduces the risk of transmission to others. In serodiscordant couples, it has been shown that HIV transmission was

significantly reduced by 96% when ART is initiated early (< 350 CD4 T cell per ul) (Cohen et al., 2011). Several other studies have shown that when ART is initiated early and the individual is virally suppressed, a significant reduction in HIV transmission was observed. The infections that occurred during these studies were attributed to infections outside the primary relationship (Grulich et al., 2015). Other trials: Sustainable East Africa Research in Community Health (SEARCH) (NCT01864603), Botswana Combination Prevention Project (BCPP) (NCT01965470), Population Effects of ART to Reduce HIV Transmission (PopART) (NCT01900977) and Impact of Immediate Versus South African Recommendations Guided ART Initiation on HIV Incidence (ARNS/TasP) (NCT01509508) are currently ongoing to provide further evidence at community level that early ART initiation results in reduced HIV transmission.

1.3.5 Mother-to-child prevention (MTCT) treatments

Involve providing ART to pregnant women living with HIV to prevent transmission of the virus to their new-borns. Without prior treatment with ART, HIV transmission from mother to child is high (15-25%) and it doubles when the baby is breastfed by an infected mother (35-40%) (Nduati et al., 2000). Transmission rate is drastically reduced (<5%) when ART is used as a prophylaxis for the baby and as treatment for the infected mother. Using ART as prophylaxis for the baby prevents the establishment of infection in the baby and when used for treating the infected mother prior to giving birth, it results in viral suppression (reduced viral load), thus making the mother less infectious (de Vincenzi et al., 2011). The WHO recommends that HIV-infected mothers continue taking ART as it provides benefits of viral suppression and prolongs life.

Furthermore, for infants, the WHO recommends that they be enrolled in a short-term ART treatment as prophylaxis (WHO consolidated guidelines).

1.3.6 Microbicides

These are topical products, such as gels, films or rings, that can be applied to the vagina or rectum to prevent HIV infection. Vaginal microbicides such as Tenofovir in CAP004 trial in South Africa have demonstrated HIV acquisition reduction by 39% overall and 54% in women with high adherence (Abdool Karim et al., 2010). A Dapivirine ring has been evaluated in different trials to show safety and effectiveness in preventing HIV acquisition (Baeten et al., 2021). Two different phase III placebo controlled trials have shown that a Dapivirine ring reduced HIV infection in ~30% of women (Baeten et al., 2016; Nel et al., 2016). In one of the trials, protection was greatest (>50%) in women aged 21 and above, who demonstrated better adherence (Baeten et al., 2016). Rectal gels are currently in development and none have been evaluated in phase III trials for efficacy (Baeten et al., 2021).

1.3.7 Passive immunization

These approaches, such as AMP (Antibody Mediated Prevention), aim to use monoclonal antibodies (mAbs) to block HIV from entering cells and prevent infection. bNAbs are rare types of antibodies that can neutralize a wide range of viral strains, rather than just one. bNAbs have been shown to be effective at suppressing viral replication and preventing infection in animal models (Parren et al., 2001; Hessell et al., 2007; Hessell et al., 2009; Moldt et al., 2012; Lewis et al., 2017). One mAb that

has been used for the purpose of passive immunization is VRC01 (Corey et al., 2021). VRC01 is a bNAb that was isolated from an HIV-infected individual and has been shown to neutralize a wide range of HIV strains (91%) with potent inhibitory concentration 50 (IC_{50}). It is a CD4 binding site specific bNAb which blocks infection by mimicking the CD4 receptor- HIV-1 Env interaction (Wu et al., 2010; Zhou et al., 2010). VRC01 is one of the potent and well-studied bNAbs. However, it is not easy to elicit by vaccination. There is abundant clinical data for use of this bNAb for passive immunization in animal models, hence, now it is being evaluated in humans for proof-of-principle HIV prevention and treatment study (Wu et al., 2010).

In the AMP trial, VRC01 was tested as a potential preventative measure against HIV infection. The trial aimed at determining the safety and efficacy of infusing VRC01 in HIV-uninfected individuals at high risk of HIV infection (Corey et al., 2021). The trial found that VRC01 was safe and well-tolerated, with no significant safety concerns reported. However, the trial did not show a statistically significant reduction in the incidence of HIV-1 infection in the VRC01 group compared to the placebo group. When data was stratified according to different virus profiles: sensitive, intermediate and resistant, VRC01 significantly reduced the risk of HIV infection against VRC01-sensitive viruses which accounted for 30% of the viruses tested (Corey et al., 2021).

While the trial did not demonstrate that a single agent bNAb such as VRC01 can provide enough protection on its own, it still provided valuable information for future HIV-1 prevention strategies, such as the use of combination of bNAbs with other prevention methods (Corey et al., 2021). Additionally, more research is needed to

understand the optimal dosing and frequency of VRC01 infusions, as well as the duration of protection. It would be interesting to see if VRC01 is effective in combination with other prevention methods such as Pre-Exposure Prophylaxis (PrEP).

1.3.8 Vaccination

This approach presents the most effective method to prevent and eradicate infectious diseases (Ehreth, 2003). An HIV vaccine able to elicit bNAbs to globally circulating viruses is widely thought to represent the best option for preventing new HIV-1 infections (Halper-Stromberg, Lu, et al., 2014). Vaccines work by priming the body's immune system against a particular pathogen using immunogens. Immunogens include attenuated versions of the pathogen and/or engineered antigens to elicit an immune response. Most licensed vaccines rely on neutralizing antibodies against the pathogen (Plotkin, 2008; Mascola and Montefiori, 2010). HIV vaccine development, however, is complicated by the rapid evolution and variability of the virus (Korber, Gaschen, et al., 2001).

There are several HIV vaccine candidates in development, following the only trial which showed modest efficacy, RV144 vaccine (Rerks-Ngarm et al., 2009). The HVTN 702 trial "Uhambo" is a follow up to RV144 and was conducted in SA. It was prematurely terminated because of the HIV-1 acquisition risk posed to patients in the vaccine arm. Data analysis showed increased susceptibility to HIV acquisition in participants enrolled in the vaccine arm of the trial and no efficacy (Gray et al., 2021). Another trial conducted is "Mbokodo" HVTN 705. This trial took place in the Sub-saharan region and the study population was women. This trial was motivated by

studies conducted in non-human primates (NHP) which showed 67% efficacy and protection in NPH vaccinated with Ad26.Mosaic.gp140.C.alum trivalent vaccine regimen (Barouch et al., 2018). Results for this trial have been recently submitted and a publication should be available soon (Feinberg et al., 2021). The “Mosaico” HVTN 706 trial in Europe, USA, Latin America and designed for MSM and transgender persons was also terminated (Feinberg et al., 2021). It is similar to HVTN 705 with slight modification to the vaccine regimen (**Table 1**). There are no official peer-reviewed publications for these studies, only press releases are available (Imbokodo and Mosaico). Lastly, the PrEPVacc, a Phase IIb three-arm, two-stage HIV prophylactic vaccine trial with a second randomisation to compare oral PrEP (TAF/FTC to TDF/FTC) is currently enrolling participants in the sub-saharan region. It aims to evaluate efficacy of two experimental HIV vaccines: DNA/AIDSVAX/B/E and DNA/CN54gp140 with placebo control. Simultaneously, daily oral PrEP is compared for efficacy against daily TDF/FTC (Truvada) and TAF/TFC (Discovy) (**Table 1**).

Currently there has not been a vaccine trial to elicit bNAbs in humans, however, early phase trials and proof-of-principle studies are being conducted. Recently, a bNAb stimulating phase I vaccine trial (eOD-GT8 vaccine) showed promise in human trials and is being pursued for subsequent phases. This trial has invigorated the bNAb field and provides proof-of-principle that it is possible to stimulate bNAb precursors using a germline-targeting vaccine strategy (see section 1.5.2) (Leggat et al., 2022). These are just a few examples of the many experimental HIV vaccines that have been tested, and research in this field is ongoing.

Table 1: HIV-1 vaccine efficacy trials conducted to date

	RV144	HVTN 702	HVTN 705	HVTN 706	PrEPVacc
Geographic region	Thailand	South Africa	Sub-Saharan Africa	Europe, United States, Latin America	Sub-Saharan Africa
Local trial name		Uhambo	Imbokodo	Mosaico	
Enrollment period	2003–2009	2016–2020	2017–2022	2019–2023	2020–2023
ClinicalTrials.gov identifier	NCT00223080	NCT02968849	NCT03060629	NCT03964415	NCT04066881
Virus Subtype	AE	C	C	B, C, and others	A, D, C
Diversity	Relatively homogeneous	Highly diverse	Highly diverse	Highly diverse	Highly diverse
Sex or gender	Male and female	Male and female	Female	MSM and transgender persons	Male and female
Vaccine features					
Adjuvant	Aluminum hydroxide	MF59	Aluminum phosphate	Aluminum phosphate	Aluminum hydroxide (AIDSVAX B/E); MPLA-L (CN54 gp140)
Regimen	Heterologous prime–boost regimen consisting of subtype AE ALVAC (vCP1521) and protein boost bivalent AE/B (A244/MN)	Heterologous prime–boost regimen consisting of subtype C ALVAC (vCP2438) and protein boost bivalent C (TV1.C/1086.C)	Heterologous prime–boost regimen consisting of tetravalent Ad26.Mos4.HIV (expressing mosaic Gag, Pol, and Env antigens) and adjuvanted clade C gp140	Heterologous prime–boost regimen consisting of tetravalent Ad26.Mos4.HIV (expressing mosaic Gag, Pol, and Env antigens) and adjuvanted clade C gp140 plus mosaic gp140	Two combination vaccine regimens with PrEP consisting of DNA/AIDSVAX B/E, DNA/CN54 gp140, plus MVA–CN54 gp140 plus MPLA-L
Protein dose	300 μg of each protein	100 μg of each protein	250 μg	80 μg clade C protein, 75 μg mosaic protein	100 μg in one regimen and 300 μg in the other
Dosing schedule	Months 0, 1, 3, and 6	Months 0, 1, 3, 6, 12, and 18	Months 0, 3, 6, and 12	Months 0, 3, 6, and 12	Months 0, 1, 6, and 12; daily PrEP
Result	**31.2% vaccine efficacy at 42 months**	**No vaccine efficacy**	**No vaccine efficacy**	**ongoing**	**Trial ongoing**

1.4 Development of antibodies and HIV bNAbs

Antibodies, also known as Immunoglobulins (Igs) are proteins produced by the immune system to specifically recognize and neutralize foreign substances, such as bacteria and viruses, in the body. Antibodies also have several key properties that are appealing for vaccine development, which include specificity, affinity, diversity and immune modulation. Antibodies can also trigger other parts of the immune system such as the complement system to destroy these foreign substances. Structurally, Igs are Y-shaped heterodimeric proteins made up of two light chains (LCs) and two heavy chains (HCs) held together by disulfide bonds (s-s) (Schroeder et al. 2010, Stanfield et al., 2014). The LC is composed of the variable (V_L) and constant (C_L) regions. The HC is composed of variable (V_H) and constant (C_H1, C_H2, C_H3 & C_H4) regions. The LCs form part of the arms "Fab-region" of this Y-shape, while HCs forms both the Fab-region and Fc-region of this Y-shape (**Fig. 5A**). The Fab and Fc regions are linked together by the "hinge region" (**Fig. 5A**), however, this is not the case for IgM and IgE (Schroeder et al. 2010, Stanfield et al., 2014; Chiu et al., 2019).

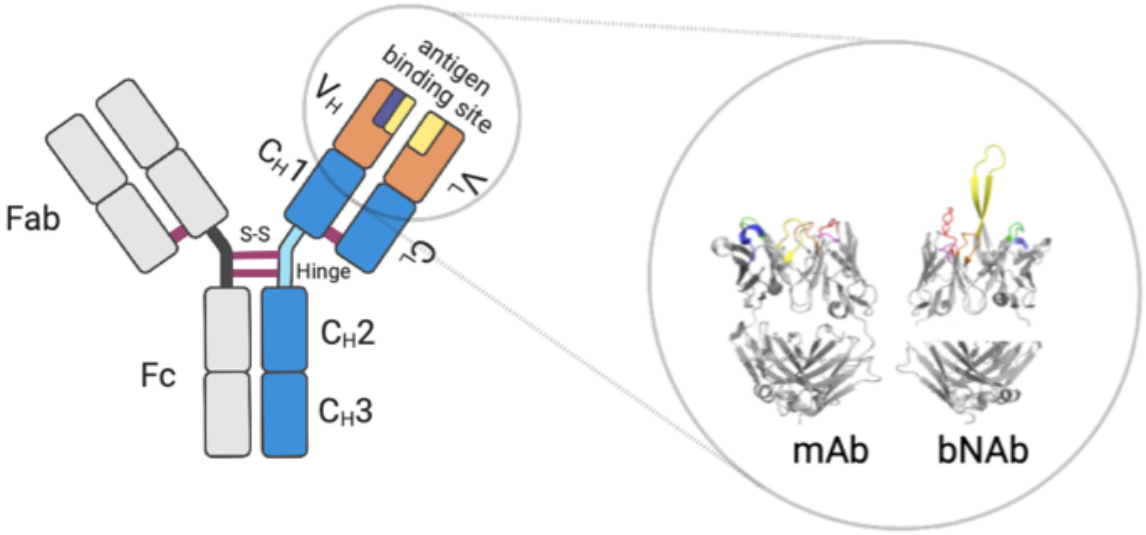

Figure 5: Antibody structure. Schematic representation of the antibody to show different regions and structural features. The antibody binding site (Fab) composed of the CDRs is highlighted to show CDR differences between antibodies and bNAbs. Ribbon structure shows the CDRs for both LC (CDR-L1, CDR-L2 & CDR-L3) and HC (CDR-H1, CDR-H2 & CDR-H3) and contrasts the mAb (PDBid 5I1A) and bNAb PGT145 (PDBid 3U1S) CDRs highlighting the unique features of bNAb Fab. Red (CDRL1), pink (CDRL2), orange (CDRL3), blue (CDRH1), green (CDRH2), yellow (CDRH3). Figure created with Biorender.

Functionally, the Fc region is responsible for activating the complement system and interacting with the Fc receptors present on immune system cells to trigger Fc-mediated functions such antibody-dependent cellular cytotoxicity (ADCC), complement dependent cytotoxicity (CDC), antibody-dependent phagocytosis (ADCP), antibody-dependent complement deposition (ADCD), antibody-dependent cellular trogocytosis (ADCT) (Schroeder et al. 2010, Chiu et al., 2019). The N-terminal tip of the Fab region is responsible for antigen binding, recognising and neutralizing of the pathogens utilising the V_L and V_H specifically. Within the V_L and V_H there are Complementarity determining regions “CDRs” and Framework regions “FRs” which

are essential in antigen binding and antibody structural conformation stability, respectively. There are three CDRs for both LC (CDR-L1, CDR-L2 & CDR-L3) and HC (CDR-H1, CDR-H2 & CDR-H3) and four FRs in the HC and LC (FR1, FR2, FR3 & FR4) (**Fig. 5B**). The antigen-binding site region is highly variable, allowing for the production of a large number of different Igs that can recognize a diverse range of antigens (Schroeder et al. 2010, Stanfield et al., 2014; Chiu et al., 2019).

1.4.1 How are antibodies generated?

Antibodies are generated by specialized white blood cells called B-lymphocytes (or B-cells) in response to exposure to foreign substances, such as bacteria, viruses, or toxins. The process is as follows: recognition, activation, differentiation, maturation and memory (Chiu et al., 2019; Stanfield et al., 2014). Initially, B-cells recognize antigens and bind to them through their B-cell receptors, then this is followed by the activation and multiplying of the B-cells, thus creating a population of identical cells known as a clone. Following activation, activated B-cells differentiate into plasma cells, which secrete large amounts of antibodies. The antibodies produced by plasma cells mature and undergo a process called affinity maturation, during which the antibodies become more specific and able to bind more tightly to the antigen (Schroeder et al. 2010, Stanfield et al., 2014; Chiu et al., 2019). Lastly, some B-cells with high affinity to the antigen remain in the body as memory cells, allowing for a faster and more effective response to a subsequent infection by the same antigen (Schroeder et al. 2010, Stanfield et al., 2014; Chiu et al., 2019). This process of antibody generation is part of the adaptive immune response, which provides specific and targeted protection against foreign invaders.

1.4.2 How is antibody antigen-binding site diversity achieved?

The diversity of the antigen-binding site is generated via VDJ recombination in the bone marrow. The process of VDJ recombination involves the rearrangement of three genetic elements: the variable (V), the diversity (D), and the joining (J) gene segments. V(D)J recombination depends on the action of the lymphoid-specific RAG-1 and RAG-2 endonucleases that initiate DNA cleavage at defined recombination signal sequences (RSS) that flank the V, D, and J gene segments. These gene segments are located on separate chromosome regions, but during B-cell development, they are brought together through a process of somatic recombination to form a functional antibody gene (Meizels et al., 2005; Nguyen et al., 2016) (**Fig. 6**). VDJ happens as a process of combinatorial assembly, whereby one segment of each type is chosen from several possibilities and assembled to form genetically diverse antibodies each with its own unique antigen-binding site. This diversity allows the immune system to respond to a wide range of antigens, increasing the chances of recognizing and neutralizing foreign invaders (Schatz et al., 2011)

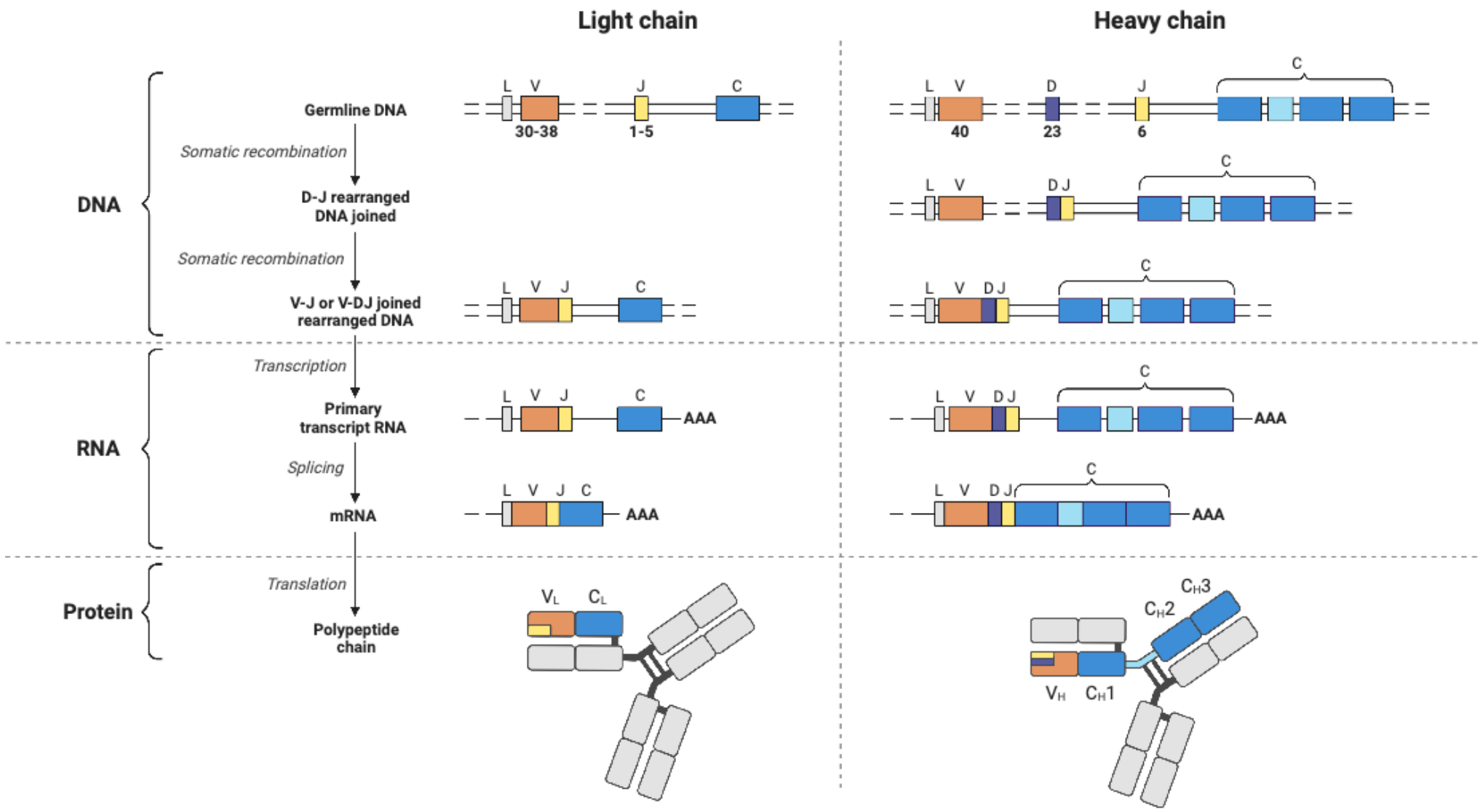
Light chain
Heavy chain
DNA
RNA
Protein
Germline DNA
Somatic recombination
D-J rearranged DNA joined
Somatic recombination
V-J or V-DJ joined rearranged DNA
Transcription
Primary transcript RNA
Splicing
mRNA
Translation
Polypeptide chain
L V J C
30-38
1-5
L V D J C
40
23
6
AAA
V_L C_L
V_H C_H1 C_H2 C_H3

Figure 6: VDJ recombination. During a V(D)J recombination process a pair of gene segments are chosen and double-strand breaks are introduced adjacent to each segment. This is followed by the deletion (or, in some cases, inversion) of the intervening DNA. Lastly, the process concludes by ligating the segments together and inserting the poly-A tail, thus forming an Ab mRNA ready to be translated into a functional and unique Ab protein. The process and sequence of events is shown on the left from DNA to protein. Variable (V), diversity (D) and joining (J) gene segments are represented as orange, purple and yellow blocks, respectively. Constant region is shown as blue blocks. Hinge region is shown as a light blue block. a poly-A tail is represented as "AAA". Figure created with Biorender

1.4.3 How is affinity maturation achieved?

Affinity maturation is a process that increases the specificity and binding affinity of antibodies over the course of an immune response. Following VDJ recombination of the antigen receptor, the B-cell expressing the assembled receptor termed immature B-cell, migrates out of the bone marrow to the spleen to form mature antigen naïve B-cells expressing both IgM and IgD isotypes. The naïve mature B-cell is then negatively screened for autoreactivity before they exit the spleen to engage with the antigen (Schatz et al., 2011). B-cells continually mature via the antigen-dependent secondary diversification events that occur following two activation-induced cytidine deaminase (AID)-dependent processes known as somatic hypermutation and class switch recombination (CSR) (Maizels et al., 2005). These AID-dependent processes occur at the germinal centre (GC). Antigen or helper T cell activated B-cells enter the GC and there, they proliferate and are subjected to AID-induced somatic hypermutation alteration and Ig class switching. The resulting B-cells after this process undergo a process of positive selection, where B-cells with high-affinity receptors are favoured

and multiplied (Maizels et al., 2005; Schroeder et al. 2010, Stanfield et al., 2014; Chiu et al., 2019).

This process of affinity maturation is critical for the immune system's ability to respond effectively to infections and other foreign invaders. By continuously improving the specificity and binding affinity of antibodies, the immune system can better neutralize antigens and clear infections. This process is responsible for the generation of bNAbs in PLWH.

1.5 bNAbs as holy grail for HIV-1 vaccine

BNAbs are a special class of antibodies that are capable of neutralizing a wide range of HIV viral variants or quasispecies (see section 1.2.1). During HIV infection, strain-specific antibodies develop in all infected individuals, and target the virus that infected the individual (the autologous virus). However, approximately 15-30% of HIV infected individuals develop bNAbs, with “elite neutralizers” able to neutralize up to 98% of heterologous viruses from different HIV clades (Simek et al., 2009; Gray et al., 2011; Euler et al., 2012; Hraber et al., 2014; Rusert et al., 2016). Several factors correlate with the development of bNAbs in these individuals, such as viral diversity (Euler et al., 2012; Liao et al., 2013; Doria-Rose et al., 2014; Bhiman et al., 2015), high viral load, duration of infection (Gray, et al., 2011) and T follicular helper cells (Tfh) (Locci et al., 2013).

BNAbs differ from most antibodies in several key ways. Compared to most antibodies, bNAbs have the ability to target conserved epitopes within the antigen, thus neutralizing multiple strains. Conversely, strain-specific antibodies are only specific to a particular strain or clade, thus they can only neutralize those particular viruses.

Structural and genetic characteristics that make bNAbs special include: particularly long CDRs (Walker et al., 2009; Doores and Burton, 2010; Pancera et al., 2010; Pejchal et al., 2010; Briney et al., 2012; Doria-Rose et al., 2014; Bhiman et al., 2015), high levels of somatic hypermutation (SHM) (Klein et al., 2013; Sok et al., 2013; Wu et al., 2015) and polyreactivity (Verkoczy et al., 2011; Moore et al., 2015). These unusual features pose significant challenges to their elicitation in a vaccine setting and, thus far, no Env immunogen has successfully elicited bNAbs. BNAbs are a valuable tool in the fight against HIV. Currently, bNAbs are being developed as therapeutics for HIV-1, and they have the potential to provide broad and long-lasting protection (Caskey, 2020).

The discovery of bNAbs in HIV infected participants revived the HIV vaccine discovery field since these bNAbs target the HIV Envelope (Env) and can neutralize the majority of globally circulating HIV strains (Mascola and Haynes, 2013). Moreover, they have been shown to be protective in non-human primate challenge models (Parren et al., 2001; Hessell et al., 2007; Hessell et al., 2009; Moldt et al., 2012; Lewis et al., 2017), thus furthermore fueling the need to understand the conserved sites they target within the Env protein.

1.5.1 bNAb targets on the HIV Envelope

The HIV-1 Env glycoprotein is the sole target of bNAb-mediated vaccine development and any neutralizing response (**Fig. 7**). It consists of three molecules of surface exposed subunit gp120 (which interacts with CD4, and the CCR5 or CXCR4 co-receptors), and three molecules of transmembrane gp41 protein. The gp120 contains variable regions (V1-V5), which play an important role in co-receptor tropism, virus sensitivity to antibody neutralization, pathogenesis and disease progression. The V1-V5 regions are joined by five conserved regions (C1-C5) (Pancera, et al., 2014). The Env protein is highly variable and surrounded by dense host-derived N-linked glycans that account for approximately half of the Env molecular mass (Behrens and Crispin, 2017). The virus uses this glycan shield to occlude important bNAb protein contacts (Pancera, et al., 2014). However, glycans are also important for neutralization for some bNAbs (Wagh et al., 2018).

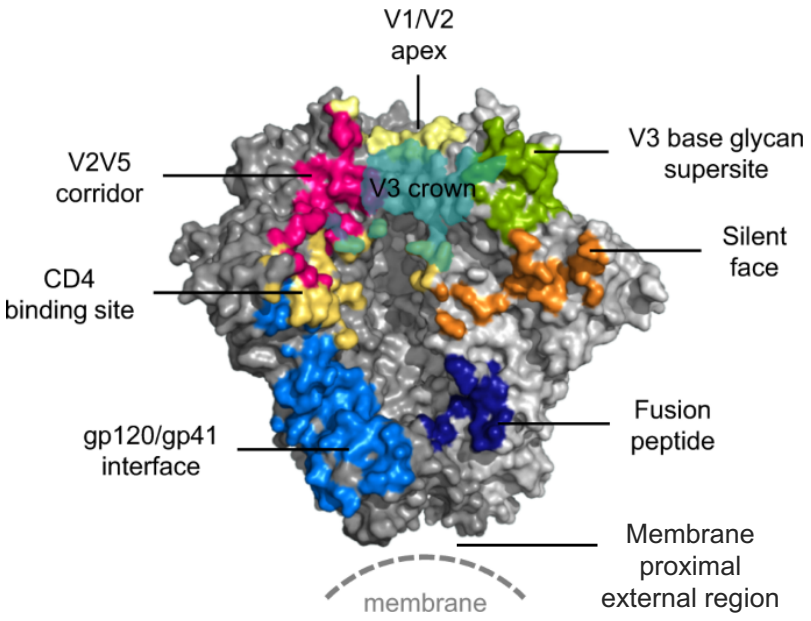

Figure 7: HIV-1 Env Trimer structure. Eight currently known bNAb epitopes are labelled and highlighted. Figure adapted from Chan et al., (2021)

To date, eight conserved bNAb epitopes have been identified on the HIV-1 Env trimer (**Fig. 7**). These include the silent face, the V3 crown epitopes, the V1/V2 site at the apex of the trimer, the V3-glycan/N332 supersite, the CD4 binding site (CD4bs), the membrane proximal external region (MPER), the gp120-gp41 interface epitope, and the fusion peptide (Blattner, et al., 2014; Huang, et al., 2014; Wibmer, et al., 2017; Kong, et al., 2016; Van Gils, et al., 2016; Zhou et al., 2018; Schoofs et al., 2019; Chan et al., 2021; Wibmer et al., 2015; Burton et al., 2016; Sok et al., 2018; Ward et al., 2017) V2/V5 corridor is also indicated.

1.5.2 Germline targeting vaccine strategy

The discovery of HIV-1 bNAbs and subsequent identification of conserved epitopes within the Env trimeric protein invigorated researchers with hope of identifying an immunogen capable of eliciting bNAb responses. However, several studies later proved that Env vaccinations failed to stimulate bNAb responses because they lacked affinity for naive bNAb precursors, thus, indicating that special immunogens with the ability to engage these rare naive bNAb precursors are needed (Xiao et al., 2009; Bonsignori et al., 2011; Hoot et al., 2013; McGuire et al., 2013; Jardine et al., 2013; Jardine et al., 2016). This realization led to the concept and strategy termed “Germline-targeting immunogen design”, in which the priming immunogen is engineered to bind single or diverse naive bNAb precursors within a bnAb class. Germline-targeting is based on selection of a transmitted/founder virus (T/F) or a specifically designed Env immunogens that can bind to the bNAb unmutated common ancestor (UCA) (Xiao et al., 2009; Haynes et al., 2012; Saunders et al., 2019; Steichen et al., 2019). Germline-targeting immunogens can be identified by *in-vitro* and by *in-silico* techniques (Haynes

et al., 2022). Identification of immunogens via *in-vitro* technique involves screening multiple Envs against the UCA and selecting Envs with high affinity to the UCA (Haynes at al., 2022). Inversely, identification of immunogens via *in-silico* technique involves using computationally inferred UCAs and T/Fs combined with mutation-guided modifications of the Env to enhance affinity for naive precursors (Haynes at al., 2022). Recently, using this strategy, a first-in-human proof-of-principle study successfully elicited VRC01 specific naive precursors thus fuelling encouragement to use this strategy for other bNAb epitopes (Leggat et al., 2022) (see section 1.3.8).

1.6 Ontogeny of bNAbs and the implications for vaccine discovery

Developmental pathways of bNAbs represent a roadmap to guide vaccine strategies. These studies link the development of bNAbs with the viral variants that engage the naïve B cell and elicit bNAb lineages (**Fig. 8**). HIV and antibody co-evolution studies have been performed in 13 infected donors. These studies include bNAb donors targeting four of the five currently known bNAb epitopes: V2 apex, V3 supersite, CD4bs and MPER epitopes (Moore et al., 2012; Liao et al., 2013; Doria-Rose et al., 2014; Bhiman et al., 2015; Wu et al., 2015; Van Gils et al., 2016; Landais and Moore, 2018). Altogether, these studies have indicated that strain-specific neutralizing antibodies (nAbs) developed breadth as a result of being exposed to different immunotypes (viral escape mutations within epitopes) and that antibody SHM enabled the immune system to adapt to the constantly evolving viral swarm (Moore et al., 2011; Moore et al., 2013; Murphy et al., 2013; Wibmer et al., 2013; Doria-Rose et al., 2014; Bhiman et al., 2015). Such studies inform lineage-specific vaccine strategies which aim to use sequential immunogens to program the antibody response of un-infected

individuals towards the development of antibodies with greater neutralization breadth (Escolano, Steichen, et al., 2016). To date, only one study looked at the ontogeny of interface-directed bNAb VRC34 (Shen et al., 2020). Thus, more studies are warranted to elucidate common signatures that favour the development of this class of bNAbs.

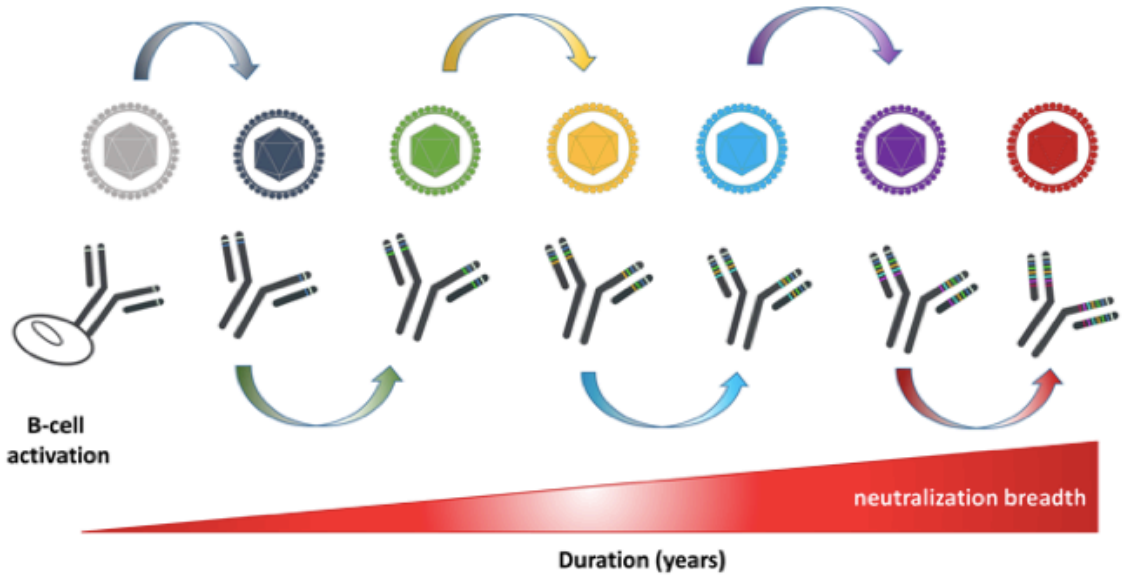

Figure 8: Virus-antibody coevolution and the development of bNAbs during HIV-1 infection. Virus-antibody coevolution is a dynamic process in which viruses and antibodies evolve in response to each other. This process occurs as viruses and antibodies adapt to each other over time, each developing new strategies to outcompete the other. When a virus infects a host, it activates a naive B cell which will in turn produce antibodies that recognize and neutralize the virus. However, viruses can evolve and mutate to evade recognition by these antibodies, leading to the development of new viral strains. In response, new antibodies that are specific to the new viral strain are produced. Over time, this coevolution can lead to the emergence of highly virulent and infectious strains of viruses. At the same time, the antibody can also evolve to become more efficient at recognizing and neutralizing diverse viruses, leading to the development of bNAbs. This process is approximately three years or more. Virus evolution is depicted by the coloured viral spheres, while antibody evolution and

maturation to becoming a bNAb is shown as grey antibodies with streaks of coloured lines symbolising mutations.

1.7 Technologies used to isolate anti-HIV-1 bNAbs

Currently there are a number of different technologies that are used to isolate and study bNAbs against HIV-1. Some of the most common and latest methods include: Hybridoma/B Cell immortalization, Phage Display and Yeast Display, B cell sorting, Cell-based assays & Single B cell sequencing (McCoy et al., 2017; Sun et al., 2018).

1.7.1 Hybridoma technology and B-cell immortalization

These are methods used to produce stable, long-term sources of specific antibodies. These techniques are often used to produce monoclonal antibodies, which are highly purified identical copies of a single type of antibody. The hybridoma technique was developed in the 1970s and involves fusing a B cell, which produces a specific antibody, with a cancer cell line that has the ability to divide indefinitely. This creates a hybrid cell, called a hybridoma, that can produce unlimited amounts of the specific antibody (Kohler et al., 1975; Sun et al., 2018). B-cell immortalization is a similar technique, in which B cells are transformed or manipulated in such a way that they can divide indefinitely, allowing for the continuous production of the specific antibody they produce (Straub et al., 1989; Sun et al., 2018). However, human B cells were shown to be difficult to immortalize via the hybridoma technique because human derived hybridoma cells react with self-antigens (Cafri et al 2013; Sun et al., 2018).

First generation bNAbs against HIV such as 2F5, 4E10, 2G12 were isolated using the hybridoma technique (Buchacher et al., 1994; McCoy et al., 2017).

1.7.2 Phage display

This is a technology that allows for the display of a large number of antibody library candidates on the surface of bacteriophage particles and exposing these to target antigen. Yeast Display, is a similar technology to phage display, but instead of bacteriophages, the antibody candidates are displayed on the surface of yeast cells (Falkowska et al., 2014; McCoy et al., 2017; Sun et al., 2018). This technique allows for antibodies to be presented in different forms as either single chain (ScFv) or Fab (Duarte et al., 2016; Sun et al., 2018). The underlying principle of the technique is the creation of recombinant antibody libraries by stochastically pairing antibody HCs and LCs V-region thus creating greater diversity of antibody pairs that can interact with a myriad of antigens (Graus et al., 1998; McCoy et al., 2017; Sun et al., 2018). Through this process it is possible to rapidly identify bNAbs that are specific to one of the eight currently identified bNAb epitopes on the HIV-1 Env. The HIV-1 bNAb b12 is considered as one of the potent neutralizing antibodies isolated by phage display technique. Generally, HIV-1 specific antibodies isolated by display techniques are less potent than those isolated by micro neutralization or single B cell sorting and cloning (Wu et al., 2009; Sun et al., 2018).

1.7.3 B cell Culture

B cell culture refers to the in vitro growth and proliferation of B cells. B cell culture has played an important role in the isolation of bNAbs by allowing for the selection and

expansion of B cells that produce specific bNAbs. The process of isolating bNAbs from B cell cultures typically involves the following steps: stimulation of B cells, screening of bNAb-producing B cells, expansion of bNAb-producing B cells, purification & characterization of bNAbs.

Initially, PBMCs from PLWH are collected and stimulated to promote antibody production in microwell plates. This is followed by screening individual wells supernatant for binding or neutralization activity. Wells that yield positive hits are then subjected to cell lysis, mRNA sequencing of the B cell, cloning of the HC and LCs, expressing and purifying the bNAb. The purified bNAbs are characterized to confirm their identity and determine their specificities, including the epitopes they recognize on the viral antigen and the viral strains they can neutralize. Currently, the bNAbs that have been isolated with this technique include: PG9, PG16, PGT145, CAP256.VRC26, CH01, PGT121, PGT128, PGT135, 10-1074, CH235, PGT151, 35022, 8ANC195 & 10E8. (McCoy et al., 2017).

1.7.4 Flow cytometry based single cell sorting and cloning

B cell sorting and FACS involves using antigen baits to isolate specific memory B cell populations and sorting them into a 96 well plate based on their surface markers. This in turn enables the sequencing of the original VH and VL gene pairs of the antibody from the individual memory B cell. These techniques allow for the rapid and efficient isolation of specific populations of B cells and the bNAbs produced by these cells.

The process of B cell sorting and FACS for bNAb isolation typically involves the following steps: Collection of PBMCs samples: PBMCs are collected from an individual

infected with HIV, and the B cells are exposed to fluorescently labelled antigenic bait leading to the identification of B cells that bind the antigen. The stained B cells are then sorted through FACS to sort the cells based on the fluorescence of the labelled B cells. The sorted bNAb-secreting B cells are then sequenced by reverse transcription PCR to amplify, clone and express the antibody genes (HC & LC). This is then followed by characterization of bNAbs to test for their ability to neutralize multiple strains of the virus. The bNAbs that have been isolated with this technique include: PGDM1400, 10-1074, VRC01, IOMA, CH103, 3BNC117, PGV04, 8ANC131, CH235, 8ANC195, ACS202 and N123-VRC34.01. (McCoy et al., 2017; Sun et al., 2018).

1. 8 Aims and Objectives

Currently there are limited ontogeny studies focusing specifically on the gp120-gp41 interface region (described in section 1.6). This makes it difficult to decipher common molecular signatures that favour the development of interface-directed bNAbs. This makes the design of lineage specific immunogens that will trigger the activation and maturation of interface directed bNAbs challenging. In this study, we aimed to close this gap in knowledge and investigated the development of a previously described interface-directed bNAb, CAP248-2B (Wibmer *et al.*, 2017)

Secondly, few studies have assessed the frequency of FP- and gp120-gp41 interface-directed responses or defined how quickly these responses emerge during infection. This is key information that will inform FP/interface vaccine development, especially given that the FP region is currently an attractive vaccine target with several promising animal proof-of-concept trials conducted to pave the way for human safety and efficacy trials (Huang et al., 2014; Landais et al., 2016; Ditse et al., 2019; Xu et al., 2018; Cheng et al., 2019; Kong et al., 2019; Mogus et al., 2020; Cheng et al., 2020; Chuang et al., 2020). Therefore, in this thesis we examined the prevalence and kinetics of FP/interface directed responses in an African clade C cohort of PLWH.

Lastly, the number of FP-directed bNAbs isolated thus far is limited (VRC34, ASC202, PGT151). The isolation of additional bNAbs to this epitope will allow for comparison of genetic signatures of such bNAbs, and enable the field to decipher common structure and biochemical features that will be valuable in the vaccine design for eliciting FP-specific responses. In this thesis we aimed to isolate and characterise additional FP-specific bNAbs and fill the defined gap in knowledge.

Chapter 2

Low Prevalence of Fusion Peptide directed antibodies in a large HIV-1 clade C infected cohort

Vincent N. Hlatshwayo[1,2], Mashudu Madzivhandila[1,2], Bronwen E. Lambson[1,2], Tandile Hermanus[1,2], Nigel J. Garrett[3], Quarraisha Abdool Karim[3,5], Salim S. Abdool Karim[3,4], Lynn Morris[1,2,3], Cathrine Scheepers[1,2], Penny L. Moore [1,2,3]

[1]Centre for HIV and STIs, National Institute for Communicable Diseases of the National Health Laboratory Service, Johannesburg 2131, South Africa. [2]SA MRC Antibody Immunity Research Unit, School of Pathology, University of the Witwatersrand, Johannesburg 2050, South Africa (AIRU). [3]Centre for the AIDS Programme of Research in South Africa (CAPRISA), KwaZulu-Natal 4013, South Africa. [4]Department of Epidemiology, Columbia University, New York, New York, USA. [5]Department of Epidemiology, Mailman School of Public Health, Columbia University, New York, NY USA

Abstract

A prophylactic HIV-1 vaccine will likely need to elicit bNAbs against conserved HIV-1 envelope epitopes. One bNAb epitope, the 8 amino acid FP, has become a focus of HIV vaccine strategies because of the isolation of FP-directed monoclonal bNAbs from chronically HIV-infected people, and promising preclinical immunogenicity animal studies. However, FP-specific bNAb vaccine strategies would benefit from understanding the population prevalence and maturation of FP-specific responses during HIV infection. Here, we assessed the prevalence of bNAbs in participants previously enrolled in the CAPRISA 004 Tenofovir gel trial (CAP004), by screening three-year plasma samples against a 44 cross-clade pseudovirus panel. We identified 8/68 (12%) of donors with bNAbs, and showed a correlation of bNAb development with low CD4 T-cell count and high viral load as previously reported. Next, we screened for FP-binding responses using three FP sequences, representative of 33% of global HIV envelope sequences. Of 68 donors tested, nine (13%) showed binding to one or more FPs at 3 years post-infection. FP-binders included donor CAP312, whose plasma bound all three peptides tested, and who exhibited 64% breadth at 3 years post-infection. Longitudinal binding studies showed that CAP312 FP-specific antibodies appeared at 35 weeks post-infection and paralleled the kinetics of neutralization breadth. Depletion of FP-specific antibodies resulted in 40-100% reduction in neutralization titers against heterologous viruses, confirming that CAP312 broad neutralization is mediated by FP-specific antibodies, which arise within a year of infection. Overall, these results show that FP-directed mAbs are infrequently elicited in clade C infection. In some cases, however, these may be elicited early in infection and mature to acquire breadth. Future studies should aim to explore the determinants of strain-specific versus broadly neutralizing FP-directed antibodies.

Introduction

A successful HIV-1 vaccine will need to elicit bNAbs targeting conserved epitopes within the HIV-1 envelope (Env) (Shingai et al., 2014; Corey et al., 2021 and Walker et al., 2021). However, to date, no vaccine strategy has achieved this goal. Several reasons have been proposed for this, including the complex nature and composition of the HIV-1 Env. The HIV-1 Env trimer is highly sequence variable and heavily glycosylated resulting in occlusion of underlying epitopes which form part of bNAb epitopes (Zhu et al., 2003; Behrens et al., 2016; Ward et al., 2015). Envs are conformationally dynamic, sparsely arranged on the virions either as functional or non-functional gp41 stumps (Moore et al., 2006). Despite this, eight bNAb epitope targets have been identified and form the basis of vaccine discovery efforts. These include the V2 apex, V3-glycan site, V3 crown, CD4bs, MPER, Silent face and gp120-gp41 interface, which includes the most recently identified viral epitope, the FP (Sok and Burton, 2018).

The FP is part of the gp120-gp41 interface region and is a critical element of the HIV-1 entry machinery (Blumental et al., 2012; Harrison et al., 2015). The gp41 transmembrane N-terminus FP comprises nine amino acids forming a hydrophobic region (residues 512–527) (Guttman et al., 2014; Kong et al., 2016). Most of the FP is occluded in the prefusion conformation of Env, and only exposed when HIV interacts with the target host cell during the fusion process when gp41 forms an extended structure called the ‘pre-hairpin’ intermediate (Harrison et al., 2008; Wyatt et al., 1998; Pierson and Doms et al., 2003).

The FP gained particular attention as a vaccine target because of the isolation of FP-directed bNAbs from chronically infected donors. These include N123-VRC34.01 which has 68% breadth, ACS202 (45% breadth) & PGT151 (73% breadth) (Kong et al., 2016; van Gils et al., 2016; Falkowska et al., 2014). This showed that it was possible to elicit broad responses to a site deeply buried in the HIV-1 Env which was previously not thought to be an bNAb epitope. The fact that these isolated bNAbs encompass a short linear nine amino acid FP target makes this peptide an appealing vaccine target (Kong et al., 2016; van Gils et al., 2016; Falkowska et al., 2014; Lee and Crotty 2021). Lastly, animal proof-of concept studies have shown that it is possible to elicit FP-specific Abs within 6 months, and that these had some cross reactivity against tier 2 viruses (Xu et al., 2018; Cheng et al., 2019; Kong et al., 2019; Mogus et al., 2020; Cheng et al., 2020; Chuang et al., 2020).

The success of an FP-vaccine in eliciting bNAbs in humans will depend on understanding these responses during infection. Several studies have assessed the prevalence of V2 apex, CD4bs, V3 glycan, MPER and gp120-gp41 interface responses (Binley et al., 2004; Walker et al., 2011; Gray et al., 2007; Zhou et al., 2015; Landais et al., 2016). However, very few studies have specifically assessed the prevalence of FP-specific responses in chronically infected human donor cohorts (Huang et al., 2014; Landais et al., 2016; Ditse et al., 2019).

In this study we have explored an HIV-1 subtype-C infected cohort, referred to as CAPRISA 004 Tenofovir gel trial (CAP004), and assessed the prevalence of bNAbs and clinical drivers of breadth. Secondly, we assessed the prevalence of FP-directed

antibodies in this cohort, and examined whether the presence of these antibodies was associated with breadth. Lastly, we defined the developmental kinetics of FP-directed responses in a broad neutralizer, CAP312. We show that FP-directed antibody responses are infrequent, and that their development is not associated with breadth. However, in one participant, CAP312, we show that FP-specific antibodies, which account for heterologous neutralization, develop within the first year of infection, suggesting that once triggered, such antibodies can rapidly mature towards breadth.

Methods

Study Samples

Plasma samples were collected at regular intervals from women who became infected with HIV-1 during the CAP004 trial. The CAP004 trial was a double-blinded, randomized controlled trial that assessed the effectiveness and safety of 1% vaginal gel formulation of Tenofovir in sexually active, HIV-1 negative women between the ages of 18-40 (Abdool Karim et al, 2010). The trial took place at urban and rural sites in Kwazulu-Natal, South Africa between May 2007 and March 2010, and the design and the results from the trial are detailed elsewhere (Abdool Karim, 2010).

Ethics approval

The CAP004 trial study/trial (NCT00441298) was approved by the ethics committees of the University of KwaZulu-Natal's Biomedical Research Ethics Committee (E111/06), Family Health International's Protection of Human Subjects Committee (#9946) and the South African Medicines Control Council (#20060835), and the University of the Witwatersrand (M190251 MED19-02-067). Donor CAP312 provided written consent for her samples to be used for further studies.

Cell Lines

HEK293T and TZM-bl cells were grown and maintained in Dulbecco's modified Eagle's medium (DMEM) (Gibco, USA) supplemented with 10% FBS (foetal bovine serum) (HyClone, USA), 0.05 mg/ml gentamicin antibiotic (Sigma Aldrich, USA) and 0.025% HEPES buffer (Gibco, USA). Cells were maintained at 37°C in a 5% CO_2

humidified incubator and sub-cultured when near confluency. Cell monolayers were disrupted by treatment with 0.25% trypsin in 1 mM EDTA every 48–72 hours.

HEK293F suspension cells, used for antibody production, were grown and maintained in 293-Freestyle media (Gibco BRL Life Technologies) at 37°C, 10% CO_2, 125 RPM and routinely sub-cultured when near-confluency.

TZM-bl cells (JC53-bl (clone 13)) were obtained from the AIDS Reagent Program and used for the neutralization assays (Montefiori, 2005). 293T cells used for transfection were obtained from George Shaw (University of Alabama, Birmingham, AL) and David Montefiori (Duke University School of Medicine, Durham, NC).

Pseudovirus production

HEK293T cells were co-transfected with an equal amount (4µg) of the cloned virus Env plasmids (mutants or wild type) and HIV backbone vector pSG3Δenv, which encodes the whole HIV genome but contains two stop codons in the env gene. Transfection of the envelope plasmids into HEK293T cells was facilitated by PEI max transfection reagent (1 mg/ml) (Polysciences). Virus-containing supernatants were harvested at 48 hours post transfection, filter sterilised, and stored at -80°C. Viral titers were determined in TZM-bl cells by expression of firefly luciferase, expressed as relative lights unit (RLU), evaluated with the Bright-Glo luciferase assay substrate (Promega, Fitchburg, WI, USA).

Env-pseudotyped neutralization assay

Neutralization was measured as a reduction in luciferase gene expression after a single round of infection of TZM-bl cells with Env-pseudotyped viruses. Titers were calculated as the inhibitor concentrations (IC_{50}) or reciprocal plasma/serum dilutions

(ID_{50}) causing a 50% reduction of relative light units (Montefiori DC. 2005). Plasma samples were screened using the TZM-bl neutralization assay against 44 different viruses. These included 6 clade A, 12 clade B, and 26 clade C envelope-pseudoviruses. The 44-virus panel is made up of 42 viruses from the different clades all isolated during acute phase infection and 2 reference control viruses Du151.12 and ConC (Blish et al., 2007; Li et al., 2005; Li et al., 2007 and Gray et al., 2007). For mapping purposes, we used an 18-viruses panel that is composed of 6 of each clade viruses (clade C: Du156.12, Du172.17, CAP45.G3, CAP239.G3, ZM197M.PB7, ZM214M.PL15; clade B: 6535.3, TRO.11, AC10.0.29, QH0692.42, PVO.4, WITO.4160 and clade A: Q23.17, Q259.d2.17, Q168.a2, Q842.d12, Q769.d22, Q461.e2). Samples were scored as positive if a virus was neutralised at titers above 1:100. Below this cut-off of 100, we observed background interference. Percent breadth was calculated based on the number of viruses that each plasma sample neutralised out of a panel of 44 viruses.

Global FP diversity and prevalence analysis

We first assessed global sequence diversity within FP sequences to maximise coverage as far as possible through combinations of peptides. We analysed 5,152 HIV-1 viral FP sequences from the Los Alamos National Laboratory (LANL) database (https://www.hiv.lanl.gov/content/sequence/ANALYZEALIGN/analyze_align.html), including all group M HIV-1 subtypes. Duplicates were removed and the prevalence of each motif calculated.

Fusion Peptide specific ELISA

We selected the three most prevalent FP sequences globally (FP8_v1, FP8_v2 and FP8_v5) (Cheng et al., 2019) and added the rare FP8_v1-514b_T peptide shown to knock-out N123-VRC34 activity to screen for FP directed responses in our CAP004 cohort using samples from 3 years post-infection. Peptides were synthesised by GenScript (Piscataway, New Jersey, United States). Lyophilised peptides were initially dissolved in 70% DMSO (Sigma-Aldrich, St. Louis, Missouri, United States) and stored at -20ºC. Fusion peptides (FP8_v1 (AVGIGAVF), FP8_v2 (AVGLGAVF), FP8_v5 (AVGIGAMI) and FP8_v1-514b_T (AVGTIGAVF)) proteins were coated at 4 µg/ml onto 96-well, high-binding plates and incubated for 1 hour at 4°C. The plates were then washed and incubated at 37°C for 1 hour in a blocking buffer (5% skimmed milk powder, 0.05% Tween 20, 1× PBS). Three years post-infection plasma samples were added at 1:100 dilution and serially diluted threefold in the blocking buffer. Following a 1-hour incubation at 37°C, plates were washed and an anti-human horseradish peroxidase-conjugated antibody was added and plates incubated for 1 hour at 37°C. The signal was developed with TMB substrate (Thermo Fisher Scientific) for 5 min at room temperature, followed by addition of 1 M H_2SO_4 stop solution. Absorbance was measured at 450 nm wavelength and data was plotted using GraphPad v9.

Adsorption of FP-specific antibodies from plasma

Fusion Peptide antibodies were depleted from the CAP312 3 years plasma sample using linear Fusion Peptides (FP8_v1: AVGIGAVF) covalently coupled to DB Myone Streptavidin C1 magnetic beads (Thermo Fisher Scientific). Briefly, positive control mAB VRC34 (50 µg/ml), negative control mAB CAP256.26 (50 µg/ml) and the 3 years plasma sample was diluted 1:20 then incubated with the FP-coupled beads and

uncoupled beads for 1 hour initially at 37^{o}C in a disk rotating shaker. After an hour, a magnetic tray was used to pellet-out the FP-coupled beads with FP-specific mAbs bound to this complex. This reaction was repeated for a second time to remove residual FP-specific mAbs that might have not been depleted in the first round. Following the second depletion and pelleting, samples were assessed in ELISAs (conditions similar to above) to confirm depletion of FP-specific antibodies and in the TZM-bl neutralization assay against HIV-1 to measure residual activity and contribution of FP-specific antibodies in neutralization activity. For the neutralization assay, the starting concentration of the sample was “neat” and serially diluted. Four heterologous pseudoviruses: CAP45, Du156, Du172 and ZM249 were tested and data plotted using GraphPad prism v9.

Results

Identification of participants with broad neutralizing antibodies in the CAP004 cohort

We first assessed the development of neutralization breadth in HIV-infected participants who were enrolled in the CAP004 trial. This cohort predominantly includes participants from the placebo arm (50/68) compared to the Tenofovir arm (18/68, labels shown in bold in **Fig. 1**) because of the reduced probability of breakthrough infections in the Tenofovir arm (Abdool et al., 2010). We screened plasma samples from three years post-infection against a 44 cross-clade pseudovirus panel (comprising 6 clade A, 12 clade B and 26 clade C pseudoviruses). On the basis of percentage breadth at three years post-infection, donors were stratified into three groups: broad neutralizers (which we define as neutralizing >40% of heterologous viruses), intermediate neutralizers (neutralizing 11-39% of viruses) and those with little to no neutralization breadth (<10% of viruses) (**Fig. 1A**). Only 8/68 (12%) individuals developed broadly neutralizing antibodies, 35/68 (51%) were defined as intermediate neutralizers, and 25/68 (37%) participants did not develop breadth. In our previous study (Gray et al., 2011), we showed bNAb responses in 17% (8/48) of participants in the CAPRISA 002 cohort (CAP002) from the same geographical location. Thus, bNAb responses in the CAP004 trial were slightly lower than those observed within the CAP002 cohort, though these differences were not statistically significant (**Fig. 1B**) (Gray et al., 2011)

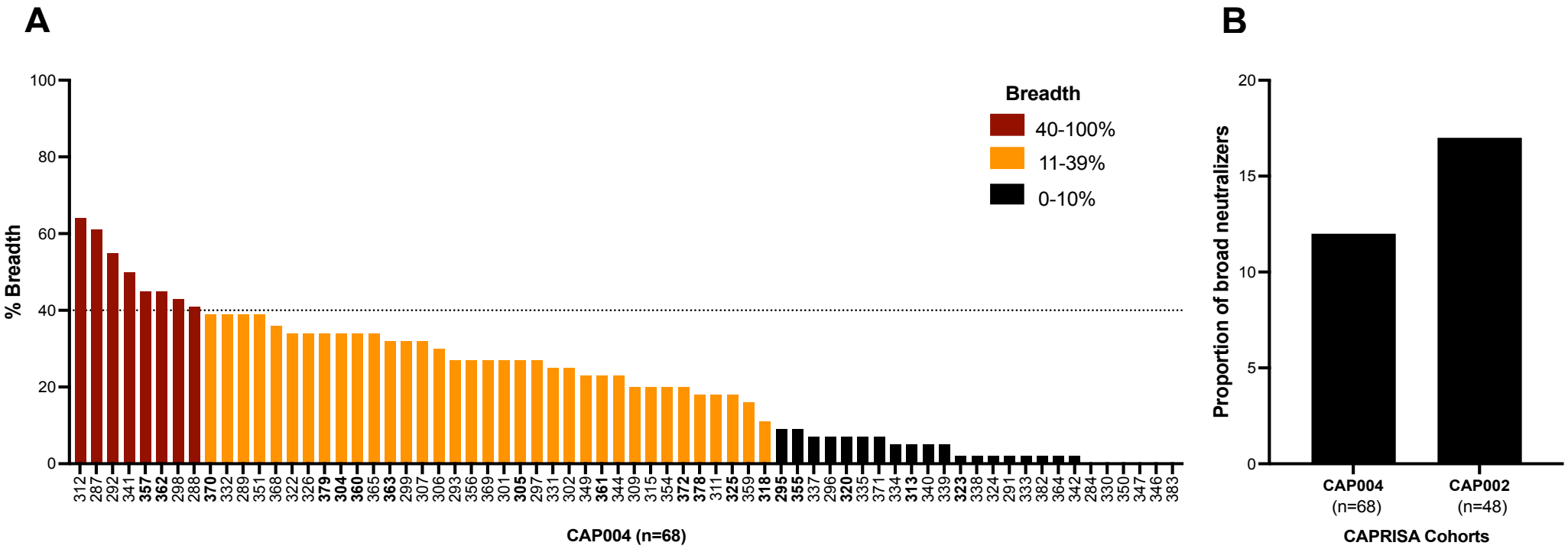

Figure 1: Neutralization breadth of CAP004 participants at 3 years post-infection. A) Participants were categorised into three groups based on the percentage of heterologous viruses neutralised: broad neutralizers 40-100% are shown in red, intermediate neutralizers 11-39% in orange and little to no breadth <10% in black. Participants who were in the Tenofovir arm of the CAP004 phase IIB trial are highlighted in bold (x-axis). B) Comparison of the proportion of broadly neutralizing CAP004 and CAP002 participants at three years post-infection.

Low CD4 and high viral load early in infection are associated with development of breadth in the CAP004 cohort

Clinical factors that have been shown to contribute to the development of broadly neutralizing antibody responses in varying cohorts include high viral load (VL) and low CD4+ T cell counts (Gray et al., 2011; Landais et al., 2016; Piantadosi et al., 2009; Sather et al., 2010). Here we assessed the correlation between breadth, VL and CD4 count at three timepoints (6 months, 12 months and 36 months post-infection) (**Fig. 2A-F**).

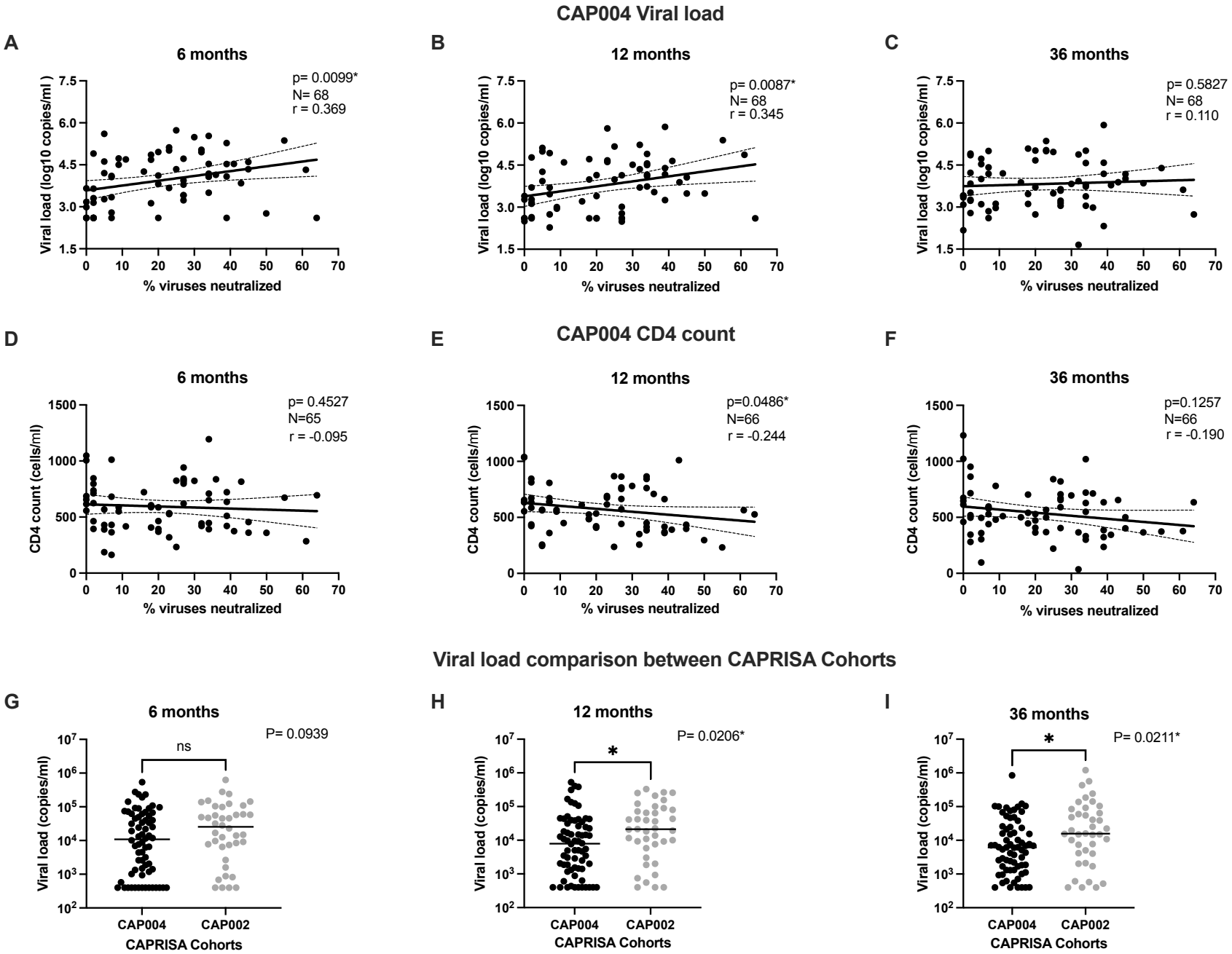
CAP004 Viral load
A
6 months
p= 0.0099*
N= 68
r = 0.369
Viral load (log10 copies/ml)
% viruses neutralized
B
12 months
p= 0.0087*
N= 68
r = 0.345
C
36 months
p= 0.5827
N= 68
r = 0.110
D
6 months
p= 0.4527
N=65
r = -0.095
CD4 count (cells/ml)
E
CAP004 CD4 count
12 months
p=0.0486*
N=66
r = -0.244
F
36 months
p=0.1257
N=66
r = -0.190
Viral load comparison between CAPRISA Cohorts
G
6 months
ns
P= 0.0939
Viral load (copies/ml)
CAP004
CAP002
CAPRISA Cohorts
H
12 months
*
P= 0.0206*
I
36 months
*
P= 0.0211*

Figure 2: Clinical factors associated with the development of broadly neutralizing antibodies in the CAP004 cohort. Correlation of breadth and viral loads (VL) (A, B, and C) and CD4+ T cell counts (D, E, and F) at 6, 12, and 36 months post-infection. VL comparisons between CAP002 and CAP004 at 6, 12, and 36 months post-infection (G, H and I). Correlations were analysed using a nonparametric Spearman's test. Trend lines with 95% confidence intervals were generated using linear regression to visualise correlations. The number of pairs (N) and P value for each correlation are shown. Statistically significant P values are marked with asterisks and non-significant values are indicated as “ns”.

We observed a significant positive correlation (p=0.0099, p=0.0087) between neutralization breadth and viral load at 6 and 12 months respectively, though correlation scores were poor: r=0.369 and r=0.345 respectively (**Fig. 2A** & **B**). No significant correlation (p=0.5872 [r=0.110]) was observed between breadth and VL at 36 months post-infection (**Fig. 2C**). A significant negative correlation (p=0.0486 [r=-0.244]) was observed between breadth and CD4 T cell count at 12 months post-infection, but not at 6 and 36 months (**Fig. 2C** & **F**). These correlations are fairly similar to those previously reported in the CAP002 cohort (Gray et al., 2011). As the percentage of broad neutralizers in CAP004 was slightly lower than in CAP002, we compared viral loads in the two cohorts at 6, 12 and 36 months (**Fig. 2G-I**). Significantly lower VLs were seen in the CAP004 cohort at 12 and 36 months post-infection (**Fig. 2H** and **I**), perhaps contributing to the slightly lower proportion of bNAb donors in this cohort.

Low prevalence of FP responses in subtype CAP004 cohort

Next, we measured the frequency of FP-directed antibody responses in the CAP004 cohort. To do this, we first assessed global sequence diversity within FP sequences to maximise coverage as far as possible through combinations of peptides. Analysis of 5,152 HIV-1 viral FP sequences from the LANL database showed that FP8_v1, FP8_v2 and FP8_v5 account for 33% of global FP sequences (**Fig. 3A**, highlighted and sequence shown). This is consistent with a report by Cheng et al., 2019 which showed that these FP-sequences are common in a 208 multi-clade virus panel (Seaman et al., 2010). We therefore used these three peptides to screen three-year plasma samples from 68 participants for FP-directed antibody responses (**Fig. 3B**). Overall, only 9/68 (13%) individuals had FP-directed antibody binding responses against any of the three peptides tested (**Fig. 3B**). Eight donors had responses specific only towards FP8_v1, four bound only FP8_v2 and two had activity only against FP8_v5 (**Fig. 3C**) suggesting that FP responses can be highly strain-specific. However, in some donors, cross-reactive binding was observed, with five donors binding at least two peptides, and one donor, CAP312, binding to all three peptides (**Fig. 3C**). Interestingly, CAP312, as seen in **Fig. 1A**, is a broad neutralizer with percentage breadth of 64% a 44 cross-clade pseudovirus panel.

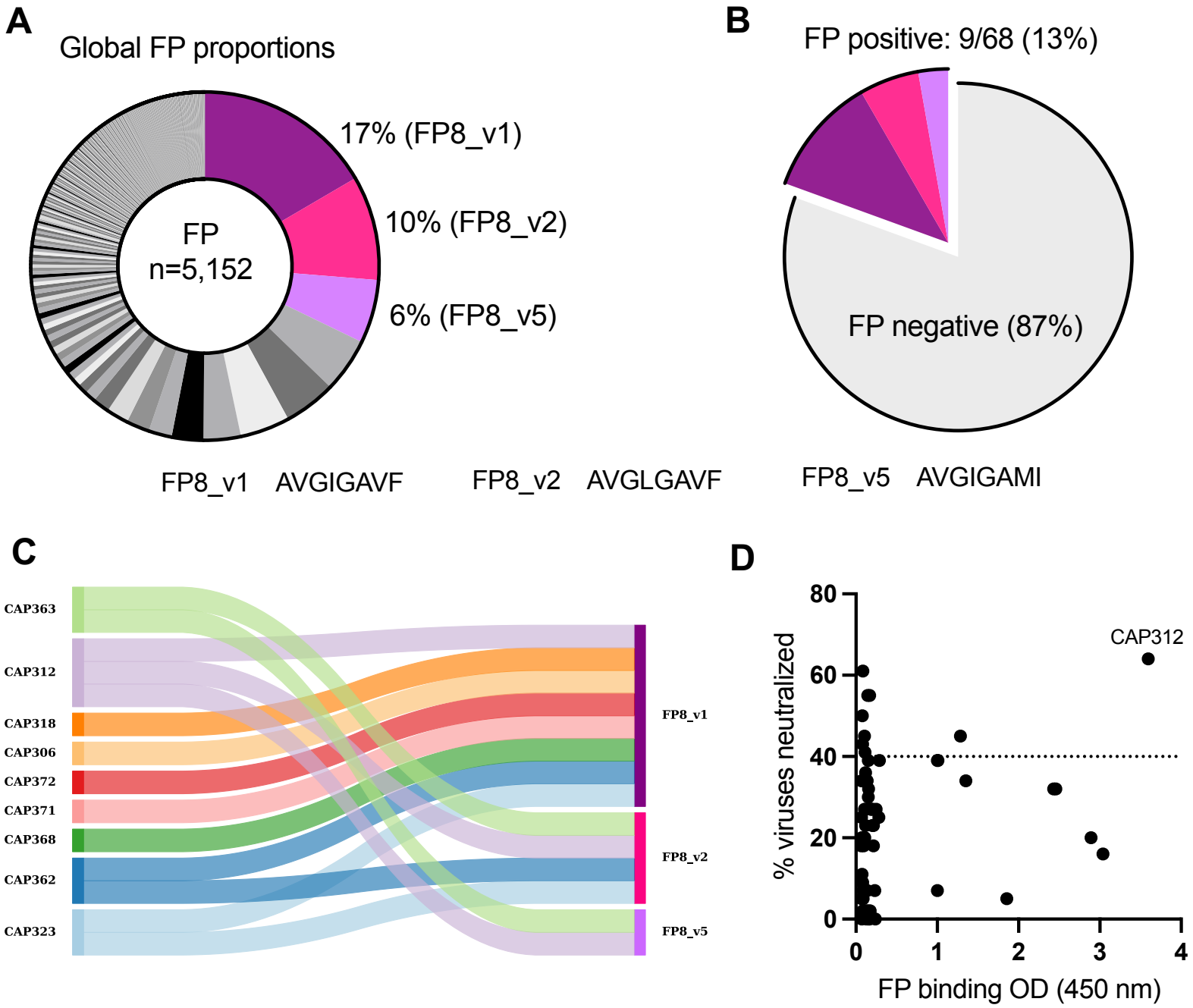
A
Global FP proportions
17% (FP8_v1)
10% (FP8_v2)
6% (FP8_v5)
FP
n=5,152
FP8_v1 AVGIGAVF
FP8_v2 AVGLGAVF
FP8_v5 AVGIGAMI
B
FP positive: 9/68 (13%)
FP negative (87%)
C
CAP363
CAP312
CAP318
CAP306
CAP372
CAP371
CAP368
CAP362
CAP323
FP8_v1
FP8_v2
FP8_v5
D
% viruses neutralized
FP binding OD (450 nm)
CAP312
0
20
40
60
80
0
1
2
3
4

Figure 3: Prevalence of FP directed antibody responses in subtype C cohorts. A) Global prevalence of the FP sequence motifs shown as a percentage. 5,152 viral FP sequences obtained from the LANL database, including all group M HIV-1 subtypes. Pink and purple shades indicate the three most prevalent sequences (FP8_v1, FP8_v2 and FP8_v5), and their respective sequence motifs are indicated below the plots. B) Prevalence of FP-binding responses in the CAP004 cohort. C) Sankey diagram showing overlapping binding profiles for nine participants with anti-FP antibody responses. Donor CAP312 which binds all three peptides is indicated D) Association between neutralization breadth and ELISA binding by CAP004 participants. Broadly neutralizing donor CAP312 with strong binding to FP is highlighted.

We next looked at the association between FP responses and breadth, to ascertain if FP responses were enriched in broad neutralizers (**Fig. 3D**). We observed no enrichment of FP-directed responses in broad neutralizers. Only two broad neutralizers developed FP specific responses, namely CAP312 and CAP362 with 64% and 45% breadth, respectively. Five participants with intermediate neutralizing profiles had FP-directed antibody responses. Furthermore, two donors with <10% breadth had FP-directed antibodies responses (**Fig. 3D**). Overall, therefore, FP-specific responses appear to develop infrequently in infection, and do not appear to be enriched in broad neutralizers.

Broad FP-specific responses develop within 1 year post-infection in donor CAP312

We next focused on the broad neutralizer CAP312, and assessed the kinetics of the FP-specific antibody response. To achieve this, we performed longitudinal FP binding

ELISAs and neutralization assays. We utilised a smaller panel of 13 pseudoviruses, all of which were known to be sensitive to the three-year plasma, and which included 11 clade C, and one each of clade B and A, to assess the maturation of heterologous cross-neutralization.

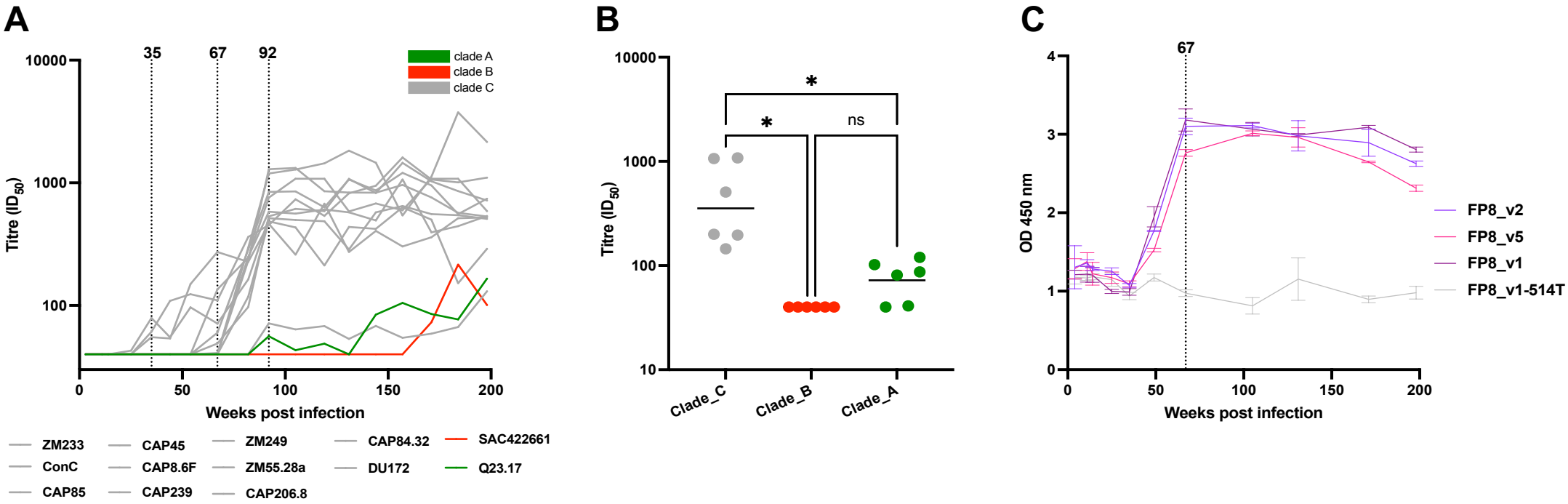
A
35
67
92
clade A
clade B
clade C
10000
1000
100
Titre (ID50)
0
50
100
150
200
Weeks post infection
ZM233
ConC
CAP85
CAP45
CAP8.6F
CAP239
ZM249
ZM55.28a
CAP206.8
CAP84.32
DU172
SAC422661
Q23.17
B
10000
1000
100
10
Titre (ID50)
*
*
ns
Clade_C
Clade_B
Clade_A
C
67
4
3
2
1
0
OD 450 nm
0
50
100
150
200
Weeks post infection
FP8_v2
FP8_v5
FP8_v1
FP8_v1-514T

Figure 4: CAP312 FP and neutralization breadth kinetics. A) Longitudinal neutralization breadth development for CAP312 against sensitive 13 cross-clade pseudovirus panel. Initial neutralization responses are indicated by a vertical line at 35 wpi, with additional responses developing at 67 wpi, for clade C and 92 wpi for clade A. B) CAP312 significantly neutralizes clade C and A but not B. C) Longitudinal binding to three different Fusion Peptides and the negative control FP8_v1-514T by CAP312 longitudinal plasma samples. One-way Anova was used for statistical analysis, ns = non-significant, significance is indicated with an asterisk (*)

Neutralization breadth in donor CAP312 developed gradually, starting around 35 wpi, where neutralization of clade C viruses CAP85, ConC and ZM233 was detected (**Fig. 4A**). Additional neutralization of clade C viruses CAP45, CAP206, ZM255.28a, Du172 is seen around 67 wpi. Peak neutralization against 10 clade C viruses is observed at 92 wpi. Neutralization activity against clade A and B viruses emerged later, with neutralization of Q23 appearing from 92 wpi and neutralization of SAC422661 appearing post 150 wpi (**Fig. 4A**, orange and green graphs against the 13 virus panel). Overall, CAP312 preferentially neutralised clade C viruses in the first two years post infection (~104 weeks post infection) and cross-clade neutralization is only seen after this time frame. This preferential early neutralization of clade C viruses was maintained at three years post infection, as shown by the geometric mean ID_{50} titres for clade C being 354 compared to 72 and 40 for clade A & B respectively (**Fig. 4B**).

FP binding against the three FPs (FP8_v1, FP8_v2 and FP8_v5) initially appeared around 49 wpi and gradually increased, peaking at 67 wpi then plateaued during the course of three years (**Fig. 4C**). Interestingly, peak FP binding coincided with increased neutralization breadth (**Fig. 4A** & **C**). Consistently, neutralization breadth

maturation paralleled longitudinal FP binding (**Fig. 4A** & **C**), suggesting that FP-specific antibodies drive heterologous neutralization. CAP312 plasma failed to bind to the negative control FP8_v1_514b_T which has a single point mutation G514T (**Fig. 4C**), suggesting that the CAP312 Abs have a similar profile to the isolated FP-specific mAb VRC34.01, which also shows no binding of FP8_v1_514T (Kong et al., 2016). Altogether, FP-binding and broad neutralization response in donor CAP312 appeared within one year post-infection.

Neutralization breadth is mediated by FP-specific antibodies

To assess whether neutralization breadth observed for donor CAP312 was due to FP-specific Abs, we depleted these from three-year plasma using FP8_v1, and tested adsorbed plasma in ELISA and neutralization assays (**Fig.5A** and **5B**). Removal of FP-specific Abs in the plasma sample resulted in binding reduction by 11.7 fold (**Fig. 5A**), similar to the positive control, mAb VRC34 (which indicates that we have successfully depleted FP-specific Abs in these samples). Neutralization activity against four heterologous viruses sensitive to CAP312 plasma, decreased by approximately 34 - 89 fold or resulting in a complete knock-out (K/O) following depletion (**Fig. 5B**), confirming that CAP312 FP binding antibodies mediate neutralization breadth.

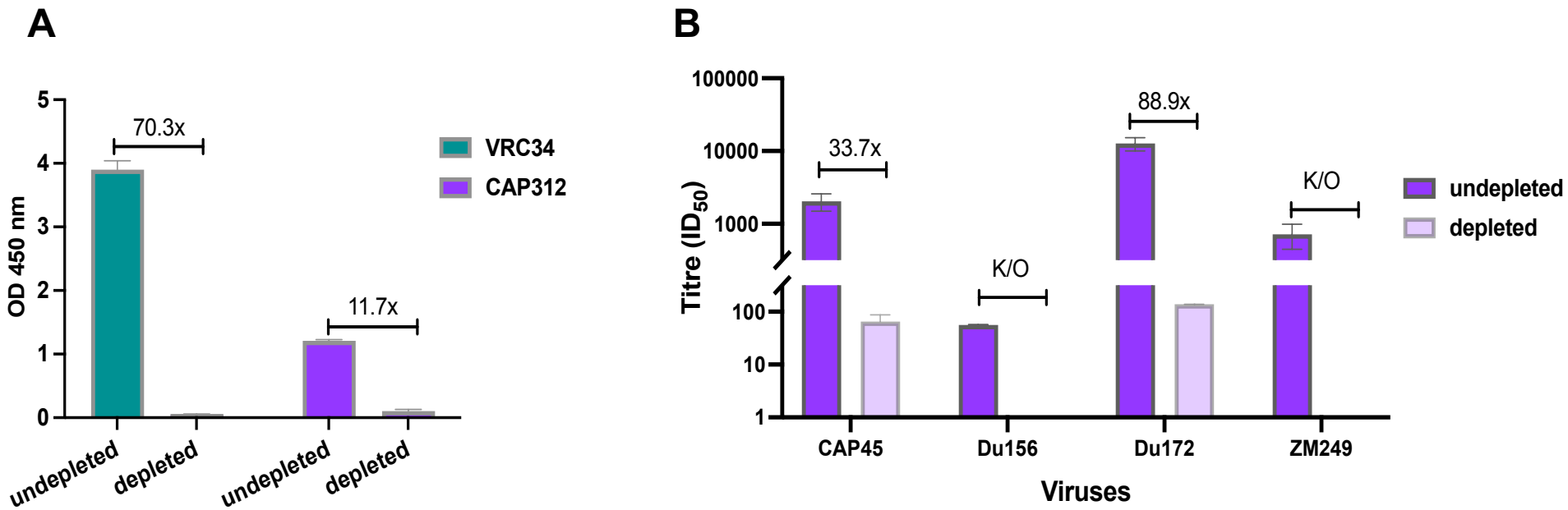

Figure 5: CAP312 plasma heterologous neutralization is mediated by FP-specific antibodies. A) VRC34 and CAP312 depletion control experiment showing successful FP-specific mAb depletion. CAP312 plasma FP binding following depletion of FP-specific antibodies was reduced. B) Heterologous neutralization profile of CAP312 3 years plasma sample following depletion of FP-specific antibodies. Fold changes are indicated for both panel A and B. K/O = knock-out. VRC34 was used as an assay-positive control.

Discussion

The identification of the eight amino acid long N-terminus FP region as a bNAb epitope and the subsequent isolation of FP-directed bNAbs has expanded the option of epitopes of interest for vaccine design against HIV-1. Here, we screened a clade C infected cohort for the development of broadly neutralizing antibodies, and then specifically screened for the prevalence of FP-directed antibodies. We show that in this cohort the prevalence of FP-directed antibodies was low, and that these antibodies were not especially enriched in donors who developed broadly neutralizing antibodies. However, in one donor, CAP312, with 64% breadth, we observed high level binding to multiple FP antigens that emerged early in infection, and which mediated heterologous neutralization.

Although many cohorts have been screened for the development of breadth, prospectively enrolled ART-naive donors are increasingly rare in the era of enhanced access to antiretroviral therapy. The CAP004 cohort was enrolled in 2007 and includes longitudinal stored samples that can be leveraged for studies to define how bNAbs mature. In this cohort of 68 subjects, we identified eight (12%) participants with breadth at three years post-infection, which is slightly lower than the levels of breadth observed in many other cohorts (Doria-Rose et al., 2009; Euler et al., 2012; Gray et al., 2007; Piantadosi et al., 2009; Sather et al., 2009; van Gils et al., 2010; Mikell et al., 2011; Gray et al., 2011; Landais et al., 2016). This is likely due to lower VLs in the CAP004 cohort compared to the CAP002 cohort (which we have previously described, and which were enrolled in the same geographic region), as high VL is a crucial driver of bNAb development (Moore et al., 2015; Moore and Landais 2018; Sather et al., 2009;

Gray et al., 2011; Landais et al., 2016; Rusert et., 2016). We speculated that the lower VL we observed in the CAP004 cohort may be due to Tenofovir exposure, however, comparison of the VLs between the placebo and Tenofovir arms of the CAP004 trial at three years post-infection showed no significant difference (data not shown). Furthermore, we note that the majority of participants in the CAP004 infection cohort were from the placebo arm of the trial, and so would not have been exposed to Tenofovir (**Fig. 1A**). The reasons underlying the lower VL observed in CAP004 remain unclear.

FP-based vaccine strategies are based on the notion that such responses can be widely triggered in vaccinated subjects, however the prevalence of FP-responses in population studies of people living with HIV (PLWH) is unclear. Our study shows that only 13% of donors mounted FP-specific responses. FP-directed responses may be expected to be rare as the FP is relatively inaccessible (Kong et al., 2016; Harrison et al., 2008; Wyatt et al., 1998). Most of the FP is occluded in the prefusion conformation of Env. This region is only easily accessible when HIV interacts with the target host cell during the fusion process (Harrison et al., 2008; Wyatt et al., 1998), which may limit the accessibility of this epitope to the immune system.

However, the low prevalence of FP-responses in our study may also be a consequence of the experimental methodology. Our study may underestimate the prevalence of FP responses because this region is highly variable. It is possible that the use of only three peptides limited our ability to detect strain-specific FP-directed responses to other less prevalent FP sequences. Future studies using a larger panel

of varying peptides, including those matched to the infecting virus, would be valuable in deciphering how common strain-specific FP-directed responses are. However, even if such strain-specific responses are more prevalent, their use for vaccine design is questionable. Our screening with only three FPs may have preferentially detected participants with more cross-reactive response. Indeed, of the nine FP-responders we identified, four bound to more than one of the three peptides we screened with.

Lastly, using biotinylated FP in ELISA might underestimate the frequency of FP-directed responses. This approach constrains the FP in one particular conformation which might not be favourable for FP-directed nAbs recognising a different orientation. A recent study by (Yuan et al., 2019) showed that the FP exists in several different orientations and bNAbs isolated thus far can bind to the FP in different angles of approach.

We note that these data differ from our previous work in a paediatric cohort (Ditse et al., 2018) where we screened 16 paediatric participants by ELISA against FP8_v1 and observed FP binding prevalence of 69% (11/16). Furthermore, these paediatric samples were tested for neutralization against viruses having single point mutations at the FP region, showing a prevalence of FP-directed neutralizing responses of 44% (7/16). However, adult and paediatric cohorts may have different neutralization profiles. Paediatric donors have been shown to develop accelerated bNAb responses during HIV infection, and isolated bNAbs from paediatric donors have low levels of SHM compared to bNAbs from adult donors (Ng et al., 2010; Goo et al., 2014; Simonich et al., 2016; Lucier et al., 2021). Furthermore, chronically infected children

have different clinical HIV phenotypes of high viral loads but normal CD4 counts, which might skew antibody specificities and frequencies (Muenchhoff et al., 2016).

Within a single donor, CAP312, we also defined the kinetics of FP-directed bNAbs and showed that these emerged within a year of infection. Although bNAbs generally take many years to develop (Gray et al., 2011; Doria-Rose et al., 2010; Landais et al., 2016), several case studies have described more rapid development of bNAbs. For example, (Sather et al., 2014) showed that MPER-directed mAb neutralizing antibodies developed in two donors within a period of a year. Furthermore, (Moore et al., 2011) described serum neutralization breadth in donor CAP256, mediated by V2-directed bNAbs, within a year. The rapid emergence of FP-directed bNAbs in CAP312 is encouraging from a vaccine perspective. However, it is not known whether this rapid emergence of breadth is a common trend among participants with FP-directed bNAb responses.

In our cohort of 68 participants, FP-directed antibodies were not significantly enriched in participants with breadth. Future studies of larger cohorts will be valuable in ascertaining whether FP responses are associated with bNAbs. Furthermore, the differences between FP-directed antibodies with breadth compared to those that are strain-specific warrants further studies. In ongoing work, we aim to isolate and compare FP-directed mAbs both from strain-specific donors and from donors with cross-reactive FP-specific responses. Lastly, antibody ontogeny studies and virological studies should compare the broad FP donor identified here (CAP312) with donors who have strain specific FP responses. These studies will provide valuable

information about the key events that differentiates the development of the broadly neutralizing lineage compared to a non-broadly neutralizing lineage.

Overall, eliciting broadly neutralizing FP-directed antibodies by vaccine will likely be complex due to low prevalence of such responses during infection. These data are consistent with animal studies conducted by Xu et al., (2018) which showed that vaccination using the FP-coupled to carrier protein and sequential boosting with modified Envs resulted in the elicitation of antibodies with limited breadth and potency. Thus, both preclinical animal studies and studies of PLWH suggest that vaccine strategies may require multiple rounds of sequential immunization to drive strain-specific antibodies towards bNAbs able to recognise an occluded, conformationally variable FP epitope that is highly sequence variable.

Chapter 3

Isolation of HIV-1 Fusion Peptide-directed broadly neutralizing antibodies from an HIV-1 clade C infected individual

Vincent N. Hlatshwayo[1,2], Nonhlanhla N. Mkhize[1,2], Bronwen E. Lambson[1,2], Nigel J. Garrett[3], Quarraisha Abdool Karim[3,5], Salim S. Abdool Karim[3,4], Lynn Morris[1,2,3], Cathrine Scheepers[1,2], Penny L. Moore [1,2,3]

[1]Centre for HIV and STIs, National Institute for Communicable Diseases of the National Health Laboratory Service, Johannesburg 2131, South Africa. [2]SA MRC Antibody Immunity Research Unit, School of Pathology, University of the Witwatersrand, Johannesburg 2050, South Africa (AIRU). [3]Centre for the AIDS Programme of Research in South Africa (CAPRISA), KwaZulu-Natal 4013, South Africa. [4]Department of Epidemiology, Columbia University, New York, New York, USA. [5]Department of Epidemiology, Mailman School of Public Health, Columbia University, New York, NY USA

Abstract

A prophylactic HIV-1 vaccine will likely need to elicit bNAbs against conserved HIV-1 envelope epitopes such as the FP. Promising preclinical immunogenicity animal studies and the isolation of FP-directed bNAbs from chronically HIV-infected donors has made this epitope an appealing vaccine target. Here, using B cell sorting, we isolated three clonally related FP-specific mAbs (AIRU-F8, AIRU-G9 and AIRU-G4) at three years from CAP312 with 64%, 45% and 5% breadth (against a 22 virus multi-clade panel), respectively. These mAbs utilise the *IGHV3-30*04/IGHJ6*02* heavy chain and *IGKV1-33*01/IGKJ3*01* light chain genes. The heavy chains have long CDRH3s (32 aa) with moderate SHM (6-15%), while LCs have 10 aa CDRL3s with 12-16% SHM. Exposure of the mAbs to trimeric and monomeric gp120 Envs resulted in strong binding to trimeric Envs forms compared to monomeric gp120 Envs, indicating that these antibodies bind to an epitope that is present in trimers and not monomeric gp120. Additionally, exposure of the mAbs to different FPs: FP8_v1, FP8_v2, FP8_5 & FP8_v1-514T resulted in strong binding preference to FP8_v1, the most prevalent FP globally. No complete loss of neutralization activity was observed when mAbs were exposed to pseudoviruses with single point tryptophan mutations within the FP known to abrogate neutralization activity of FP-specific bNAbs VRC34 and ACS202. Similarly, no knock-out of neutralization activity was observed against viruses with glycan knock-out mutations surrounding the gp120-gp41 interface region. Both these findings suggest that the isolated mAbs are glycan independent and two or more FP mutation combinations are required for neutralization escape. Using longitudinal CAP312 Env sequences from 2 - 157 wpi we trace the evolution of the glycan shield in CAP312 Envs, and showed that at 2 wpi the Env had an intact glycan shield, while at 157 wpi (the time CAP312 mAbs were isolated) the Env had a

significant glycan hole exposing the FP. Overall, we have isolated additional FP-specific mAbs which recognise a unique epitope yet to be determined.

Introduction

The goal of an effective prophylactic HIV-1 vaccine is to induce potent bNAbs that have the ability to neutralize diverse HIV-1 strains. This approach is favoured because several proof-of-principle studies in animal and human trials have shown that bNAbs can prevent infection (Gautam et al., 2016; Deruaz et al., 2016; Hua and Ackerman, 2017; Corey et al., 2021). Currently there are several bNAbs that have been isolated from chronically infected HIV individuals which led to the identification and classification of eight bNAb epitopes (Sok and Burton, 2018). One of these epitopes that is currently of interest in the field is the FP, especially the first 9 amino acids at the gp41 N-terminus because of the isolation of FP-specific bNAbs N123-VRC34.01 (68% breadth), ACS202 (45% breadth) & PGT151 (73% breadth) which target these residues (Kong et al., 2016; van Gils et al., 2016; Falkowska et al., 2014). This has indicated that it is possible to elicit broad neutralizing antibodies to a site deeply buried in the HIV-1 Env which was previously not thought to be a bNAb epitope.

The currently isolated bNAbs targeting the FP are trimer specific and were isolated through B-cell sorting using native-like trimers. FP-specific bNAbs isolated to date usually require conserved glycans to fully exert their broadly neutralizing activity (Sok et al., 2018). Glycan knock-out at positions 88 and 611 affect neutralization potency of VRC34, ACS202 and PGT151 (Kong et al., 2016; van Gils et al., 2016; Falkowska et al., 2014). Residues E83, V85, E87 and N229, all located close to the N88 glycan, were also found to be critical for ACS202 neutralization. Furthermore, loss of neutralization activity for VRC43 and ACS202 was observed when sequentially mutating one of the 9 amino acid residues of the FP at positions 512, 514, 515, 517, 518 (Kong et al., 2016; van Gils et al., 2016). Distal mutations in the HIV-1 Env also

affect the overall neutralization potency of these mAbs (van Gils et al., 2016; Kong et al., 2016).

We previously identified a participant in the CAPRISA 004 Tenofovir gel trial (CAP004), CAP312, who developed 64% neutralization breadth against a 44 cross-clade viruses panel at three years post infection. CAP312 developed breadth from 35 weeks post infection (wpi) and mapping indicated that CAP312 has FP-specific monoclonal antibodies (mAb). Depletion of FP-specific antibodies from the three years plasma sample resulted in significant loss of breadth confirming that this epitope is the dominant target of bNAbs in this donor (refer to chapter 2).

The aim of this study was to isolate and characterise FP-specific bNAbs from a clade C infected donor CAP312 by B-cell sorting using a simple linear eight amino acid long FP probe, an approach that is different from what other groups have used to isolate FP-specific mAb. For example, N123-VRC34 was isolated using a trimeric HIV-1 Env BG505 SOSIP.664.T332N gp140 with an Avi tag (GLNDIFEAQKIEWHE) (Kong et al., 2016). While ACS202 was isolated using BG505SOSIP.664-AviB, 94UG103 gp120-AviB or MGRM-C026 gp120-AviB probes (van Gils et al., 2016). Here, we used this FP-focused probe isolation technique to isolate and characterise two FP-specific bNAbs and one non-bNAb and show that these mAbs are clonal relatives. We show that these bNAbs have extraordinarily long CDRH3s and are moderately mutated. Furthermore, we show that they are FP- and trimer-specific. Lastly, we evaluated the evolution of Env glycan shield surrounding the FP region using a glycan shield mapping tool and 2 - 157wpi longitudinal Env sequences and observed that the

presence of glycan holes and glycan shield is a dynamic process and this may have influenced the development of these isolated FP-specific mAbs.

Methods

Study Samples

PBMC samples were collected at regular intervals from donor CAP312 who became infected with HIV-1 during the CAP004 trial. The CAP004 trial was a double-blinded, randomized controlled trial that assessed the effectiveness and safety of 1% vaginal gel formulation of Tenofovir in sexually active, HIV-1 negative women between the ages of 18-40 (Abdool Karim et al, 2010). The trial took place at urban and rural sites in Kwazulu-Natal, South Africa between May 2007 and March 2010, and the design and the results from the trial are detailed elsewhere (Abdool Karim, 2010).

Ethics approval

The CAP004 trial (NCT00441298) was approved by the ethics committees of the University of KwaZulu-Natal's Biomedical Research Ethics Committee (E111/06), Family Health International's Protection of Human Subjects Committee (#9946) and the South African Medicines Control Council (#20060835), and the University of the Witwatersrand (M190251 MED19-02-067). Donor CAP312 provided written consent for her samples to be used for further studies.

Cell Lines and Pseudovirus production

For these methods, refer to chapter 2 methods section.

Neutralization assay

Neutralization was measured as a reduction in luciferase gene expression after a single round of infection of TZM-bl cells with Env-pseudotyped viruses. Titers were

calculated as the inhibitor concentrations (IC_{50}) or reciprocal plasma/serum dilutions (ID_{50}) causing a 50% reduction of relative light units (Montefiori DC. 2005).

Staining and sorting of B-cell populations.

Cryopreserved PBMCs isolated at 157 weeks post infection (wpi) were selected for memory B-cells marked as CD3-, CD14-, CD16-, CD19+, IgD- (all BD Biosciences) and Aqua Vital Dye (Life Technologies) negative. Biotinylated fusion peptide FP8_v1: was labelled with Brilliant Violet 421 (BV421, Biolegend) or AlexaFlour 647 (AF647, Life Technologies) fluorochromes via biotin-streptavidin interaction. Viable cells, that bound the fusion peptides were single sorted using a BD FACSMelody (BD Biosciences, San Jose, CA) into 96-well PCR plates containing 20µl/well of RT reaction buffer that included 5µl First strand cDNA buffer, 0.5 µl RNAseOut (Invitrogen, Carlsbad, CA), 1.25µl DTT, 0.0625µl Igepal and 13.25µl dH2O. Data were analysed using FlowJo (Tree Star, Ashland, OR). Sorted plates were stored at −80°C prior to PCR.

Isolation of Ig variable gene transcripts.

The genes encoding Ig variable region gene segments of heavy chain (VH) and light chain (VL) were amplified by reverse transcription-PCR. RNA from single B cells sorted in 96-well plates was reverse transcribed using Superscript III in the presence of random hexamers specific for human IgG, IgM, IgD, IgA1, IgA2, kappa (K), and lambda (L) constant gene regions to yield cDNA. The VH, VK, and VL genes were then amplified from the cDNA by nested PCR and analysed on 1% agarose gels. The nested PCR includes a second-round PCR with primers that have tag sequences at the 5′ which allows assembling of the VH and VL genes into functional linear Ig gene

expression cassettes (Liao et al. 2009). Second-round PCR products were purified and sequenced. The variable gene segments, gene usage and productivity of the immunoglobulin were determined using the IMGT-V QUEST (an online platform).

Antibody production

Plasmids separately encoding heavy and light chain genes were co-transfected and expressed in HEK293F cells (NIH AIDS Reagent Program) with PEI-MAX (1 mg/ml) (Polysciences). Cells were maintained in 293-FreeStyle 293 Expression Medium (GIBCO) at 37°C, 5% CO2, 70% humidity and 125 rpm. Cultures were harvested after seven days by centrifugation at 4000x g, and supernatants were filtered through a 0.22mm filter. Filtered supernatant antibodies were purified by chromatography using protein A-Agarose (BioVision). Purified antibodies were tested for neutralization and binding activity.

Results

Isolation and characterisation of CAP312 antibodies

In chapter two we demonstrated that CAP312, an HIV-1 clade C infected participant in the CAP004 Tenofovir microbicide clinical trial, developed FP-specific broadly neutralizing antibodies, which emerged at 35 wpi. Peripheral blood memory B cells from this donor were sorted using the globally common and CAP312 plasma sensitive FP8_v1 (AVGIGAVF) as a probe to isolate FP-specific B-cells (**Fig. 1A)**. Using this approach, 72 cells were sorted (shown as orange dots in panel five of **Fig. 1A**) and of these, 27 HC and LC pairs were amplified, of which 14 HCs and 27 LCs were predicted to be productive using IMGT HighV-QUEST. Nucleotide analysis of these HC and LC genes revealed diverse genetic usage within these sorted cells, with *IGHV3-30*04* (29%), *IGKV1-33*01* (44%) and *IGLV2-14*01* (33%) genes being the most commonly represented for the HC, kappa and lambda LCs, respectively (**Fig. 1B**).

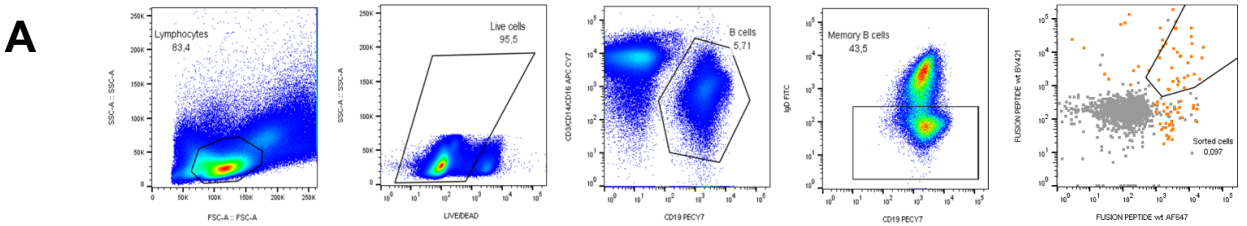

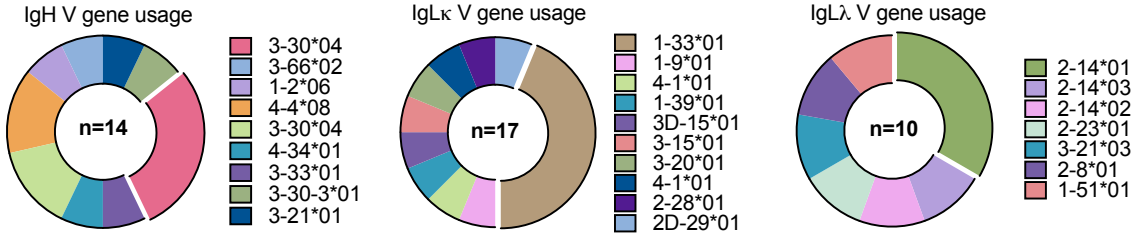

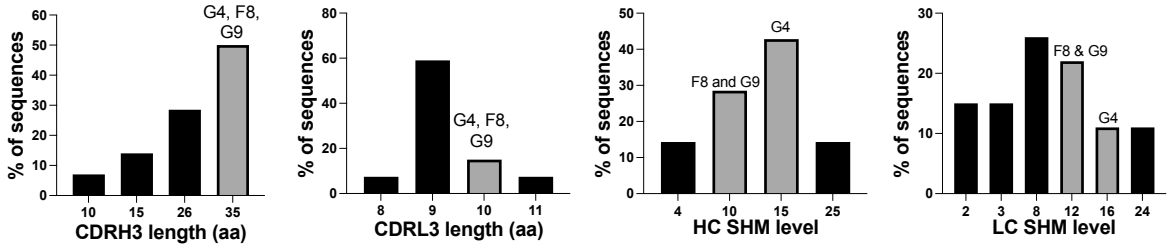

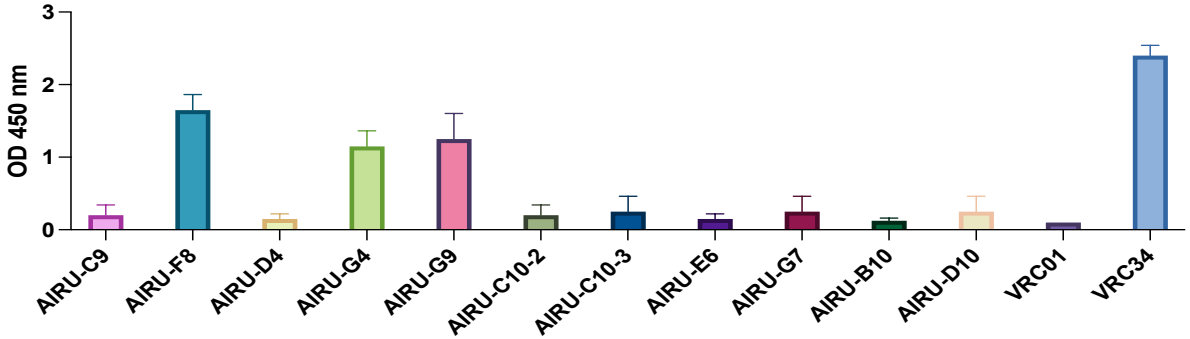

E

```
                                FW1                 CDRH1       FW2         CDRH2                FW3                                 CDRH3
                                10        20        30          40        50         60        70        80        90                      99        109
                     ....|....|....|....|.... |....|... .|....|....|....| ....|... .|....|....|....|....|....|....|....|... .|....|....|....|....|....|... .|....|....
IGVH3-30*4/IGHJ6*02  QVQLVESGGGVVQPGRSLRLSCAA SGFTFSSYA MHWVRQAPGKGLEWVAV ISYDGSNK YYADSVKGRFTISRDNSKNTLYLQMNSLRAEDTAVYYCAR                YYYYGMDV WGQGTTVTVSS
X97051|IGHD1-1*01                                                                                                                                GTTGT
X97051|IGHD5-24*01                                                                                                                               VEMATI
AIRU-F8 (7.3%)       .F..................... ......H.. ................. M...E... ....F....Y.....F.................H..T DRGGPKQAQLVRQGDSPYFQYQ..... ..........
AIRU-G9 (6.6%)       .F..................... ......H.. ................. M...E... ....F....Y.....................H..T DRGGPKQAQLVRQGDSPYFEYQ..... ..........
AIRU-G4 (14.6%)      E...................... ......DF. .....L.........G ....E.H. F.T.........F.....D......N.K.D.......T DRGGAKQRLLLPLGDGPYYQYH..... ..........
```

```
                                FW1                 CDRL1       FW2         CDRL2          FW3                                 CDRL3
                     ....|....|....|....|.... |....|... .|....|....|....| ....|... .|....|....|....|....|....|....|....|... .|....|....|....|....|....|...
IGKV1-33*01/IGKJ3*01 DIQMTQSPSSLSASVGDRVTITC QASQDISNY LNWYQQKPGKAPKLLIY DASN LETGVPSRFSGSGSGTDFTFTISSLQPEDIATYY CQQYDNLPFTF GPGTKVDIK
AIRU-F8 (12.9%)      E.VL.................I... ......KNS ....KH...ID.....F ..TT .AG..S.............L......S....... CQQYHDLSFSF .....L...
AIRU-G9 (12.9%)      E.VL.................I... ......KNS ....KH...ID.....F ..TT .AG..S.............L......S....... CQQYHDLSFNF .....L...
AIRU-G4 (15.4%)      E.VL.........F......... ..T...KTS .....H......R.... ...K .AGT.....T............T.......G... CQQYHDLSFTF .....LN..
```

Figure 1: Isolation of FP-specific memory B cells and characterization of isolated antibodies. (**A**) Sorting strategy used to isolate FP-specific antibodies from CAP312 PBMCs at visit code 4230 (i.e., 158 weeks post infection). Panel 1 shows the gated lymphocytes, panel 2 shows positive selection of live cells, panel 3 shows positive selection of B cells, panel 4 shows positive selection of memory B cells and panel 5 shows antigen positive B-cells that were sorted. The gated orange cells in panel 5, represents double-positive FP cells that were sorted and further analysed to assign gene usage. (**B**) Gene usage of the sorted heavy chains (HC) and light chains (HC). A total of 14 productive heavy chains (HC) were obtained. A total of 27 productive light chains (LC) were obtained, which were composed of 17 kappa LC and 10 lambda LC sequences. The exploded pie portions represent the most common heavy/light chains used. (**C**) Average CDR3 lengths and SHM of the sorted HCs and LCs. Grey shading shows the SHM and CDRs of the three mAbs that bind FP8_v1 in ELISA (**D**) Linear cassettes of the 11 paired HC/LC binding to FP8_v1. VRC01 and VRC34 are negative and positive controls respectively. (**E**) HC and LC sequences of the three FP-specific Abs that had high binding and appeared to be clonally related. Germline *IGVH3-30*04, IGVK1-33*01, IGHJ6*02, IGKJ3*01 and IGHD1-1*01* and *IGHD5-24*01* genes are also shown in this alignment. SHM levels are indicated next to the sequence name.

Genetic analysis indicated that all the 27 linear cassette antibody pairs have varied CDRH3, CDRL3 lengths (**Fig. 1C**). SHM analysis indicated that the sorted pairs have varied SHM levels, ranging from 11-26% and 14-43% for LC and HC respectively (**Fig. 1C**). We next generated linear cassettes to perform small scale antibody expressions and screened 11/27 linear cassette antibody pairs for functionality using an IgG ELISA, since the remaining 16 pairs failed to bind to primers and amplify (**Fig. 1D**). We identified three linear cassette antibody pairs; AIRU-F8, AIRU-G9 & AIRU-G4, which showed binding to FP8_v1, while the remaining eight linear cassette antibody pairs had little to no binding (**Fig. 1D**). The three pairs (AIRU-F8, AIRU-G9 & AIRU-G4)

which bound to FP8_v1, had unusually long CDRH3 (32 aa) but average length CDRL3 (9 aa) (**Fig. 1C**). Heavy chain SHM levels for the three FP-specific mAbs ranged from 10-15%, and those for the LCs from 12-16% (**Fig. 1C**, grey highlighted). Nucleotide sequence analysis of the three candidate mAbs using IGMT/HighV-QUEST showed that they all share the same *IGHV3-30*04/IGHJ6*02* and *IGKV1-33*01/IGKJ3*01* genes, with junction sequences of identical lengths, thus suggesting they are clonal relatives (**Fig. 1E**). Furthermore, at amino acid level, AIRU-F8 and AIRU-G9 (7.3 & 6.6% SHM, respectively) had fewer mutations compared to AIRU-G4, which was highly mutated (14.6%) and had only 2 aa differences between them (**Fig. 1E**). All three mAbs have CDRH3 region flanked by a string of tyrosines, each having four tyrosines forming a "YYYY-motif" (**Fig. 1D**). AIRU-F8, AIRU-G9 & AIRU-G4 were cloned as full length mAbs and further characterised.

FP-specific CAP312 isolated mAbs recognise trimeric Env forms and have neutralization breadth.

We evaluated the binding of the three FP-specific mAbs against four different FPs, including the sorting antigen, FP8_v1 (AVGIGAVF). The other three peptides tested were FP8_v2 (AVGLGAVF), FP8_v5 (AVGIGAMI) and FP8_v1-514T (AVGTIGAVF). Combined, these peptides account for 33,2% of global HIV-1 sequences in the LANL database. All three mAbs showed binding to FP8_v1, FP8_v2 and FP8_v5, with preferential binding seen for the sorting antigen (FP8_v1) compared to the other two (**Fig. 2A**). No binding to FP8_v1-514T was observed, as seen for the positive control mAb VRC34 (**Fig. 2A**). Taken together, the data confirms that the isolated mAbs are FP-specific and capable of binding different FPs.

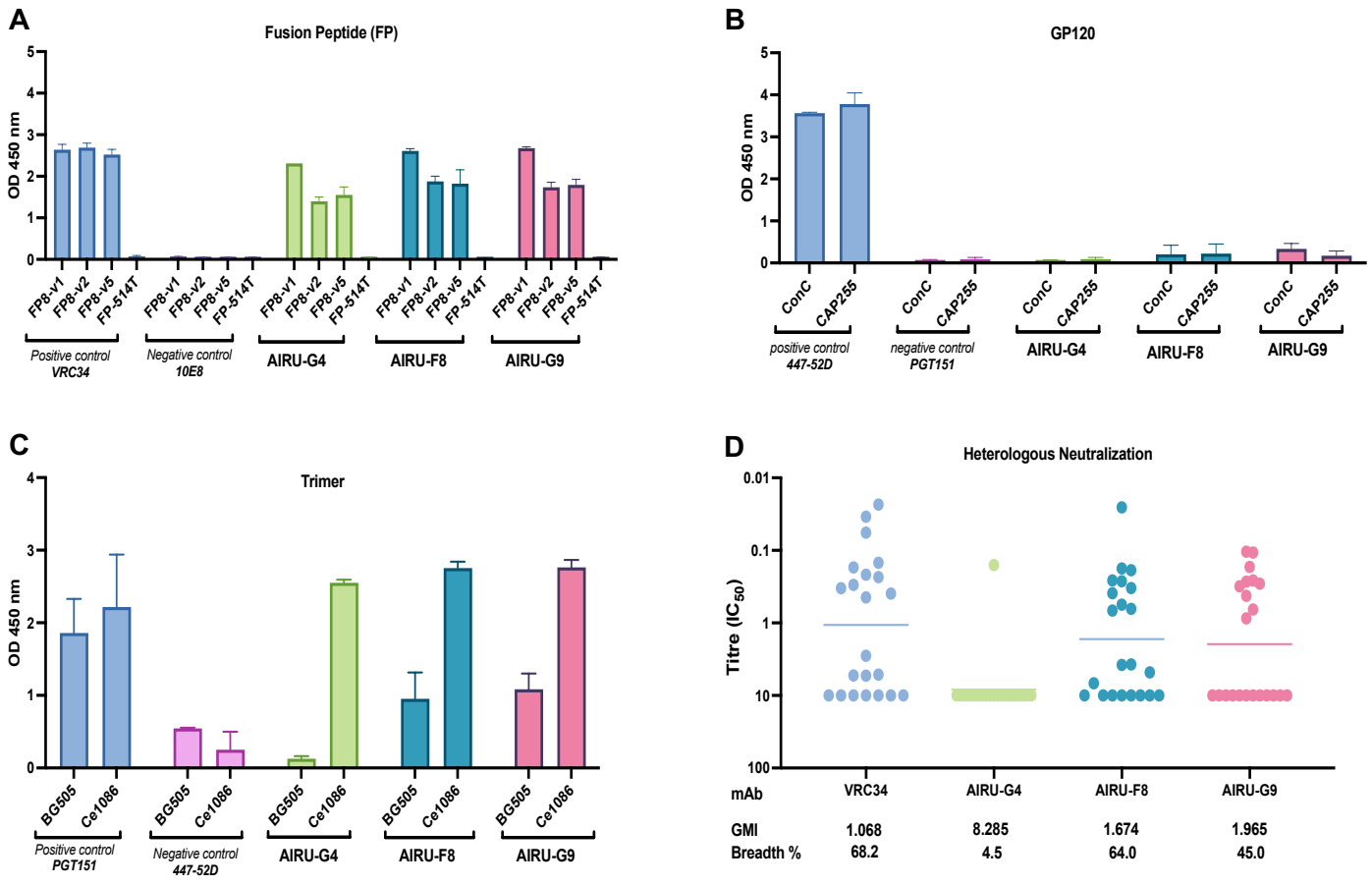

Figure 2: Functional characterization of the three isolated FP-specific antibodies. Three linear cassette pairs that bind FP8_v1 from **Fig. 1D** were cloned and expressed as full Abs then examined by ELISA and neutralization assay to see whether they are FP-specific, gp120 specific, and trimer specific. Breadth and potency was also assayed against 22 virus panel: (**A**) CAP312 mAbs AIRU-G4, AIRU-F8 and AIRU-G9 were examined for binding to four FPs: FP8_v1, FP8_v2, FP8_v5 and FP-514T. bNAbs VRC34 and 10E8 were used as positive and negative controls, respectively. (**B**) CAP312 mAbs AIRU-G4, AIRU-F8 and AIRU-G9 were exposed to ConC and CAP255 gp120 Envs. bNAb PGT151 and Ab 447-52D were used as negative and positive controls respectively. (**C**) To check if the isolated mAbs bind to an epitope present in trimeric Env and not monomeric Envs, CAP312 mAbs AIRU-G4, AIRU-F8 and AIRU-G9 were assayed against Ce1086 and BG505 trimeric Envs. bNAb PGT151 and Ab 447-52D were used as positive and negative controls respectively. (**D**) Breadth and potency of CAP312 mAbs AIRU-G4, AIRU-F8, AIRU-G9 and VRC34 was evaluated against a 22 virus panel. GMI

and IC_{50} values were calculated for all mAbs. bNAb VRC34 was used as control. GMI= geometric mean IC_{50}.

We next assessed whether the three FP-specific isolated mAbs bound preferentially to monomeric HIV-1 gp120 or trimeric Envs (**Fig. 2B** & **C**). Two different Env trimers (BG505 and Ce1086) and two gp120 (ConC and CAP255) were used because the CAP312 plasma neutralized their respective pseudoviruses (see chapter 3, **Fig. 1A**). All three mAbs failed to bind to the monomeric gp120 much like the negative control mAb PGT151, despite neutralization potency ranging from 1.674 to 8.285 ug/ml (**Fig. 2B**). However, they were able to bind to the Env trimers, with all mAbs showing strong binding (2.5, 2.8 & 2.8 OD for AIRU-G4, AIRU-F8 & AIRU-G9, respectively) to Ce1086 and only AIRU-F8 and AIRU-G9 showing modest binding (~ ±1 OD) to the BG505 Env trimer (**Fig. 2C**). Further confirming their dependence on FP, since soluble monomeric HIV-1 Env lacks the fusion peptide. Combined, these observations indicate that the three isolated CAP312 mAbs recognise an epitope that is present in a trimeric HIV-1 Env and not monomeric Envs.

Next, we evaluated the neutralization breadth and potency of the three isolated FP-specific mAbs. To achieve this, we performed neutralization assays and calculated IC_{50} values using 22 cross-clade HIV-1 pseudoviruses, which included eight clade C, and seven each of clade B and A (**Fig. 2D**). AIRU-F8 and AIRU-G9 neutralized 64% (14/22) and 45% (10/22) of the viruses respectively. Conversely, AIRU-G4 only neutralized 4.5% (1/22) of the viruses (**Fig. 2D**). The most broad mAb, AIRU-F8, has the same neutralization breadth as seen in plasma at three years post-infection, in donor CAP312, from which this mAb was isolated (data shown in Chapter 3, **Fig. 1A**). AIRU-F8, AIRU-G9 and AIRU-G4 have a geometric mean IC_{50} (GMI) IC_{50} of 1.67 ug/ml, 1.97

ug/ml and 8.29 ug/ml, respectively (**Fig. 2D**). Neutralization potency of AIRU-F8 and AIRU-G9 in this 22 cross-clade virus panel is comparable to that of the FP-specific bNAb VRC34 (**Fig. 2D**). Overall, these data indicate that using a linear FP8_v1 probe, we have isolated FP-specific mAbs with comparable neutralization and potency to currently isolated FP-specific bNAbs (Kong et al., 2016; van Gils et al., 2016).

Purified CAP312 mAbs are FP-specific and mediate heterologous neutralization seen in CAP312 plasma.

To further provide evidence that the observed heterologous neutralization in donor CAP312 is mediated by the isolated FP-specific mAbs, we performed antibody depletion/adsorption assay. Following purification and elution of CAP312 mAbs, these were resuspended in the PBS buffer. PBS-resuspended mAbs were then subjected to depletion using FP8_v1 as a bait. Depleted and undepleted samples were then tested for percentage binding using ELISA (**Fig. 3**) and neutralization reduction using a neutralization assay (**Fig. 4**). We observed significant reduction in binding to FP8_v1 resulting in fold change differences ranging from 4-7 times for all three mAbs and VRC34 following FP-specific mAb depletion (**Fig. 3**). This binding experiment (**Fig. 3)** was done to verify if the purified mAbs are FP-specific just like the linear cassettes (**Fig. 1D**). Findings depicted below (**Fig. 3**) indicate that we successfully depleted FP-specific mAbs in these samples.

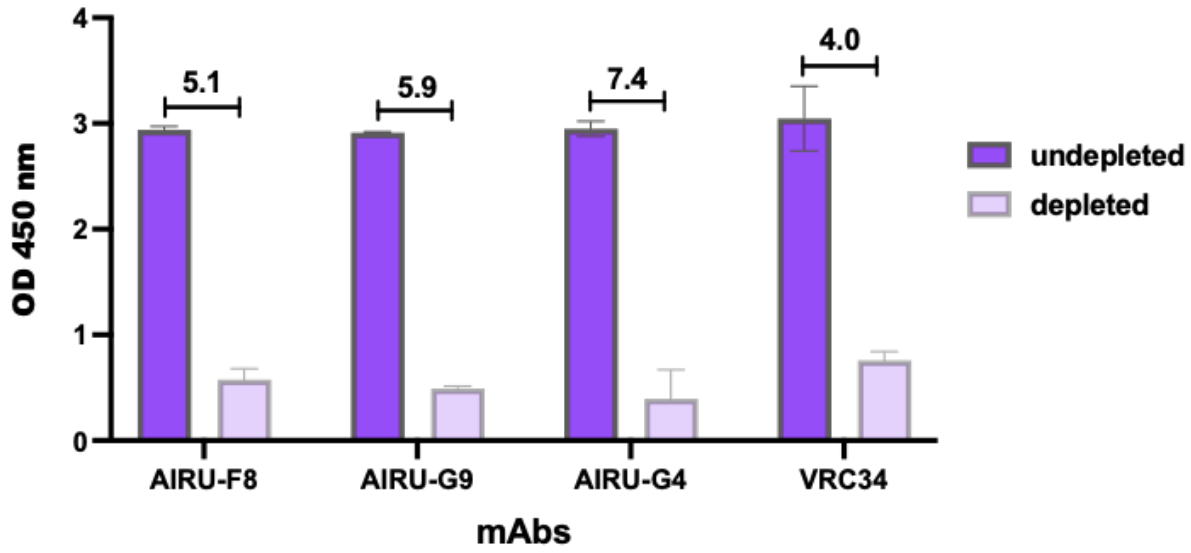

Figure 3: FP-specific CAP312 mAbs resuspended in PBS buffer were successfully depleted from solution. FP binding by CAP312 mAbs before and after depletion of FP-specific antibodies with FP8_v1 peptide. VRC34 depletion control experiment showing successful FP-specific mAb depletion. OD Fold changes are indicated for all mAbs. VRC34 was used as an assay-positive control.

We then tested the ability of the depleted and undepleted mAbs to neutralize three heterologous viruses which are sensitive to both plasma and mAbs neutralization (ZM214, Du422 & Q168) (**Fig. 4**). As anticipated, marked neutralization reduction was observed for VRC34, the positive control, following depletion of FP-specific mAbs (approximately 13.2 -109.3 fold) (**Fig. 4**). Complete knock-out (K/O) in neutralization activity was observed for AIRU-F8 following depletion, this suggests that all of FP-specific mAbs in AIRU-F8 were completely depleted. However, only a subtle decrease in neutralization was observed for AIRU-G9 (approximately 2.4 - 4 fold). Thus, not all FP-specific mAbs were depleted from this sample (**Fig. 4**). While, no marked change in neutralization activity was observed for AIRU-G4, the non-broadly neutralizing mAb, against the three heterologous viruses (approximately 0.7 - 1 fold change) following

depletion of FP-specific mAbs (**Fig. 4**). This was expected because AIRU-G4 does not neutralize the three tested viruses. Comparison of the broadly neutralizing mAbs AIRU-F8 and AIRU-G9, suggests that the mAbs bind to the FP with different affinities, with AIRU-F8 having strong affinity to FP8_v1 while AIRU-G9 has weaker affinity (**Fig. 4**). The small fold change differences for AIRU-G9 suggest that it dissociates from FP8_v1 faster than AIRU-F8, hence, FP-specific Abs were partially depleted resulting in marginal neutralization difference and not complete K/O.

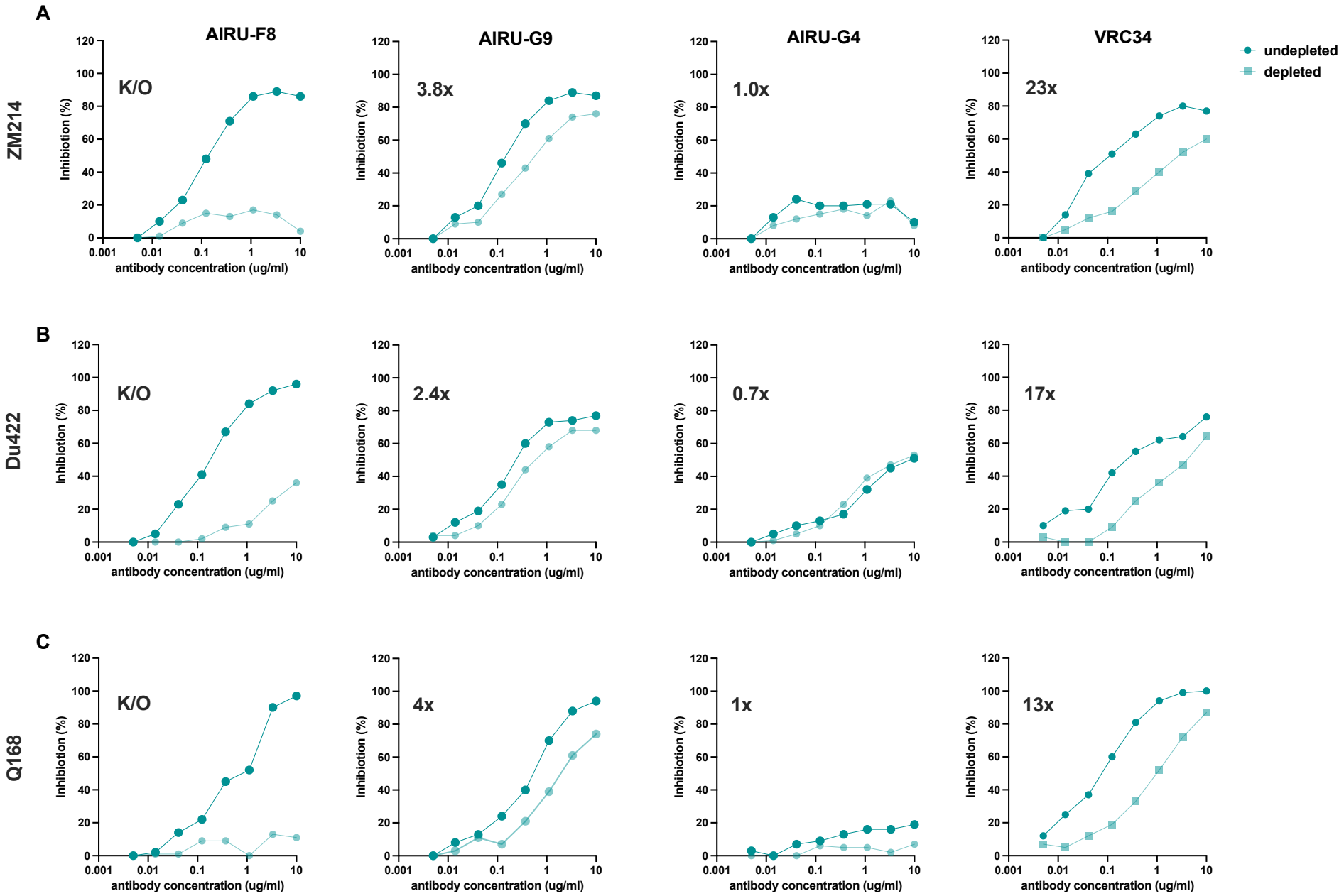
A
B
C
ZM214
Du422
Q168
AIRU-F8
AIRU-G9
AIRU-G4
VRC34
K/O
3.8x
1.0x
23x
2.4x
0.7x
17x
4x
1x
13x
undepleted
depleted
Inhibiotion (%)
antibody concentration (ug/ml)
0.001
0.01
0.1
1
10
0
20
40
60
80
100
120

Figure 4: Heterologous neutralization by CAP312 mAbs is mediated by FP-specific Abs. Neutralization profiles of three isolated CAP312 mAbs AIRU-F8, AIRU-G9 and AIRU-G4 (indicated at the top of the columns) and VRC34 against three heterologous viruses ZM214, Du422 and Q186 (indicated at the top of the rows) following depletion of FP-specific antibodies using FP8_v1 as bait. IC_{50} Fold changes (mut/wt) are indicated in the plots. K/O = knock-out. VRC34 was used as an assay-positive control.

CAP312 mAbs have a unique mode of interaction with the FP epitope

To assess whether the glycans that surround the gp120-gp41 interface region, and are proximal to the FP epitope were required for neutralization, we tested AIRU-F8, AIRU-G9, AIRU-G4 and VRC34 against knock-out mutants. Mutants tested included: N88A, N276D, N442K, N611A, N616A, N625A, N637A and N674A in pseudovirus CAP45 (which is highly sensitive to neutralization by CAP312 plasma and mAbs) (**Fig. 5A**). Dotted line in figure 5 represents a three-fold cut-off. As expected, VRC34 neutralization was enhanced by the removal of glycan N611 (indicated by S613A and N611D mutations) but negatively affected by the removal of the N88 glycan (Kong et al., 2016) (**Fig. 5A**). Slight enhancement in neutralization was seen by the removal of N611 glycan for AIRU-F8, AIRU-G9 and AIRU-G4, with only AIRU-G4 being above three-fold (**Fig. 5a**). However, unlike VRC34, but similar to nAb CAP248-2B, neutralization titres of the three isolated mAbs were not negatively affected by any of the glycan knock-out mutants (Wibmer et al., 2017) (**Fig. 5A**).

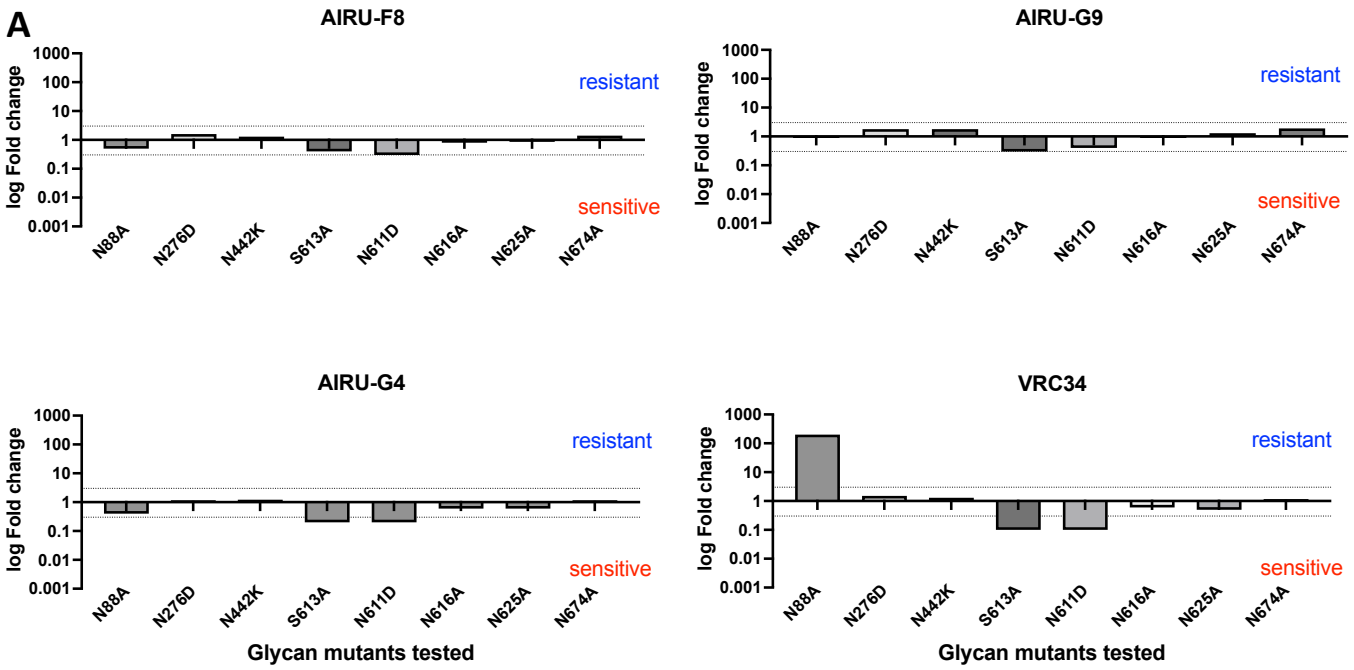
A
AIRU-F8
AIRU-G9
AIRU-G4
VRC34
log Fold change
1000
100
10
1
0.1
0.01
0.001
resistant
sensitive
N88A
N276D
N442K
S613A
N611D
N616A
N625A
N674A
Glycan mutants tested

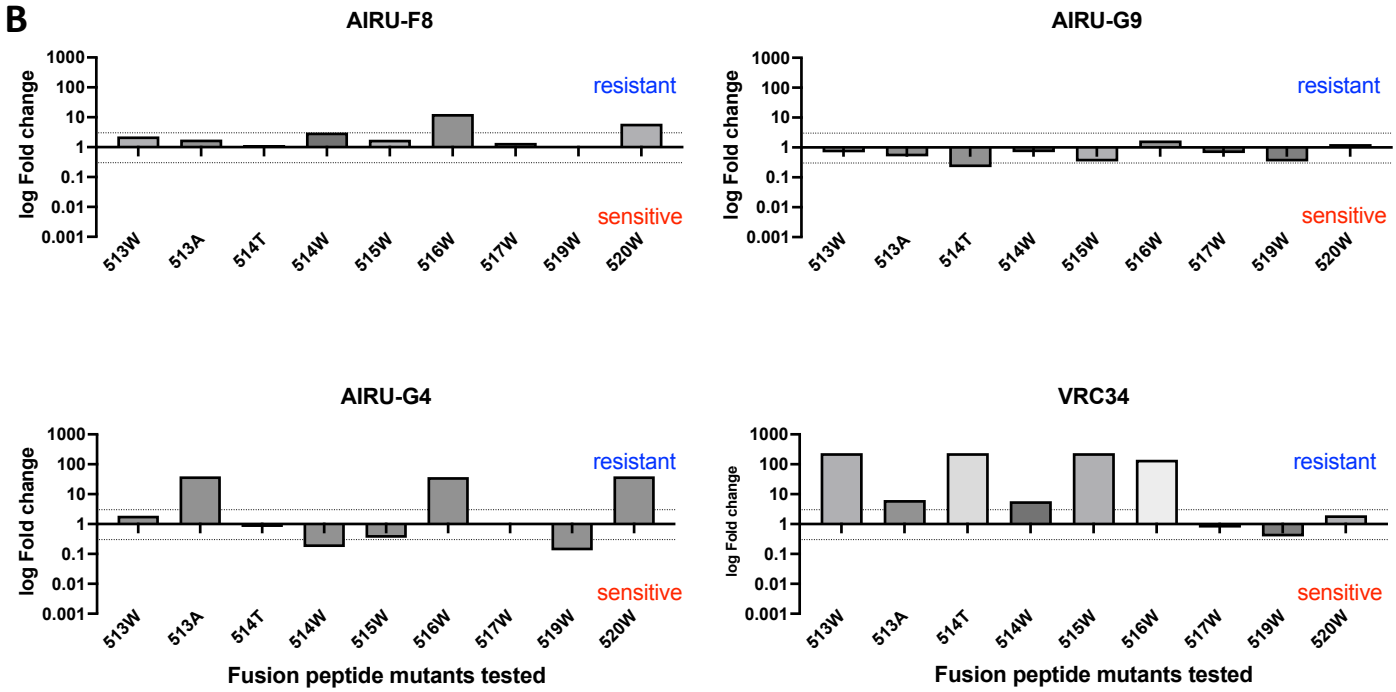
B
AIRU-F8
AIRU-G9
AIRU-G4
VRC34
log Fold change
1000
100
10
1
0.1
0.01
0.001
resistant
sensitive
513W
513A
514T
514W
515W
516W
517W
519W
520W
Fusion peptide mutants tested

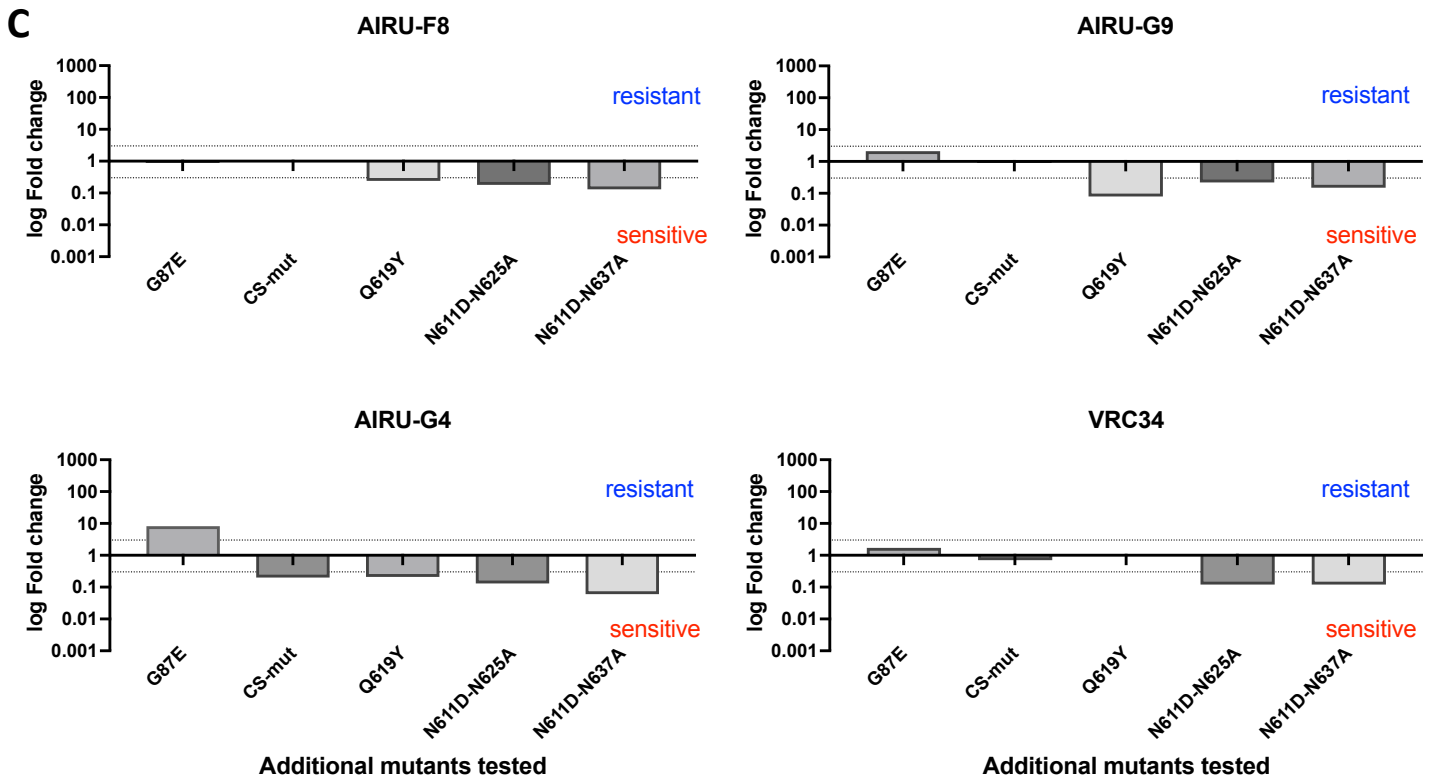

Figure 5: Fine mapping the epitope of the isolated CAP312 mAbs. (**A**) Glycan knockout mutagenesis. CAP312 mAbs were tested against CAP45 single point and double glycan mutants that surround the gp120-gp41 interface and FP region. (**B**) Substitution of FP residues with tryptophan. CAP312 mAbs were tested against CAP45 single point FP tryptophan mutants. (**C**) Additional mutants shown to affect neutralization activity of gp120-gp41 interface- and FP-specific bNAbs. Fold changes were calculated for all glycan, FP and additional mutants as mutant IC_{50}/wild-type IC_{50}. A value larger than 3 indicates that the mutant is more resistant (blue), while a value less than 0.3 indicates that the mutant is more sensitive (red) as shown by the dotted line. VRC34 was added as a control.

Furthermore, we assessed whether the mutations within the FP were required for neutralization. Fusion peptide tryptophan and alanine mutants in CAP45 (V513W, V513A, G514W, G514T, I515W, G516W, A517W, L519W & L520W) were tested for sensitivity to the three isolated mAbs (**Fig. 5B**). The A512W and V518W mutants failed to grow despite several attempts, hence, they were not included in the analysis. Differences in IC_{50} above three-fold (which represents the error within the

neutralization assay), were considered significant (the three-fold cut-off is represented as a dotted line in (**Fig. 5B**)). Similar to findings by (Kong et al., 2016), we noticed that changes within the FP at positions 513W, 513A, 514T, 514W, 515 & 516 negatively affected VRC34 (positive control) neutralization, resulting in loss of neutralization by 235, 6, 235, 6, 235 & 141x respectively (**Fig. 5B**). AIRU-F8 and AIRU-G4 were also negatively affected by some of these mutations though to a lesser extent than VRC34, with AIRU-F8 showing 3-fold resistance at position 514 and AIRU-G4 showing 40-, 37- and 40-fold increased resistance at position 513, 516, and 520 (**Fig. 5B**). Unlike, VRC34, AIRU-G9 and AIRU-G4 showed neutralization potency enhancement by changes at position 514 (4.5 & 5x respectively), with AIRU-G4 having further enhancement at position 519 (10 fold) (**Fig. 5B**). Overall, this data suggests that single point mutations within the FP of CAP45 virus are not sufficient to knock-out neutralization activity of CAP312 isolated mAbs. Therefore, we hypothesise that double or multiple mutations occurring simultaneously within the FP of virus CAP45 are needed to completely escape neutralization by these mAbs.

Additional CAP45 mutations tested included G87E, Q619Y, N611D-N625A, N611D-N637A and CS-mut (which is composed of six mutations: E500K, R502K, V505M, E507G, R508K, E509G that were shown to abrogate neutralization by CAP248-2B, a gp120-gp41 interface-directed nAb (Wibmer et al., 2017)) (**Fig. 5C**). G87E resulted in an 8-fold reduction in neutralization for AIRU-G4, but did not have a negative effect on AIRU-F8 and AIRU-G9 (**Fig. 5C**). CS-mut resulted in potency enhancement for AIRU-G4 (5.5x) but not for AIRU-F8 (1x) or AIRU-G9 (1x) (**Fig. 5C**). A Du422 Q619Y change resulted in potency enhancement for AIRU-G4, AIRU-G9 & AIRU-F8 (4.7, 11.8 & 4.2x respectively) (**Fig. 5C**). These three changes (G87E, Q619Y and CS-mut) did not affect

VRC34 neutralization (1.7, 1 & 0.7x respectively) (**Fig. 5C**). Lastly, for all mAbs including VRC34, double glycan mutants N611D-N625A and N611D-N637A resulted in potency enhancement (**Fig. 5C**). All together, these data suggest that CAP312 mAbs have a unique neutralization profile to the positive control VRC34 and CAP248-2B which is significantly affected by CS-mut as previously reported (Wibmer et al., 2017) (**Fig. 5C**).

Tracking the evolution of glycans surrounding the FP region

To explore the lack of glycan usage by the mAbs, we analysed the CAP312 viral env sequences at four time points (2, 4, 67 & 157 weeks post infection (wpi)) obtained by SGA and mapped the glycans onto the env using glycan shield mapping tool from LANL database (GlycanShieldMapping) (**Fig. 6**).

Focusing on the gp120-gp41 interface and FP region we observed a fluctuating trend in glycosylation pattern. Initially, at two wpi, the envelope had an intact glycan shield surrounding the gp120-gp41 interface and FP region with all the glycans (N88, N625, N616, N625 and N637) present and no evidence of glycan hole (**Fig. 6**). However, at four wpi, there was evidence of glycan holes with glycans N88 and N637 missing (**Fig. 6**). At 67 wpi, the glycan hole was filled, with all glycans present and no evidence of glycan hole (**Fig. 6**). At 158 wpi, when CAP312 mAbs were isolated, the envelope had lost glycans N611, N625 and N637 resulting in a glycan hole that exposed the gp120-gp41 interface region including FP. Previous study (Wagh et al., 2018) showed that Env glycan evolution is dynamic and fluctuates overtime as a result of the “arms race” between the immune system pressure and virus escape. We note that at 4 and 157wpi the Env sequences are few, which is a limitation in this analysis.

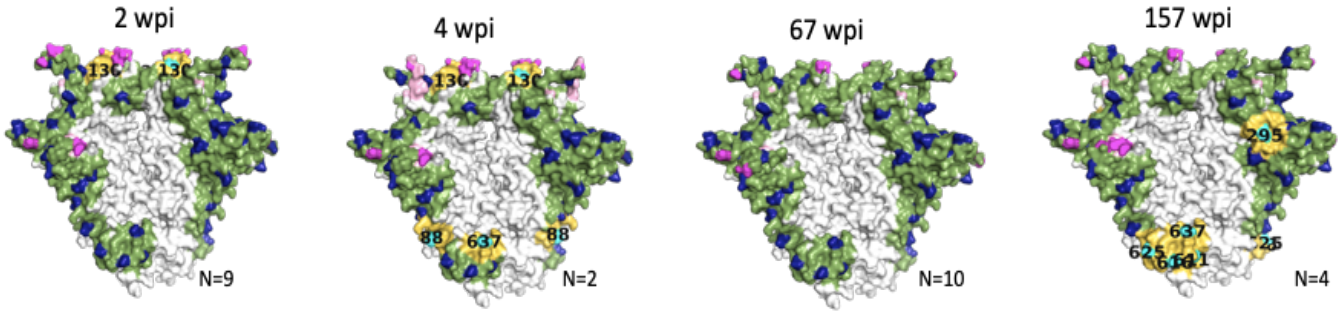

Figure 6: Evolution of glycans surrounding the FP region. Longitudinal CAP312 Envs were assayed for the glycosylation patterns by Glycan hole mapping. CAP312 Envs with glycans highlighted as blue spheres, missing glycans as cyan spheres and glycan position indicated. Rare glycan holes = pink. Hole area created by the missing glycan = Yellow. Time point of the envelope is indicated on top of the trimer structure. Number of sequences used for glycan shield analysis are indicated at the bottom right of trimers

Discussion

The recent keen interest in the nine amino acid long FP as a vaccine target has fuelled the isolation and characterisation of FP-specific bNAbs from chronically infected individuals. In this study we have isolated and characterised three FP-specific mAbs, two with good neutralization breadth and one with poor neutralization breadth. We show that the isolated mAbs are clonal relatives with exceptionally long CDRH3s and average length CDRL3s. Furthermore, the isolated mAbs have a different mode of neutralization compared to currently isolated FP-specific bNAbs, showing no apparent dependence on glycans, and not markedly affected by point mutation changes within the FP region.

CAP312 mAbs share *IGHV* and *IGHJ* gene usage with currently isolated FP-specific bNAbs

Similar to all the currently isolated FP-specific bNAbs, CAP312 mAbs recognised trimeric Envs (Falkowska et al., 2014; Kong et al., 2016; van Gils et al., 2016; Yuan et al., 2019). At the genetic level, the isolated mAbs share similar gene usage with bNAbs ACS202 and PGT151 using the HC germline gene *IGHV3-30*04* (van Gils et al., 2016; Falkwoska et 2014). VRC34 uses a different germline gene *IGHV1-2*. Further, all the FP-specific bNAbs and CAP312 mAbs share the same *IGHJ* germline gene encoded by the common *IGHJ6*02* gene (Ye et al., 2013). This gene has a conserved YYYY motif that is present in bNAbs PGT151 and ACS202 which elongated their CDRH3s, however, VRC34 lacks this motif resulting in a shorter CDRH3 (Yuan et al., 2019). This YYYY motif has been associated with favourable interaction with FP for bNAbs ACS202 and PGT151 (Yuan et 2019; Falkowska et al., 2014). Furthermore, when ACS202 CDRH3 was altered at the YY^{100}YY motif by replacing Y^{100} for H^{100} the

binding to FP weakened resulting in poor neutralization. AIRU-G4, the poor neutralizer of the CAP312 mAbs has the H^{100} phenotype as well, which is different from AIRU-F8 and AIRU-G9 having the Y^{100} phenotype. This suggests that CAP312 mAbs recognise the FP in an similar way to ACS202. Despite the shared YYYY-motif with PGT151 and ACS202, CAP312 mAbs have even longer CDRH3s (32 amino acids) compared to all the isolated FP-specific bNAbs CDRH3s (26, 18 & 13 amino acids) for PGT151, ACS202 and VRC34, respectively. Comparison of PGT151 & ACS202 sequences with CAP312 mAbs shows that they use different IGHD genes (*IGHD3-10*01 & IGHD2-8*02*, respectively), while CAP312 mAbs use *IGHD1-1*/5-24*01* which results in longer CDRH3s for these mAbs compared to shorter CDRH3s for bNAbs.

CAP312 mAbs interact with the FP with different affinities

The neutralization profile following depletion of FP8_v1 specific mAbs in our antibody samples suggests that CAP312 mAbs recognise and bind to different FP versions with varied affinities. Based on the current results, this suggests that CAP312 mAbs have an epitope within the gp120-g41 interface including the fusion peptide region that is yet to be determined. This is because none of the single point FP mutations markedly affected the neutralization of these mAbs. This suggests that CAP312 mAbs may require two or more mutations within the FP region to completely abrogate neutralization. Conversely, all of the current isolated bNAbs share the epitope and are negatively affected by single point changes in FP. This implies that CAP312 mAb have an increased viral escape tolerance compared to currently isolated FP-specific bNAbs. We hypothesise that the angle of approach and FP recognition by CAP312 mAbs is different to that of the isolated bNAbs, thus presenting us with the opportunity to elucidate a novel FP recognition by FP-specific mAbs. Future studies will elucidate

this epitope by crystallisation of the CAP312 mAb with SOSIP trimers as this will allow us to determine precisely the mode of binding and specific residues within the trimer that interact with CAP312 mAbs.

Long CDRH3 is useful for penetrating and avoiding dense glycan shield

We hypothesise that CAP312 mAbs may be glycan independent because the long CDRH3 they possess allows these mAbs to penetrate through the dense glycan shield and avoid steric clashes that would otherwise affect overall neutralization activity (**Fig. 6**). Furthermore, it is possible that the overtime evolution of the glycan shield shaped the glycan independence for these mAbs, resulting in direct interaction with the FP epitope and avoiding glycans surrounding the gp120-gp41 interface region. Future studies to prove this hypothesis will be to shorten the CDRH3s of these mAbs and assay these for altered neutralization activity. Furthermore, crystallisation studies with envelopes that are fully glycosylated at the gp120-gp41 interface region will provide some insights.

Altogether, our findings demonstrate how CAP312 mAbs may have evolved to avoid the glycan shield surrounding the gp120-gp41 interface region to directly interact with the underlying FP and neutralize heterologous viruses. Additionally, our findings expand on isolated FP-specific mAbs and identified FP-specific mAbs with a unique mode of interaction with the FP epitope. Further characterisation and precise elucidation of the CAP312 mAbs epitope could therefore provide insight on pathways through which these mAbs develop and interact with the Env.

Chapter 4

Tracking the evolution of the interface-directed nAb CAP248-2B, reveals that the unique paratope features are redundant for heterologous neutralization

Vincent N. Hlatshwayo[1,2], Dale Kitchin[1,2], Constantinos K. Wibmer[1], Zanele Makhado[1,2], Bronwen E. Lambson[1,2], Nigel J. Garrett[3], Salim S. Abdool Karim[3], Lynn Morris[1,2,3], Cathrine Scheepers[1,2], Penny L. Moore [1,2.3]

[1]Centre for HIV and STIs, National Institute for Communicable Diseases of the National Health Laboratory Service, Johannesburg 2131, South Africa. [2]SA MRC Antibody Immunity Research Unit, School of Pathology, University of the Witwatersrand, Johannesburg 2050, South Africa. [3]Centre for the AIDS Programme of Research in South Africa (CAPRISA), KwaZulu-Natal 4013, South Africa nod

Abstract

An understanding of how bNAbs develop in HIV-1-infected individuals is needed to provide a roadmap for vaccine design strategies. Specifically, the understanding of how the paratope of these bNAbs develop overtime. Several proof-of-concept studies have recently shown both the feasibility of eliciting and prevalence of gp120-gp41 interface-directed responses in different cohorts, thus making this a vaccine development target. We have previously isolated a bNAb that targets this region and we showed that this antibody interacted with the HIV-1 Env trimer through a long light chain CDRL3 that inserts into the viral membrane and a heavy chain CDRH1 ^{32}ED^{33} motif that interacted with gp41. In this study we delineated its development by tracing the evolutionary pathways utilising longitudinal samples from 11-281 weeks post infection (wpi). We made chimeric heavy and light chain antibodies focusing on the paratope changes and tested these for neutralization activity. We show that the long CDRL3 in the CAP248-2B light chain appeared 2 years post infection due to a 9 amino acid insertion. Further, we showed that this long CDRL3 is functionally redundant against heterologous viruses because its deletion resulted in improved heterologous neutralization. We also show that the heavy chain ^{32}ED^{33} motif appeared sporadically in the lineage due to amino acid toggling as early as 11 wpi, but was later replaced with the conserved ^{32}VD^{33} motif. Lastly we show that the glycan shield at the interface region obscures the epitope of CAP248 lineage members, negatively affecting their neutralization activity. Overall, our study outlines the kinetics of development of CAP248-2B paratope and identified random events that deviated the lineage development from the path of breadth towards the path of limited breadth.

Introduction

The development of an HIV vaccine, which will likely require the elicitation of neutralizing antibodies, remains a major public health priority. BNAbs capable of neutralizing globally circulating viruses, develop in a subset of HIV positive individuals. Several studies have mapped the antibody specificities responsible for breadth (Landais & Moore, 2018), and identified eight bNAb sites (Moore 2018; Williams et al., 2021) namely, V2 apex, V3 supersite, V3 crown, CD4bs, MPER, gp120-gp41 interface including the FP and the silent face of the HIV envelope (Moore, Gray, et al., 2012; Liao et al., 2013; Doria-Rose et al., 2014; Bhiman et al., 2015; Wu et al., 2015; Van Gils et al., 2016; Landais and Moore, 2018; Schoofs et al., 2019; Shen et al., 2020, Chan et al., 2021). Many vaccine strategies against HIV-1 are epitope specific, aiming to elicit a single class of bNAbs that target one of the eight bNAb epitopes identified to date (Landais & Moore, 2018). For example, several groups are working to elicit neutralizing responses to FP. However, the feasibility of eliciting that particular response may depend on understanding the maturation of such antibodies.

In recent years, HIV and antibody co-evolution studies have been performed in 14 infected individuals. These studies include bNAb donors targeting five of the eight currently known bNAb epitopes: CD4bs, V2 apex, V3 supersite, MPER and FP epitopes (Liao et al., 2013; Doria-Rose et al., 2014; Bhiman et al., 2015; Wu et al., 2015; Bonsignori et al., 2017; Shen et al., 2020; Landais and Moore, 2018). Altogether, these studies have indicated that strain-specific neutralizing antibodies (nAbs) developed breadth as a result of being exposed to different immunotypes (viral escape mutations within epitopes) and that antibody somatic hypermutation (SHM) enabled the immune system to adapt to the constantly evolving viral quasispecies (Moore et

al., 2011; Moore et al., 2013; Murphy et al., 2013; Wibmer et al., 2013; Doria-Rose et al., 2014; Bhiman et al., 2015). Such studies inform lineage-specific vaccine strategies which aim to use sequential immunogens to program the antibody response of un-infected individuals towards development of broader neutralizing antibodies with greater neutralization breadth (Escolano et al., 2016).

In this study we will be focusing on delineating an antibody lineage directed towards the gp120-gp41 epitope. The rationale for focusing on this epitope is based on recent data indicating that trimer-based vaccine regimens elicited strain-specific neutralizing responses to the interface in non-human primates, rabbits, guinea pigs and mice (Kong et al., 2016; McCoy et al., 2016; Xu et al., 2018 Cheng et al., 2019). Moreover, antibodies targeting the gp120-gp41 interface excluding the FP epitope were predicted to be present in 38% of the participants in a small HIV subtype B infected cohort of 34 donors (Huang et al., 2014). Additionally, 12% of individuals in a large clade C had gp120-gp41 interface specific responses (Landais et al., 2016). Meanwhile, in a small South African cohort of 16 subtype C infected paediatric donors, 25% had interface responses and 38% had fusion peptide responses (Ditse et al., 2018). These findings suggest that a vaccine aimed at eliciting interface-directed antibody responses would be challenging since these responses are not common.

We previously isolated and characterised an interface directed nAb called CAP248-2B, from donor CAP248 (Wibmer et al., 2017). We showed that this antibody interacted with the HIV-1 Env trimer through a long light chain CDRL3 that inserts into the viral membrane and a heavy chain CDRH1 ^{32}ED^{33} motif that interacted with gp41.

Here we trace the developmental pathway of the CAP248-2B lineage and functionally characterised the antibody intermediates using pseudovirus neutralization assays. Our findings suggest that persistent antibody evolution within crucial paratopes in this lineage beyond those observed in CAP248-2B failed to improve neutralization breadth and potency. Findings presented here have implications for the design of lineage-specific vaccines targeting the gp120-gp41 interface epitope.

Methods

Study Samples

The CAPRISA longitudinal cohort 002 was established in 2004 and has followed participants (specifically high-risk women in the KZN region, South Africa) from acute HIV infection up until ART initiation (Loggerenberg, Mlisana, et al., 2008). CAP248, a CAPRISA 002 cohort participant, was infected with an HIV-1 subtype C virus. PBMC, serum and plasma samples were collected at regular intervals from seroconversion, and were cryopreserved. Peripheral blood mononuclear cells (PBMCs) from 11 - 281 weeks post-infection were collected and stored at -80°C and later used for antibody Next Generation Sequencing (NGS) studies.

Ethics approval

The CAPRISA 002 study was approved by the ethics committees of the University of KwaZulu-Natal (E013/04), the University of Cape Town (025/2004) and the University of the Witwatersrand (M190251 MED19-02-067). Donor CAP248 provided written consent for her samples to be used for further studies.

Cell Lines and Pseudovirus production

For these methods, refer to chapter 2 methods section.

Neutralization assay

Neutralization was measured as a reduction in luciferase gene expression after a single round of infection of TZM-bl cells with Env-pseudotyped viruses. Titers were

calculated as the inhibitor concentrations (IC_{50}) or reciprocal plasma/serum dilutions (ID_{50}) causing a 50% reduction of relative light units (Montefiori DC. 2005).

CAP248-2B lineage next generation sequencing

Total RNA was extracted from cryopreserved PBMC at 10 different time-points (11, 20, 35, 48, 106, 163, 202, 255, 268 and 281 wpi) using the AllPrep DNA/RNA mini kit (QIAGEN). cDNA synthesis was carried out using Random Hexamers (Integrated DNA Technologies) and Superscript III RT enzyme (Invitrogen). Lineage specific forward primers bound leader regions of *IGHV4-31* and *IGLV2-14* and included the Illumina MiSeq barcodes to allow sequencing on the MiSeq. Samples from each time point were amplified as seven replicates for both the heavy and light chains, to ensure adequate coverage and to minimize PCR bias. PCR conditions were based on previous experiments (Scheepers et al., 2015) but modified by altering the annealing temperature and reducing cycles to 25. Nextera XT unique dual indexing combinations selected from Illumina Indexing Kit V2 Set B were added to the pooled MiSeq amplicon libraries. All products were checked on an Agilent Bioanalyser High Sensitivity DNA kit (Diagnostech) and Qubit dsDNA HS assay (ThermoFischer Scientific) and cleaned-up using 0.75X Ampure Beads (Beckman-Coulter). A final concentration of 4.5 pM denatured DNA library with 10% PhiX control (Illumina) was run on the Illumina MiSeq, using the MiSeq reagent kit (version 3) with 2 x 300 paired-end reads.

CAP248-2B lineage analysis

Paired-end MiSeq reads were merged into full-length reads for each time point using PEAR (Zhang et al., 2014). Paired sequences were then de-replicated using USEARCH (Edgar, 2010) resulting in unique reads. The SONAR bioinformatics

pipeline (Schramm et al., 2016) was used to identify CAP248-2B clonally related reads. In brief, germline V and J genes were assigned, the CDR3 regions were identified, and identity to CAP248-2B for each of the reads was calculated. Clonally related sequences were selected based on germline gene usage and CDR3 identity of 80% HC and 85% LC to CAP248. To account for sequencing and/or PCR error, all singletons were removed and the remaining sequences were clustered at 99% identity using USEARCH, and the most abundant representative was selected from clusters with three or more transcripts for downstream analyses. Tools from the immcantation portal were used to reconstruct the antibody lineage and create the phylogenetic tree (Gupta et al., 2015). Briefly, clonally related heavy chain sequences were submitted to IMGT High V-quest (Alamyar et al., 2012; Li et al., 2013) for analysis and the resulting summary files were then parsed into a Change-O database. The UCA of the lineage was used as the germline sequence for the reconstruction. Within R, the Alakazam package (Stern et al., 2014) was used to read in the Change-O database and reconstruct the lineage creating clones and introducing inferred sequences using buildPhylipLineage. The resulting tree was plotted using igraph (Csardi and Nepusz, 2006). The edge lengths of the tree were further modified to be proportional to the number of mutations between nodes.

Antibody production

All heavy and light chain clonally related sequences were paired with the mature CAP248-2B light/heavy chain. Selected clonally related heavy and light chain sequences were ordered from GenScript. For CAP248-2B and the intermediate chimeric antibody expression, plasmids separately encoding heavy and light chain genes were co-transfected and expressed in HEK293F cells (NIH AIDS Reagent

Program) with PEI-MAX (1mg/ml) (Polysciences). Cells were maintained in 293-FreeStyle Expression Medium (GIBCO) at 37°C, 5% CO2, 70% humidity and 125 rpm. Cultures were harvested after seven days by centrifugation at 4000 x g, and supernatants were filtered through a 0.22mm filter. Filtered supernatant antibodies were purified by chromatography using protein A-Agarose (BioVision). Purified antibodies were tested for neutralization activity against pseudoviruses produced as stated above.

Results

CAP248-2B lineage continues to evolve beyond CAP248-2B isolation

In this study longitudinal deep B-cell receptor sequencing was used to trace the evolution of the CAP248-2B lineage, specifically focusing on the long CDRL3 and CDRH1 ^{32}ED^{33}-motif, previously identified as key elements of the CAP248-2B paratope (Wibmer et al., 2017). Sequencing was performed for both the light and heavy chain on the Illumina MiSeq platform from peripheral blood mononuclear cells (PBMCs) at ten time points (11, 20, 35, 48, 106, 163, 202, 255, 268 and 281 wpi). These time points span the development of autologous neutralization (indicated by dark grey boxes, **Fig. 1A**) through increasing plasma breadth (orange and red boxes, **Fig. 1A**), and span the time point at which CAP248-2B was isolated at 189 weeks. Identity-divergence heat map plots, showing the level of divergence away from the heavy and light chain germline genes (x-axis) and percentage identity to CAP248-2B (y-axis), were generated to visualise the sequencing data, with each point representing a unique sequence and the colour indicating relative abundance of the sequences (**Fig. 1A**). Lineage specific sequences appeared as soon as 11 weeks post infection (wpi), followed by the appearance of segregated groups of clonally related heavy and light chain sequences from 106 wpi (**Fig. 1A**). The most pronounced islands of sequences with high levels of SHM and identity to CAP248-2B were observed between 255 - 281 wpi, which also coincided with increased plasma neutralization breadth, as indicated by the red boxes.

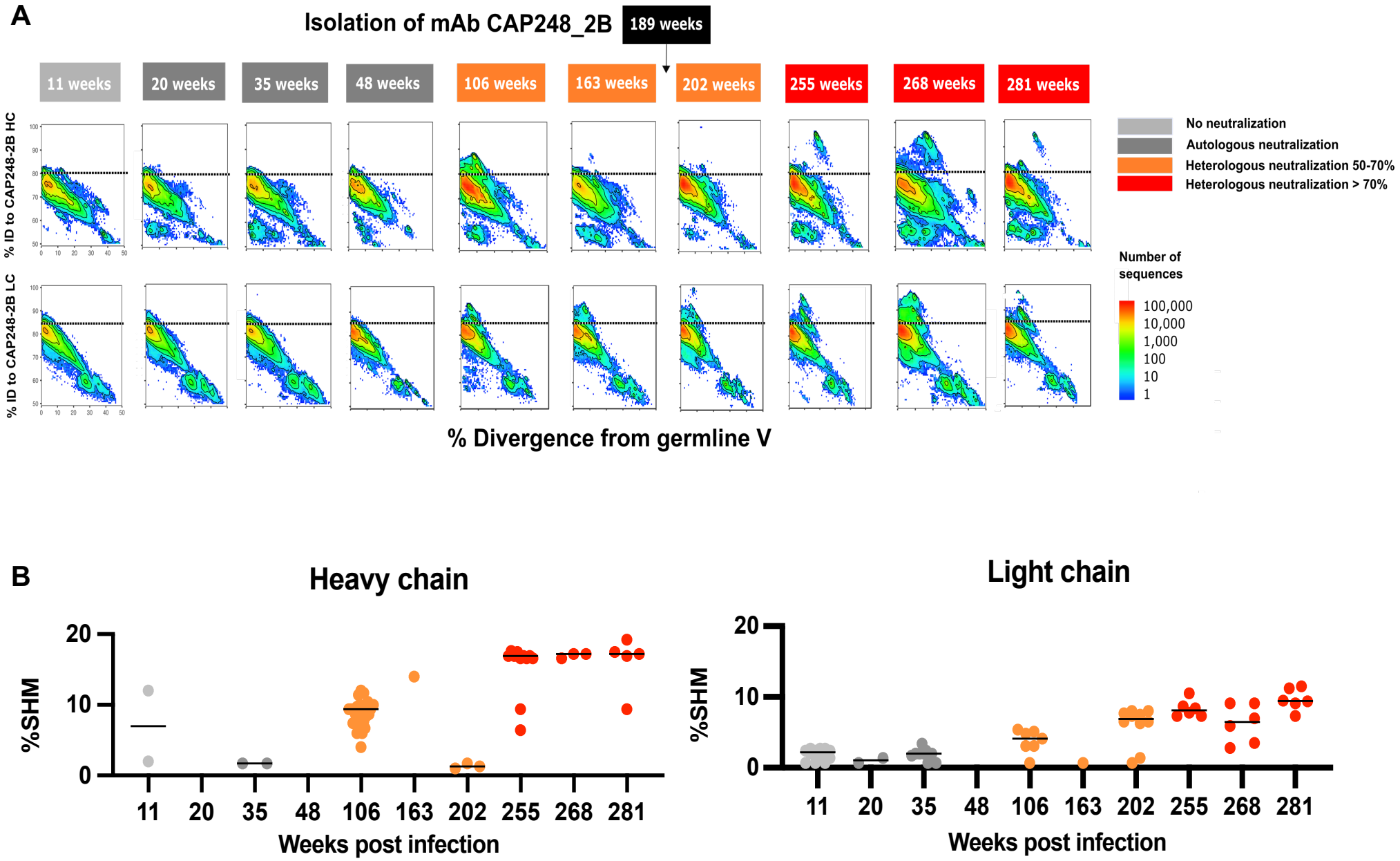
A
Isolation of mAb CAP248_2B
189 weeks
11 weeks
20 weeks
35 weeks
48 weeks
106 weeks
163 weeks
202 weeks
255 weeks
268 weeks
281 weeks
% ID to CAP248-2B HC
% ID to CAP248-2B LC
No neutralization
Autologous neutralization
Heterologous neutralization 50-70%
Heterologous neutralization > 70%
Number of sequences
100,000
10,000
1,000
100
10
1
% Divergence from germline V
B
Heavy chain
Light chain
%SHM
Weeks post infection
11
20
35
48
106
163
202
255
268
281

Figure 1: Identification of CAP248-2B lineage members and level of SHM. (**A**) Timeline in weeks post infection (wpi) spanning the time points when antibody NGS was performed over the course of infection in donor CAP248 is shown as boxes above the identity-divergence plots. Colours indicate plasma heterologous neutralization percentage. The time point at which the CAP248-2B monoclonal antibody was previously isolated (Wibmer et al., 2017) is highlighted in black. Identity-divergence heat map plots showing sequence identity to isolated nAb CAP248-2B (y-axis) versus germline divergence (x-axis) for NGS data are shown below the timeline. Sequences above the dashed line are those with > 80% identity to CAP248-2B HC and > 85% to CAP248-2B LC most likely representing lineage related reads (62 & 47 reads for LC & HC, respectively) and were thus chosen for further investigation. Relative sequence abundance is indicated by the colour (the warmer the colour, the higher the abundance). (**B**) Level of SHM in heavy (left panel) and light chain SHM (right panel) clonally related sequences, compared with their germline genes (*IGHV4-31*05* and *IGLV2-14*01*). For each time-point the solid line represents the average SHM. Clonally related reads for each time-point are coloured according to the level of plasma heterologous neutralization breadth shown in panel **A**.

The level of SHM in both heavy and light chain clonally related reads increased during the course of infection (**Fig. 1B**), with the heavy chain showing higher levels of SHM (maximum: 19.2%) than the light chains (maximum: 11.5%). This data indicates that the lineage continued to evolve beyond CAP248-2B, isolated at 189 wpi and which had moderate SHM (heavy chain = 13% SHM and light chain = 8.3% SHM). The increased SHM within the lineage from 255 wpi, when plasma breadth increased, suggests that there may be broader and more potent mAbs circulating at these later time-points.

Elongation of the functionally important CDRL3 occurs through a nine amino acid long insertion two years after infection

We have previously showed that CAP248-2B interacted with the HIV-1 Env trimer through a long light chain CDRL3 that inserts into the viral membrane (Wibmer et al., 2017). Here we assessed when the extended CDRL3 emerged. We show that the long CDRL3, was absent in the UCA, but appeared from 106 wpi, as a result of a 9 amino acid insertion (**Fig. 2A**). Thereafter, this insertion persisted throughout the lineage (shown in orange in **Fig. 2A and B**). Apart from the nine amino acid insertion in the CDRL3, several other mutations were seen throughout the light chain (**Fig. 2A**). Most notable are charge changes or polar mutations seen in the CDRL2 and FW3/CDRL3 which persist throughout most of the sequences in the lineage.

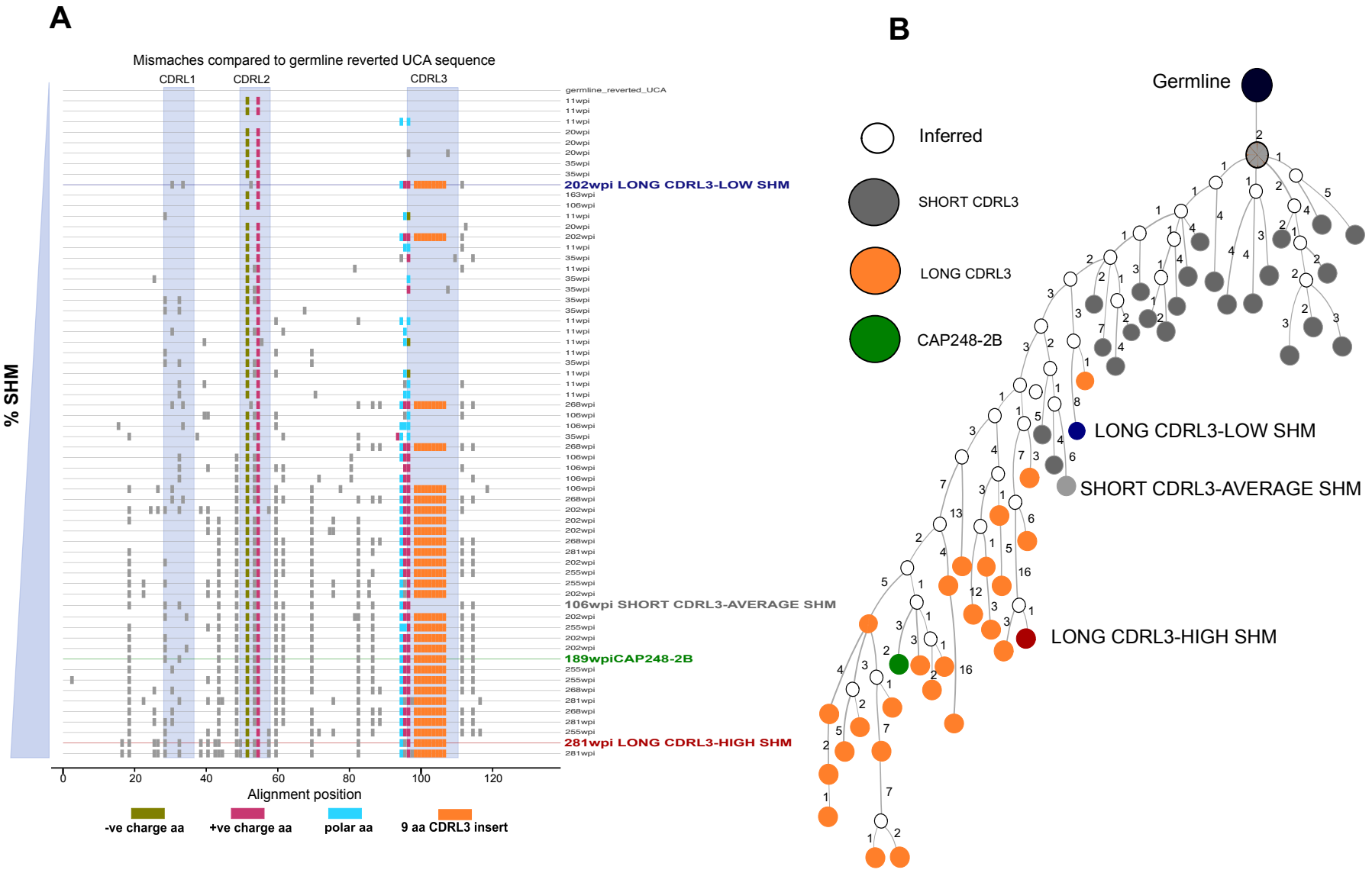
A
Mismaches compared to germline reverted UCA sequence
CDRL1
CDRL2
CDRL3
% SHM
germline_reverted_UCA
202wpi LONG CDRL3-LOW SHM
106wpi SHORT CDRL3-AVERAGE SHM
189wpiCAP248-2B
281wpi LONG CDRL3-HIGH SHM
0
20
40
60
80
100
120
Alignment position
-ve charge aa
+ve charge aa
polar aa
9 aa CDRL3 insert
B
Germline
Inferred
SHORT CDRL3
LONG CDRL3
CAP248-2B
LONG CDRL3-LOW SHM
SHORT CDRL3-AVERAGE SHM
LONG CDRL3-HIGH SHM

Figure 2: Maturation of the CAP248-2B light chain lineage revealed by NGS. (**A**) Highlighter plot showing the appearance of SHM and the extended CDRL3 in the CAP248-2B lineage members. The long CDRL3 is coloured in orange. Light chain sequences used for downstream phenotypic analyses ("SHORT CDRL3-AVERAGE SHM", "LONG CDRL3-LOW SHM" and "LONG CDRL3-HIGH SHM" as well as the sequence of CAP248-2B) are coloured and labelled in grey, blue, red, and green respectively. (**B**) Antibody-lineage reconstruction with sequences coloured by CDRL3 length. Sequences inferred by Change-O, part of the immcantation portal, are indicated as small, transparent grey circles, whereas coloured circles indicate nodes observed in NGS sequences. The number of mutations between nodes is shown as integers, and line lengths between nodes are proportional to those. Nodes indicating the mature (CAP248-2B) sequence, and three light chain sequences used for downstream analyses (denoted as "LONG CDRL3-LOW SHM", "LONG CDRL3-HIGH SHM" & "SHORT CDRL3-AVERAGE SHM") are coloured as in (**A**).

Increasing light chain SHM, rather than the extended CDRL3, is associated with increased neutralization potency.

In order to test the influence of the long CDRL3 and light chain SHM on neutralization breadth we selected three light chain sequences within the lineage for downstream analysis (labelled in **Fig. 2**). These light chains included one sequence with a short CDRL3 and average SHM (7.6%, light grey, chosen because it has SHM similar to nAb CAP248-2B of 8.3%), one with a long CDRL3 but low SHM (1.4%, blue) and one with a long CDRL3 and high levels of SHM (12%, red) (**Fig. 2**). These light chains were paired with the heavy chain of CAP248-2B, and the chimeric antibodies were tested for neutralization against a panel of 11 heterologous pseudoviruses. Titers were compared with the CAP248-2B wild-type nAb (green, **Fig. 3**).

We observed that the antibody with high SHM and a long CDRL3 (red) showed enhanced neutralization potency for all 11 heterologous viruses compared to CAP248-2B (green), as reflected by an upward shift of neutralization plateaus (**Fig. 3**). This increased potency resulted in increased breadth for this antibody, which neutralised six viruses at IC50> 10ug/ml (CAP45, CAP206, CNE52, ZM249, ZM233 and CAP85), compared to only three viruses for CAP248-2B. The difference in neutralization between these two long CDRL3 antibodies, implicates SHM in increased potency. This finding was further corroborated by the comparison of CAP248-2B with the chimeric antibody with a long CDRL3 but low SHM (blue), which showed dramatically reduced titers compared to CAP248-2B for all 11 heterologous viruses, and failed to neutralise any virus with IC50> 10ug/ml. In fact, for 7/11 viruses (ZM233, CAP85, CAP228, Du156, ConC, CAP210 & Du151) neutralization was reduced to less than 20% inhibition at 10 ug/ml. Furthermore, when comparing CAP248-2B with an antibody with similar but not identical levels of SHM, but which did not have a long CDRL3 (grey), we observed enhanced neutralization of all 11 viruses compared to CAP248-2B, and more similar neutralization to the antibody with high levels of SHM (but containing the CDRL3). This finding suggests that the long CDRL3 does not significantly enhance neutralization, and indeed in the context of CAP248-2B, may actually reduce neutralization.

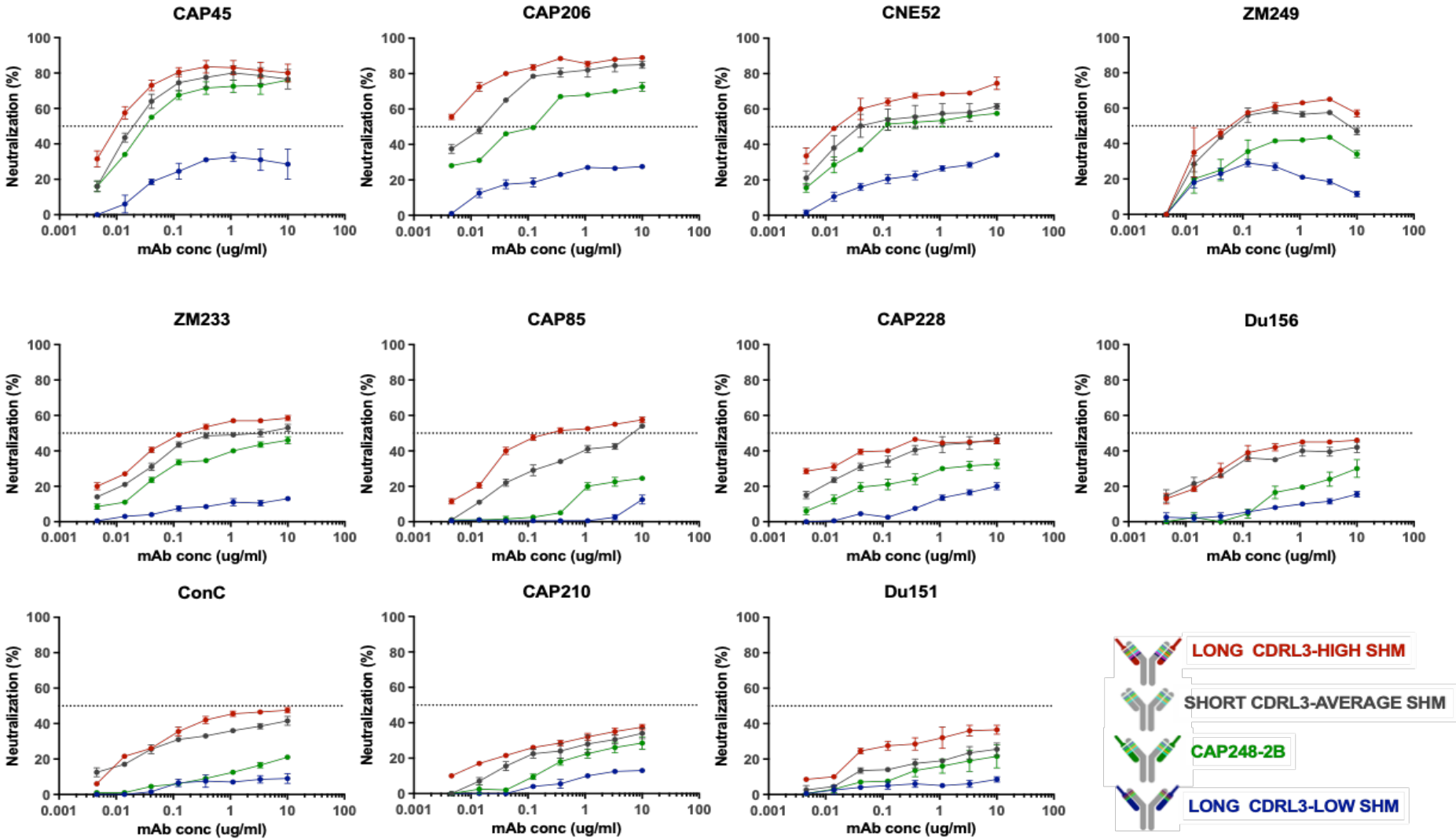
CAP45
CAP206
CNE52
ZM249
ZM233
CAP85
CAP228
Du156
ConC
CAP210
Du151
Neutralization (%)
mAb conc (ug/ml)
0.001
0.01
0.1
1
10
100
0
20
40
60
80
LONG CDRL3-HIGH SHM
SHORT CDRL3-AVERAGE SHM
CAP248-2B
LONG CDRL3-LOW SHM

Figure 3. The effect of increasing SHM and the CDRL3 insertion on neutralization potency. Pseudovirus neutralization plots showing percentage inhibition on the y-axis and antibody concentration on the x-axis. The dotted line depicts 50% inhibition. Antibodies are coloured as follows: LONG CDR3-HIGH SHM in red, SHORT CDRL3-AVERAGE SHM in grey, CAP248-2B in green and LONG CDR3-LOW SHM in blue.

Functionally important CDRH1 ED-motif is rare within the CAP248-2B lineage

We next examined the maturation of the ^{32}ED^{33}-motif within the CDRH1 in the heavy chain, which we have shown to play a crucial role in neutralizing heterologous viruses by CAP248-2B (Wibmer et al., 2017). Within the lineage, sequences with limited evolution, shown on the upper left side of **Fig. 4A**, showed toggling at this position involving ^{32}GY^{33}, ^{32}GD^{33}, ^{32}SD^{33}, ^{32}DE^{33}, ^{32}ED^{33} and ^{32}VD^{33} motifs, away from the ^{32}GG^{33}-motif encoded in the germline of *IGHV4-31*. Thereafter, highly mutated sequences which persisted beyond 255 wpi, maintained the ^{32}VD^{33} motif, with only CAP248-2B isolated at 189 wpi having an ^{32}ED^{33} motif (**Fig. 4B**). This data suggests that the ^{32}VD^{33} motif observed within the lineage may likely be a result of affinity maturation and therefore, is crucial for enhancing neutralization against autologous viruses.

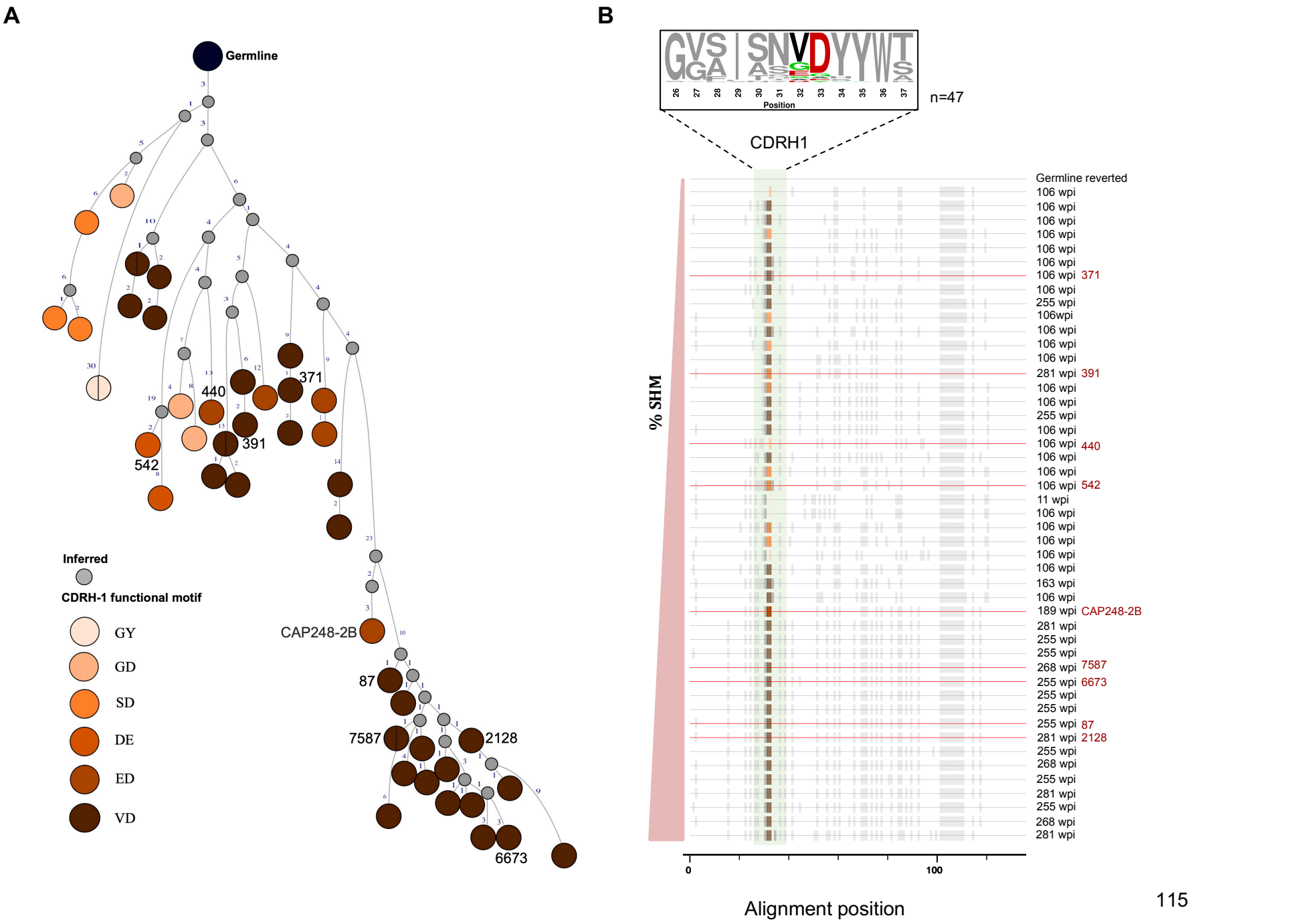
A
Germline
371
440
391
542
CAP248-2B
87
7587
2128
6673
Inferred
CDRH-1 functional motif
GY
GD
SD
DE
ED
VD
B
n=47
Position
CDRH1
% SHM
Germline reverted
106 wpi
106 wpi
106 wpi
106 wpi
106 wpi
106 wpi
106 wpi 371
106 wpi
255 wpi
106wpi
106 wpi
106 wpi
106 wpi
281 wpi 391
106 wpi
106 wpi
255 wpi
106 wpi
106 wpi 440
106 wpi
106 wpi
106 wpi 542
11 wpi
106 wpi
106 wpi
106 wpi
106 wpi
106 wpi
163 wpi
106 wpi
189 wpi CAP248-2B
281 wpi
255 wpi
255 wpi
268 wpi 7587
255 wpi 6673
255 wpi
255 wpi
255 wpi 87
281 wpi 2128
255 wpi
268 wpi
255 wpi
281 wpi
255 wpi
268 wpi
281 wpi
0
100
Alignment position

Figure 4: Tracing the evolution of CAP248 HC functional 32ED33-motif. (**A**) Antibody-lineage reconstruction with sequences coloured by functional 32/33-motif. Sequences inferred by Change-O, part of the immcantation portal, are indicated as transparent grey small circles, whereas coloured circles indicate nodes observed in NGS sequences. The number of mutations between nodes is shown as integers, and line lengths between nodes are proportional to those. (**B**) Highlighter plot showing the appearance of SHM and the different CDRH1, CDRH2, CDRH3 of the CAP248-2B lineage members. The heavy chain sequences used for downstream phenotypic analyses ("371", "391", "440", "542", "7587", "6673", "87", and "2128" as well as the sequence of CAP248-2B) are coloured and labelled in maroon. The Logogram representative of the 47 lineage sequences, shows amino acid toggling at the CDRH1 of the CAP248-HC antibody intermediates. The functional ^{32}ED^{33}-motif is highlighted, showing amino acid toggling. Sequences are aligned according to the level of SHM as indicated by the peach shaded triangle.

Persistent VD-motif alone does not enhance neutralization breadth or potency

In order to test the role of the ^{32}VD^{33} motif, on neutralization breadth and potency, eight heavy chain sequences, with differing levels of SHM and representing different motifs at position 32-33 (labelled in **Fig. 4**), were paired with the CAP248-2B light chain and tested against a panel of six heterologous viruses (CAP45, CAP228, Du151, Du172, WITO and ZM249). The chimeric antibodies were compared to CAP248-2B wild-type that showed different sensitivities to these viruses (i.e. sensitive - 98% plateau, moderate - 52-56% plateau and resistant - 20-34% plateau), (**Fig. 5**).

Our data shows that early intermediates containing a ^{32}DE^{33} motif (542) and ^{32}GD^{33}-motifs (440) had poor neutralization activity compared to CAP248-2B, containing the ^{32}ED^{33} motif (**Fig. 5**). We noted a wide range of neutralization profiles amongst the

antibodies containing the ^{32}VD^{33}-motif. Surprisingly, despite the persistence of the ^{32}VD^{33} motif within the lineage, the majority of the ^{32}VD^{33} mAbs tested showed reduced neutralization compared to CAP248-2B (**Fig. 5**). The more mutated of the ^{32}VD^{33} motif mAbs (87 and 2128), however, were able to neutralise one additional virus (ZM249) compared to CAP248-2B though they had overall lower geometric mean of maximum inhibition (GMI) across all viruses. This data suggests that the introduction of the ^{32}VD^{33} motif alone is not enough to improve neutralization breadth and potency.

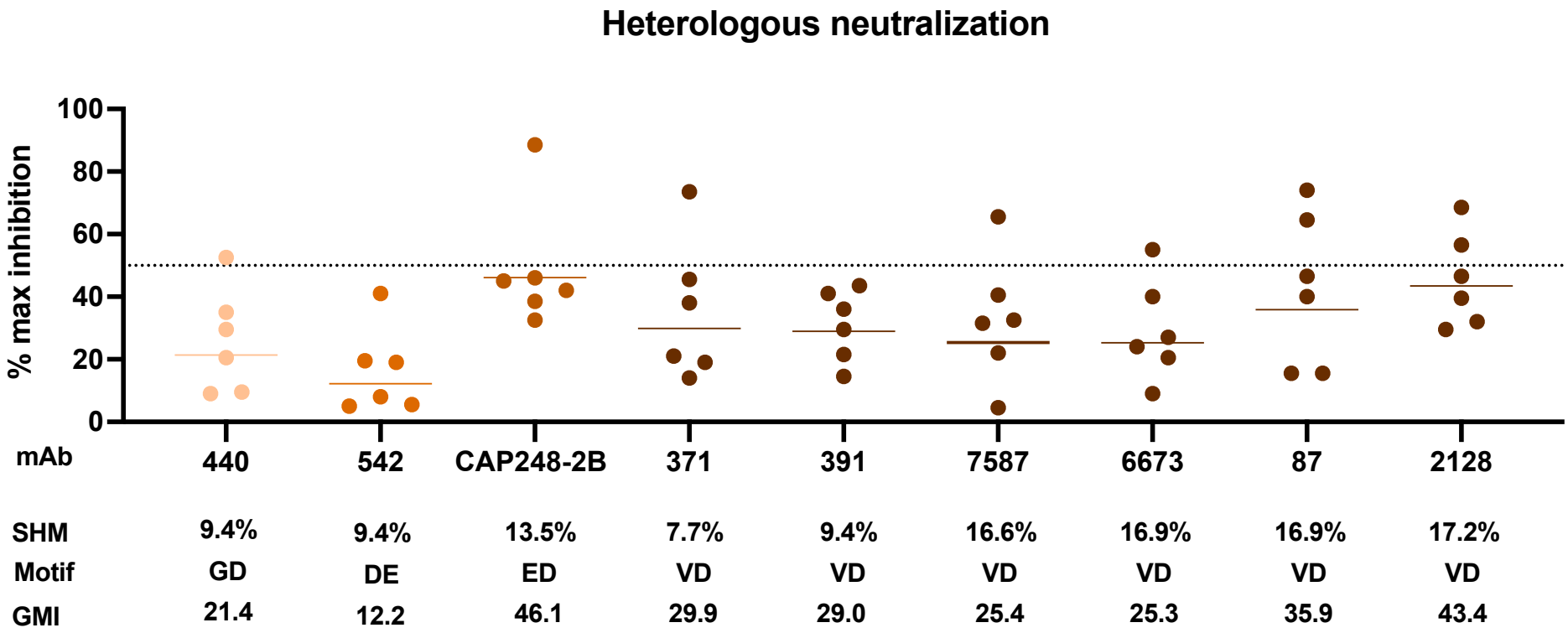

Figure 5: Neutralization profiles of CAP248 lineage antibodies. Heterologous neutralization of CAP248 lineage members. CAP248 chimeras and CAP248-2B were tested against six heterologous viruses (CAP45, CAP228, Du151, Du172, WITO & ZM249). Shown are the % maximum neutralization for each antibody where the solid horizontal line represents geometric mean inhibition. The level of SHM, specific motif within the CDRH1 (DE/GD/ED/VD) and geometric mean inhibition are shown for each mAb below the graph.

CAP248-2B lineage members share similar glycan shield interactions to CAP248-2B.

BNAbs targeting the gp120-gp41 interface, identified to date, depend on various highly conserved glycosylation sites for neutralization, excluding 3B315 (Lee et al., 2015). The CAP248-2B epitope is close to several N-linked glycans in Env, specifically N88, N611, N616, N625, and N637. We have previously shown that some of these glycans (N88, N230 and N625) obscure the CAP248-2B epitope and that their removal enhances the neutralization potency of CAP248-2B (Wibmer et al., 2017). To test the influence of these glycans on lineage members, we made glycan knock-out mutants in CAP45 (which is neutralised by the majority of the CAP248-2B lineage heavy chain mAbs) and tested for altered sensitivity compared to CAP45 wild-type (**Fig. 6**). Like CAP248-2B, the majority of the lineage members tested showed enhanced neutralization potency of CAP45 after the removal of the glycans N88, N616, N625 and N637 (**Fig. 6B**). However, the early intermediates (391 and 542 as labelled in **Fig. 6B**) showed weak neutralization resulting in little improvement especially against N616A, N625A, S613A and N637A (**Fig. 6B**). The removal of the N611 glycan (by mutating the amino acid at position S613) had little effect on mAb 371 and CAP248-2B (**Fig. 6B**, labelled), consistent with our previous report (Wibmer et al., 2017). However other lineage members showed reduced neutralization potency to CAP45 when the N611 glycan was removed, though this was not statistically significant (**Fig. 6B**). Overall this data suggests that CAP248-2B lineage members share similar interactions with the glycan shield around the gp120-gp41 interface as CAP248-2B.

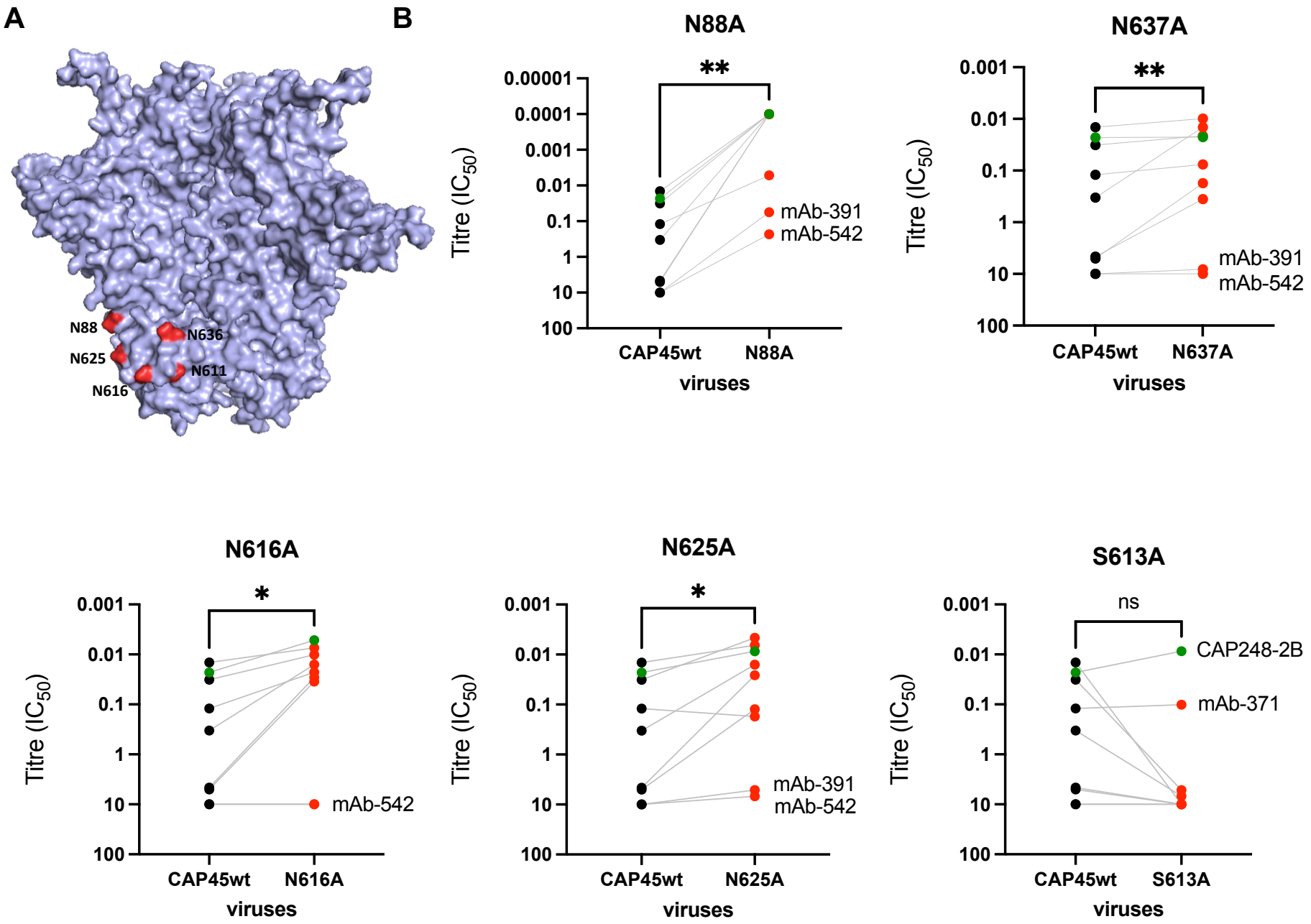
A
B
N88
N636
N625
N611
N616
N88A
**
0.00001
0.0001
0.001
0.01
0.1
1
10
100
Titre (IC50)
mAb-391
mAb-542
CAP45wt
N88A
viruses
N637A
**
0.001
0.01
0.1
1
10
100
Titre (IC50)
mAb-391
mAb-542
CAP45wt
N637A
viruses
N616A
*
0.001
0.01
0.1
1
10
100
Titre (IC50)
mAb-542
CAP45wt
N616A
viruses
N625A
*
0.001
0.01
0.1
1
10
100
Titre (IC50)
mAb-391
mAb-542
CAP45wt
N625A
viruses
S613A
ns
0.001
0.01
0.1
1
10
100
Titre (IC50)
CAP248-2B
mAb-371
CAP45wt
S613A
viruses

Figure 6: Glycan shield around the gp120-gp41 interface obscures CAP248-2B lineage neutralization. (**A**) The HIV-1 HXB2 envelope structure showing the positions of the glycans in 3D that we tested. (**B**) The antibody IC_{50} and neutralizing activity of the CAP248 lineage antibodies ($n = 9$) against CAP45 wild-type and CAP45 glycan mutants. Green colour shows CAP248-2B. Labelled mAbs in panel B show subtle to no neutralization enhancement. P values shown in the figures were determined using Wilcoxon matched-pairs signed rank test (* $P < 0.05$, ** $P < 0.005$, ns = non-significant).

Discussion

Lineage-specific vaccine strategies which aim to use sequential immunogens to program the antibody response of un-infected individuals towards the development of broad neutralizing antibodies will be possible only if we deeply understand ontogeny of HIV bNAbs during HIV infection. There are several HIV-1 bNAb ontogeny studies that have been conducted to date (Moore et al., 2012; Liao et al., 2013; Doria-Rose, Schramm, et al., 2014; Bhiman et al., 2015; Wu et al., 2015; Van Gils et al., 2016; Landais and Moore, 2018; Shen et al., 2020). These studies have provided a roadmap for eliciting lineage-specific vaccine responses. Our group has previously isolated and characterised an interface-directed nAb called CAP248-2B, showing that this mAb interacted with the HIV-1 Env trimer through a long light chain CDRL3 that inserts into the viral membrane and a heavy chain CDRH1 ^{32}ED^{33} motif that interacted with gp41 (Wibmer et al., 2017). Here we sought to define the development of these two key features of CAP248-2B by longitudinally sequencing PBMCs from donor CAP248. We show that the long CDRL3 came about during SHM involving a nine amino acid insert and that the CDRH1 motif at position 32-33 was under immune pressure early on in the lineage displaying a number of different motifs, with ^{32}ED^{33} being rare (both in frequency and mutational event). Overall, these results delineate the pathways associated with development of the CAP248 lineage which gave rise to CAP248-2B, a modestly neutralising gp120-gp41 interface-specific antibody.

Despite the interaction of the long light chain CDRL3 of CAP248-2B with the HIV-1 Env trimer (Wibmer et al., 2017), we showed that it did not confer a neutralization breadth benefit. It is intriguing therefore that this long CDRL3 persists throughout the

lineage. This is likely due to maturing against CAP248 autologous viruses which have accumulated uncommon mutations at the gp120-gp41 interface (Wibmer et al., 2017), and, hence, it might be beneficial for the neutralization of CAP248 autologous viruses and not heterologous viruses.

We hypothesise that a shorter CDRL3 presents the antibody with a plethora of options for binding and angles of approach and thus resulting in improved neutralization plateaus against heterologous viruses. Whereas the long CDRL3 seen in CAP248-2B may impose structural constraints that force CAP248-2B to be orientated in one specific conformation with an angle of approach that does not promote favourable interactions with the epitope. This is in line with previous studies on CD4bs bNAbs, which showed that these Abs have shorter loops that bind favourably to their epitope by avoiding steric clashes and thus improving neutralization (Zhou et al., 2013; Jardine et al., 2013 and Zhou et al., 2015).

Here we further provide evidence that increased light chain SHM slightly improves neutralization. Analysis of light chain lineage sequences shows that the majority of SHM is found at the FWs regions. Therefore, suggesting that the SHM likely contributes to potency by stabilising the paratope in a favourable conformation rather than interacting with the antigen directly. This is in line with previous studies that showed that the FWs in bNAbs are crucial for maintaining conducive structural orientations, and hence, changes in these regions can have deleterious or beneficial effects on bNAbs (Klein et al., 2013; Kondo et al., 2019).

Our data show that the CDRH1 is subject to early immune selection pressure, specifically at the positions 32 and 33, known to be key contact sites (Wibmer et al., 2017). This is in line with other studies that have shown that paratopes evolve with their epitopes to neutralize the pathogen (Landais and Moore 2018). Furthermore, the lineage development of the interface mAb VRC34.01 also depended on mutations at position 33 in the CDRH1 (Shen et al., 2020) similar to our findings. We looked at the types of mutations that occurred in the HCs of lineage members to ascertain whether they are “common” or “rare”. “Common” mutational events are characterised by single nucleotide base pair changes (Sacks et al., 2019). Conversely, “rare” mutational events are characterised by two nucleotide base pair changes (Sacks et al., 2019). Looking at the kind of mutations at nucleotide level for early members of the lineage we showed that they tend to be single base pair changes, thus resulting in “common” mutational events. Conversely, the nucleotide changes seen for later lineage members including ^{32}ED^{33} and ^{32}VD^{33} tend to be as a result of two base pair changes, thus making these changes “rare” mutational events. This is in line with previous studies which have shown that rare and improbable mutations are responsible for the development of bNAbs (Shen et al., 2020, Sacks et al., 2019 and Wiehe et al., 2018). Altogether, this suggests that the CAP248-HC lineage evolution against autologous virus, favoured the accumulation of rare amino acids at the CDRH1 ^{32}ED^{33} and ^{32}VD^{33} -motif as a result of affinity maturation process.

Similar to what has been reported in the literature for bNAb evolution (Sok et al., 2013), we showed that SHM in these lineage members correlates with increased breadth or potency. However, the observed improvement is not drastic, especially for the heavy chains. This might be due to the both HCs and LCs SHM being in the framework

regions which supports the flexibility of binding rather than being at the active site and interacting with the antigen. This trend has also been observed in other studies (Walker et al., 2009, Walker et al., 2011, Jardine et al., 2016 and Griffith et al 2021). Another possible reason for the observed modest neutralization by the more mutated lineage members is that we have tested these HCs in isolation by artificially pairing them with CAP248-2B LC, which has modest SHM instead of pairing it with a highly mutated LC as seen in later lineage members. Therefore, because this is not the native pairing of HCs and LCs, it is possible that this artificial pairing may be obscuring the contribution of the persistent VD-motif and SHM.

A previous report by (Wibmer et al., 2017) showed that the nAb CAP248-2B is glycan independent, because removal of glycans surrounding the interface region did not result in improved or knock out neutralization. Here, we show that the glycan shield at the interface region negatively affects the neutralization profiles of CAP248 lineage mAbs because removal of these interface surrounding glycans resulted in improved neutralization potency. This suggests that much like CAP248-2B, the lineage members target the underlying residues. Similarly, mAb-371 and mAb-2B were not negatively affected by a glycan change at position 611 (N611A), while the rest of the lineage members were negatively affected. This implies that these mAbs seem to be N611 glycan dependent. This is similar to what has been seen in other gp120-gp41 interface-specific bNAbs like PGT151 which is N611-dependent (Falkowska et al., 2014).

Overall, our findings demonstrate how the critical antibody paratope has evolved overtime to give rise to a modestly neutralizing gp120-gp41 interface nAb CAP248-

2B. Moreover, we show that during antibody evolution the pathway taken does not always result in the development of potent bNAbs. The data presented here also suggest that in order to elicit potent and broad interface-directed bNAbs, it is imperative to understand the ontogeny of the bNAb responses we want to elicit and then use tailored sequential immunogens that precisely favour the selection of the respective bNAb response.

Chapter 5

Conclusion

An effective vaccine against HIV will likely need to elicit bNAbs that target conserved epitopes within the HIV-1 Env. In the early 1990s only four bNAb epitopes had been identified: (1) the CD4-binding site (Barbas et al., 1992; Burton et al., 1994); (2) the membrane proximal external region (Muster et al., 1993; Stiegler et al., 2001; Zwick et al., 2001); (3) a glycan patch on gp120 that includes the N332 glycan (Trkola et al., 1996); and (4) the tip of the V3 loop (Gorny et al., 1992). These were targeted by first generation bNAbs such as b12, 2F5, 4E10, 2G12, and 447-52D which had limited levels of breadth and potency. Since those early discoveries, a total of eight bnAb epitopes on the HIV-1 Env have been identified and are targeted by the highly potent and broad next generation bNAbs subsequently isolated as technological advances were made. This has refuelled the interest in eliciting such responses by vaccination. The continued identification of new targets on the Env and subsequent isolation of bNAbs targeting these new sites has expanded our understanding of shared traits between bNAbs in terms of their developmental kinetics, shared germline genetics and their structural properties. Furthermore, these studies may lead to the design of immunogens capable of eliciting bNAbs while circumventing the restrictive immunological regulation checkpoints, thus expanding avenues to explore for HIV vaccine development.

The HIV-1 FP was not known to be a target of bNAbs until mAbs VRC34 and ASC202 targeting this site were isolated, and it has subsequently become a major vaccine target (Kong et al., 2016; van Gils et al., 2016). Several preclinical studies in animal

models have shown the possibility of eliciting FP directed bNAbs, further fueling the interest in developing a vaccine scheme that will elicit such responses in humans (Xu et al., 2018; Cheng et al., 2019; Kong et al., 2019; Mogus et al., 2020; Cheng et al., 2020; Chuang et al., 2020). Many studies have also outlined the complexity of eliciting HIV-1 bNAb responses by traditional approaches, and thus suggested the use of lineage-based vaccination followed by a sequential immunization scheme. This approach is reliant on understanding both the evolution of strain-specific responses and autologous virus escape throughout the course of infection. Unfortunately, since few FP-specific bNAbs have been isolated, little is known about their virus-antibody coevolution. This presents limitations for eliciting FP-specific responses by vaccination using the currently pursued lineage-based and immunofocusing approach. This further highlights the need for more studies to fully understand the developmental kinetics, shared germline genetics and structural properties of FP-specific bNAbs.

Functionally, the FP is used by HIV-1 for the fusion process between the virus and the host-cell during infection. It is part of a larger epitope, located in the gp120-gp41 interface region-a bNAb epitope that is also of great interest to the field. Because of this, in this thesis we have focused on understanding the factors that influence the development of the responses directed to these two epitopes. Here, we have explored the prevalence of FP-directed Ab responses in an African PLWH cohort, and isolated three new FP-specific mAbs (AIRU-G4, AIRU-G9 & AIRU-F8). Furthermore, we elucidated the ontogeny of gp120-gp41 interface specific neutralizing mAb CAP248-2B. These studies may contribute towards the development of a successful FP-specific HIV-1 bNAb lineage vaccine.

In chapter two we show that the prevalence of FP-specific responses is 13% in our cohort, which is lower than observed in other cohorts which was recorded as 38% (Ditse et al., 2018; Huang et al., 2014). This suggests, with the caveats associated with our screening approach, that FP-directed mAbs may be infrequently elicited in adult clade C infection. In some rare cases, as we observed for CAP312, however, these may be elicited early in infection and mature overtime to acquire breadth. This suggests eliciting FP responses will likely be complex and lengthy just like eliciting a CD4bs specific response, which is not ideal for a vaccine. Furthermore, compounding this observation is that the FP is genetically diverse among circulating viruses, therefore using a single FP immunogen, designed based on the FP sequence commonly seen in circulating viruses such as “AVGIGAVF”, will likely not elicit the desired broad FP responses in the majority of people. This suggests that in order to elicit the desired broad FP responses in the majority of people by vaccination, and thus achieve a higher prevalence, multiple FP immunogens may need to be used simultaneously. Also, this suggests that these FP immunogens may need to be precisely designed by mutation guided approaches and used for sequential immunization to shepherd and immunofocus the responses towards the FP region. However, even if better breadth can be achieved with FP-directed bNAbs alone, a protective and efficacious HIV-1 vaccine will likely require simultaneous targeting of two or more epitopes.

Current studies that have shown the prevalence of interface responses (Landais et al., 2016; Huang et al., 2014) have not used specific FP mutants and peptides in their screening process. In this study we have identified gaps which include the need to

look at more adult cohorts with different HIV-1 subtypes using FP specific mutants to explore if indeed FP responses are infrequently elicited in adults and why if that is the case. Furthermore, the use of only three FPs in screening and determining the prevalence of such responses in natural infection is a limitation. This is because only participants with mAb responses directed to the peptides we used were identified, and participants with autologous responses to FPs we did not use were likely not detected. Future studies should aim to use autologous (sequence-matched) FPs and expand the peptides used for screening purposes. Additionally, more longitudinal studies are warranted in different cohorts and donors because these may enable us to understand predictive pathways for FP responses, as it has been done for CD4bs, V2, MPER and N332 responses (Briney et al., 2016; Sok et al., 2016; Tian et al., 2016; Andrabi et al., 2015; Gorman et al., 2016; Moore et al. 2017; Bonsignori et al., 2017; McLeod et al., 2017; Scheepers et al., 2022; Irimia et al., 2016). Lastly, future studies will need to link the autologous sequences to FP-directed responses, to assess whether some viral FP sequences are more likely to imprint FP bNAbs or not, just as seen in macaque studies by Cheng et al., (2020). Such studies will benefit the development of a FP-based vaccine.

The isolation and characterisation of new FP-specific antibodies, as shown in chapter three, revealed a trend of shared gene usage and bNAb structural features between isolated bNAbs and our bNAbs. Here we have uncovered the genetic convergence between FP antibodies towards IGHV3-30, which are also shared by FP-directed mAbs ACS202 and PGT151 (van Gils et al., 2016; Falkwoska et 2014). A study by Scheepers et al., (2015) showed that this IGHV3-30 gene, shared by FP bNAbs, is commonly present in PLWH genome. This shared germline usage phenomenon is

similar to that of many CD4bs-targeting bNAbs that share IGHV1-2, MPER bNAbs which share IGHV1-69 and the N332 specific bNAbs sharing IGHV4-34 gene (Wu et al., 2010; Zhou et al., 2015; Roskin et al., 2020; Scheepers et al., 2022; Moyo et al., 2020). This suggests that there are public B cell clonotypes in unrelated PLWH from different cohorts, as has been reported for other pathogens such as influenza and SARS-CoV-2 (Joyce et al., 2016; Pappas et al., 2014; Zost et al., 2021; Sui et al., 2009; Wheatley et al., 2015; Dong et al., 2021; Nielsen et al., 2020; Yuan et al., 2020; Robbiani et al., 2020; Pushparaj et al., 2023). Furthermore, this highlights that people may be intrinsically capable of eliciting anti-HIV-1 bNAbs if the correct immunogen targeting a specific common germline (germline-targeting) was used.

Given the commonality of the IGHV3-30 gene in PLWH, this suggests that germline targeting vaccination to stimulate protective FP-specific responses may widely trigger such responses and therefore, it is worth exploring further. However, a common concern is that the bNAb germline-targeting strategy will only work if people have the rare subset of naive B cells germline immunoglobulin alleles that are being targeted (Moore 2022). Additionally, our experience of germline-targeting immunogens thus far is that even if the correct responses are triggered in animal models and human studies, they are often weak and elicit narrow immune responses in animal models and human studies, which may not be sufficient to protect against HIV-1 infection, and hence, additional boosting will be required to enhance these responses. In summary, despite the challenges we currently have, there are potential avenues to elicit FP responses by vaccine that will need further exploration and refined understanding.

In addition to shared germline gene usage, bNAbs have unusual features such as the long CDHRs and high SHM and these correlate with increased neutralization breadth (Klein et al., 2013; Sok et al., 2016; McLeod et al., 2016; Griffith et al., 2021). Although these features are often required for breadth, emerging evidence suggests that not all such unusual features nor levels of high SHM necessarily contribute to increased breadth (Sacks et al., 2019; MacLeod et al., 2016). As a further example of this, we show in chapter four of this thesis that the long CDRL3 observed for the gp120-gp41 interface specific neutralizing mAb CAP248-2B that we assumed might be essential for breadth, was in fact associated with reduced heterologous neutralization effects. Moreover, for CAP248 we confirm that SHM was not necessarily important for breadth, because highly mutated CAP248-2B lineage members did not exhibit significantly improved neutralization breadth compared to the CAP248-2B neutralizing mAb. However, we note that antibodies develop against autologous viruses, therefore, in CAP248, it is possible that these unusual features are needed to potently neutralize autologous viruses but they are not necessary for heterologous viruses.

Here, we further showed that the appearance of the unusual and long CDRL3 occurred early on during antibody evolution against CAP248 autologous viruses. Furthermore, the appearance of the crucial ^{32}ED^{33} motif at the CDRH1 region of CAP248-2B nAb was not present in early lineage members, but appeared sporadically and was replaced by the ^{32}VD^{33} motif in later lineage members. This suggests that possibly during autologous virus escape against the lineage, a rare evolutionary event triggered the appearance of the ^{32}ED^{33} motif. These findings show that lineage development does not always necessarily result in lineage members with broader neutralization activity, however, breadth and heterologous potency are sometimes serendipitous by-

products of evolution against certain autologous viruses. Our findings provide information on how complex immunological responses are following infection while also highlighting the complexity and stochastic nature of shepherding the strain-specific responses towards broader responses. Overall, our CAP248-2B ontogeny study identified random events that deviated the lineage development from the path of breadth towards the path of limited breadth. More ontogeny studies of other gp120-gp41 interface-directed bNAbs are warranted to identify common, productive routes to breadth for this epitope.

Limitations identified in this study include not using paired antibody deep sequencing to define the ontogeny of the gp120-gp41 interface specific CAP248-2B mAb. This would have enabled us to amplify the heavy and light chains as they naturally occur in a B-cell, compared to the artificial pairing technique we have used here. The use of more recent technologies like LibraSeq would have provided a wealth of data linking the antigens and the paired antibody heavy- and light chains per B-cell (Setlif et al., 2019). For CAP248, using autologous derived viruses would allow us to precisely trace the development and evolution of the bNAb and non-bNAb lineages, thus allowing us to deeply understand the determinants of breadth for broader lineage vs non-broad lineage. However, still few studies for the other epitopes have not used this technology, raising questions such as: by not using this technology, have we identified all the possible mechanisms that influence lineage development in these donors?

Focusing on the virological features that influenced the development of the CAP248-2B lineage, we show that unlike other interface directed bNAbs, CAP248-2B and the intermediate mAbs do not appear to rely on glycans for neutralization. This is shown

in chapter four that removal of the glycans surrounding the gp120-gp41 interface resulted in improved neutralization instead of knock-out. This data further suggest that to elicit CAP248-2B-like bNAbs, the immunogens must have glycan holes at the interface region as this will expose the epitope targeted by such antibodies. For vaccine immunogen design this is ideal as it reduces the complexity of immunogen design to elicit bNAb responses. Another limitation in our study is that we did not evaluate autologous virus evolution to identify the viral variants that drove the development of the limited neutralization breadth lineage. Future studies should focus on the use of the PacBio approach to do deep sequencing of the autologous viruses as this can sequence the *env* gene at once without the need to do manual alignments of partially sequenced gene segments. Using PacBio would provide us the opportunity to precisely determine and trace the viral variants that could potentially shepherd the lineage towards broader and more potent bNAb intermediates.

Future studies should aim to precisely determine the epitope of the isolated FP-specific mAbs while defining the mechanism of virus escape and elucidate their maturation pathways. Such studies would provide insight into the binding and interaction of these mAbs with Envs which may inform the design of germline targeting immunogens to trigger FP responses. Also, future studies should focus on performing antibody-trimer structural analyses and explore the determinants of strain-specific versus broadly neutralizing FP directed antibodies. In the past, such studies led to discoveries of unmutated common ancestor (UCA), transmitted founder virus (T/F), improbable mutations concept, B cell lineage immunogen design, germline-targeting, mutation-guided immunogen design, and structure-based immunogen design, all of which are yielding promising data in preclinical trials and proof-of-concept studies

(Haynes et al., 2012; Jardine et al., 2016; Wiehe et al., 2018; Burton et al., 2017; Kepler et al., 2014; Keele et al., 2008). In summary, continued research into the mechanisms of bNAb development, the identification of new bNAb specificities, and the development of novel immunization strategies will be critical in the effort to combat HIV/AIDS.

References

1. Barré-Sinoussi, F. *et al.* Isolation of a T-lymphotropic retrovirus from a patient at risk for acquired immune deficiency syndrome (AIDS). *Science* **220**, 868–71 (1983).
2. Barré-Sinoussi, F., Ross, A. L. & Delfraissy, J.-F. Past, present and future: 30 years of HIV research. *Nat. Rev. Microbiol.* **11**, 877–883 (2013).
3. Maartens, G., Celum, C. & Lewin, S. R. HIV infection: epidemiology, pathogenesis, treatment, and prevention. *Lancet* **384**, 258–271 (2014).
4. Deeks, S. G., Overbaugh, J., Phillips, A. & Buchbinder, S. HIV infection. *Nat. Rev. Dis. Prim.* **1**, 15035 (2015).
5. Abdool Karim, Q., Baxter, C. & Birx, D. Prevention of HIV in Adolescent Girls and Young Women. *JAIDS J. Acquir. Immune Defic. Syndr.* **75**, S17–S26 (2017).
6. van Heuvel, Y., Schatz, S., Rosengarten, J. F. & Stitz, J. Infectious RNA: Human Immunodeficiency Virus (HIV) Biology, Therapeutic Intervention, and the Quest for a Vaccine. *Toxins 2022, Vol. 14, Page 138* **14**, 138 (2022).
7. Joseph, S. B., Swanstrom, R., Kashuba, A. D. M. & Cohen, M. S. Bottlenecks in HIV-1 transmission: insights from the study of founder viruses. *Nat. Rev. Microbiol. 2015 137* **13**, 414–425 (2015).
8. Abdool Karim, Q. *et al.* Effectiveness and safety of tenofovir gel, an antiretroviral microbicide, for the prevention of HIV infection in women. *Science* **329**, 1168–74 (2010).
9. Parren, P. W. H. I. *et al.* Antibody Protects Macaques against Vaginal Challenge with a Pathogenic R5 Simian / Human Immunodeficiency Virus at Serum Levels Giving Complete Neutralization In Vitro. **75**, 8340–8347 (2001).
10. Hessell, A. J. *et al.* Broadly Neutralizing Human Anti-HIV Antibody 2G12 Is Effective in Protection against Mucosal SHIV Challenge Even at Low Serum Neutralizing Titers. **5**, (2009).
11. Korber, B. *et al.* Evolutionary and immunological implications of contemporary HIV-1 variation. *Br. Med. Bull.* **58**, 19–42 (2001).
12. Moldt, B. *et al.* Highly potent HIV-specific antibody neutralization in vitro translates into effective protection against mucosal SHIV challenge in vivo. *Proc. Natl. Acad. Sci. U. S. A.* **109**, 18921–5 (2012).

13. Lewis, G. K., Pazgier, M. & DeVico, A. L. Survivors Remorse: antibody-mediated protection against HIV-1. *Immunol. Rev.* **275**, 271–284 (2017).
14. Corey, L. *et al.* Two Randomized Trials of Neutralizing Antibodies to Prevent HIV-1 Acquisition. *N. Engl. J. Med.* **384**, 1003–1014 (2021).
15. Wu, X. *et al.* Rational design of envelope identifies broadly neutralizing human monoclonal antibodies to HIV-1. *Science* **329**, 856–61 (2010).
16. Zhou, T. *et al.* Structural basis for broad and potent neutralization of HIV-1 by antibody VRC01. *Science* **329**, 811–7 (2010).
17. Ehreth, J. The value of vaccination: a global perspective. *Vaccine* **21**, 4105–4117 (2003).
18. Halper-Stromberg, A. *et al.* Broadly neutralizing antibodies and viral inducers decrease rebound from HIV-1 latent reservoirs in humanized mice. *Cell* **158**, 989–999 (2014).
19. Plotkin, S. A. Correlates of Vaccine-Induced Immunity. *Clin. Infect. Dis.* **47**, 401–9 (2008).
20. Stanfield, R. L., Wilson, I. A. & Crowe, J. E. Antibody Structure. (2014). doi:10.1128/microbiolspec.AID
21. Maizels, N. Immunoglobulin Gene Diversification. *https://doi.org/10.1146/annurev.genet.39.073003.110544* **39**, 23–46 (2005).
22. Nguyen, T. V., Pawlikowska, P., Firlej, V., Rosselli, F. & Aoufouchi, S. V(D)J recombination process and the Pre-B to immature B-cells transition are altered in Fanca−/− mice. *Sci. Reports 2016 61* **6**, 1–11 (2016).
23. Bhiman, J. Viral variants that initiate and drive maturation of V1V2-directed HIV-1 broadly neutralizing antibodies. *Nat. Med.* **21**, 1332–1336 (2015).
24. Locci, M. *et al.* Human circulating PD-1 + CXCR3-CXCR5+ memory Tfh cells are highly functional and correlate with broadly neutralizing HIV antibody responses. *Immunity* **39**, 758–769 (2013).
25. Walker, L. M. *et al.* Broad and Potent Neutralizing Antibodies from an African Donor Reveal a New HIV-1 Vaccine Target. *Science (80-.).* **326**, 285–289 (2009).
26. Doores, K. J. & Burton, D. R. Variable Loop Glycan Dependency of the Broad and Potent HIV-1-Neutralizing Antibodies PG9 and PG16 □. **84**, 10510–10521 (2010).
27. Pancera, M. *et al.* Crystal Structure of PG16 and Chimeric Dissection with

Somatically Related PG9 : Structure-Function Analysis of Two Quaternary-Specific Antibodies That Effectively Neutralize HIV-1 □ §†. **84**, 8098–8110 (2010).

28. Pejchal, R. *et al.* Structure and function of broadly reactive antibody PG16 reveal an H3 subdomain that mediates potent neutralization of HIV-1. (2010). doi:10.1073/pnas.1004600107
29. Briney, B. S., Willis, J. R. & Crowe, J. E. Human Peripheral Blood Antibodies with Long HCDR3s Are Established Primarily at Original Recombination Using a Limited Subset of Germline Genes. **7**, 1–13 (2012).
30. Klein, F. *et al.* Somatic mutations of the immunoglobulin framework are generally required for broad and potent HIV-1 neutralization. *Cell* **153**, 126–38 (2013).
31. Sok, D. *et al.* The Effects of Somatic Hypermutation on Neutralization and Binding in the PGT121 Family of Broadly Neutralizing HIV Antibodies. *PLoS Pathog.* **9**, e1003754 (2013).
32. Wu, X. *et al.* Maturation and Diversity of the VRC01-Antibody Lineage over 15 Years of Chronic HIV-1 Infection Article Maturation and Diversity of the VRC01-Antibody Lineage over 15 Years of Chronic HIV-1 Infection. 1–16 (2015). doi:10.1016/j.cell.2015.03.004
33. Schatz, D. G. & Ji, Y. Recombination centres and the orchestration of V(D)J recombination. *Nat. Rev. Immunol. 2011 114* **11**, 251–263 (2011).
34. Verkoczy, L., Kelsoe, G., Moody, M. A. & Haynes, B. F. Role of immune mechanisms in induction of HIV-1 broadly neutralizing antibodies. *Curr Opin Immunol* **23**, 383–390 (2011).
35. Moore, P. L., Williamson, C. & Morris, L. Virological features associated with the development of broadly neutralizing antibodies to HIV-1. *Trends Microbiol.* **23**, 204–211 (2015).
36. Caskey, M. Broadly-Neutralizing Antibodies (bNAbs) for the Treatment and Prevention of HIV Infection. doi:10.1097/COH.0000000000000600
37. Mascola, J. R. & Haynes, B. F. HIV-1 neutralizing antibodies: understanding nature's pathways. *Immunol. Rev.* **254**, 225–244 (2013).
38. Pancera, M. Structure and immune recognition of trimeric pre-fusion HIV-1 Env. *Nature* **514**, 455–461 (2014).
39. Behrens, A. J. & Crispin, M. Structural principles controlling HIV envelope

glycosylation. *Current Opinion in Structural Biology* (2017). doi:10.1016/j.sbi.2017.03.008

40. Blattner, C. *et al.* Structural delineation of a quaternary, cleavage-dependent epitope at the gp41-gp120 interface on intact HIV-1 Env trimers. *Immunity* **40**, 669–680 (2014).
41. Huang, J. *et al.* Broad and potent HIV-1 neutralization by a human antibody that binds the gp41–gp120 interface. *Nature* **515**, 138–142 (2014).
42. Wibmer, C. K. *et al.* Structure and Recognition of a Novel HIV-1 gp120-gp41 Interface Antibody that Caused MPER Exposure through Viral Escape. *PLOS Pathog.* **13**, e1006074 (2017).
43. Kong, R. *et al.* Fusion peptide of HIV-1 as a site of vulnerability to neutralizing antibody. *Science (80-.).* **352**, 828–833 (2016).
44. Simek, M. D. *et al.* Human immunodeficiency virus type 1 elite neutralizers: individuals with broad and potent neutralizing activity identified by using a high-throughput neutralization assay together with an analytical selection algorithm. *J. Virol.* **83**, 7337–48 (2009).
45. Van Gils, M. J. *et al.* An HIV-1 antibody from an elite neutralizer implicates the fusion peptide as a site of vulnerability. *Nat. Microbiol.* **2**, 1–10 (2016).
46. Zhou, T. *et al.* A neutralizing antibody recognizing primarily N-linked glycan targets the silent face of the HIV envelope. *Immunity* **48**, 500e6-513e6 (2018).
47. Schoofs, T. *et al.* Broad and Potent Neutralizing Antibodies Recognize the Silent Face of the HIV Envelope. *Immunity* **50**, 1513-1529.e9 (2019).
48. Wibmer, C. K., Moore, P. L. & Morris, L. HIV broadly neutralizing antibody targets. *Curr Opin HIV AIDS* **10**, 135 (2015).
49. Burton, D. R. & Hangartner, L. Broadly neutralizing antibodies to HIV and their role in vaccine design. *Annu Rev Immunol* **34**, 635–659 (2016).
50. Sok, D. & Burton, D. R. Recent progress in broadly neutralizing antibodies to HIV. *Nat. Immunol. 2018 1911* **19**, 1179–1188 (2018).
51. Ward, A. B. & Wilson, I. A. The HIV-1 envelope glycoprotein structure: nailing down a moving target. *Immunol. Rev.* **275**, 21–32 (2017).
52. Gray, E. S. *et al.* The Neutralization Breadth of HIV-1 Develops Incrementally over Four Years and Is Associated with CD4+ T Cell Decline and High Viral Load during Acute Infection. *J. Virol.* **85**, 4828–4840 (2011).
53. Euler, Z. *et al.* Longitudinal Analysis of Early HIV-1-Specific Neutralizing Activity

in an Elite Neutralizer and in Five Patients Who Developed Cross-Reactive Neutralizing Activity. 2045–2055 (2012). doi:10.1128/JVI.06091-11

54. Hraber, P. *et al.* Prevalence of broadly neutralizing antibody responses during chronic HIV-1 infection. *AIDS* **28**, 163–169 (2014).
55. Rusert, P. *et al.* Determinants of HIV-1 broadly neutralizing antibody induction. *Nat. Med.* **22**, 1260–1267 (2016).
56. Liao, H.-X. *et al.* Co-evolution of a broadly neutralizing HIV-1 antibody and founder virus. *Nature* **496**, 469–476 (2013).
57. Doria-Rose, N. A. *et al.* Developmental pathway for potent V1V2-directed HIV-neutralizing antibodies. *Nature* **509**, 55–62 (2014).
58. Xiao, X. *et al.* Germline-like predecessors of broadly neutralizing antibodies lack measurable binding to HIV-1 envelope glycoproteins: Implications for evasion of immune responses and design of vaccine immunogens. *Biochem. Biophys. Res. Commun.* **390**, 404–409 (2009).
59. Bonsignori, M. *et al.* Analysis of a Clonal Lineage of HIV-1 Envelope V2/V3 Conformational Epitope-Specific Broadly Neutralizing Antibodies and Their Inferred Unmutated Common Ancestors. *J. Virol.* **85**, 9998–10009 (2011).
60. Hoot, S. *et al.* Recombinant HIV Envelope Proteins Fail to Engage Germline Versions of Anti-CD4bs bNAbs. *PLoS Pathog.* **9**, e1003106 (2013).
61. McGuire, A. T. *et al.* Engineering HIV envelope protein to activate germline B cell receptors of broadly neutralizing anti-CD4 binding site antibodies. *J Exp Med* **210**, 655–663 (2013).
62. Jardine, J. *et al.* Rational HIV Immunogen Design to Target Specific Germline B Cell Receptors. *Science (80-.).* **340**, 711–716 (2013).
63. Jardine, J. G. *et al.* HIV-1 broadly neutralizing antibody precursor B cells revealed by germline-targeting immunogen. *Science (80-.).* **351**, 1458–1463 (2016).
64. Haynes, B. F., Kelsoe, G., Harrison, S. C. & Kepler, T. B. B-cell–lineage immunogen design in vaccine development with HIV-1 as a case study. *Nat. Biotechnol.* **30**, 423 (2012).
65. Saunders, K. O. *et al.* Targeted selection of HIV-specific antibody mutations by engineering B cell maturation. *Science (80-.).* **366**, (2019).
66. Steichen, J. M. *et al.* A generalized HIV vaccine design strategy for priming of broadly neutralizing antibody responses. *Science (80-.).* **366**, (2019).

67. Haynes, B. F. *et al.* Strategies for HIV-1 vaccines that induce broadly neutralizing antibodies. *Nat. Rev. Immunol.* 1 (2022). doi:10.1038/S41577-022-00753-W
68. Moore, P. L. *et al.* Evolution of an HIV glycan-dependent broadly neutralizing antibody epitope through immune escape. *Nat. Med.* **18**, 1688–1692 (2012).
69. Landais, E. & Moore, P. L. Development of broadly neutralizing antibodies in HIV-1 infected elite neutralizers. *Retrovirology* **15**, 61 (2018).
70. Moore, P. L. *et al.* Potent and broad neutralization of HIV-1 subtype C by plasma antibodies targeting a quaternary epitope including residues in the V2 loop. *J. Virol.* **85**, 3128–41 (2011).
71. Moore, P. L. *et al.* Multiple Pathways of Escape from HIV Broadly Cross-Neutralizing V2-Dependent Antibodies. *J. Virol.* **87**, 4882–4894 (2013).
72. Murphy, M. K. *et al.* Viral Escape from Neutralizing Antibodies in Early Subtype A HIV-1 Infection Drives an Increase in Autologous Neutralization Breadth. **9**, (2013).
73. Wibmer, C. K. *et al.* Viral Escape from HIV-1 Neutralizing Antibodies Drives Increased Plasma Neutralization Breadth through Sequential Recognition of Multiple Epitopes and Immunotypes. *PLoS Pathog.* **9**, (2013).
74. Escolano, A. *et al.* Sequential Immunization Elicits Broadly Neutralizing Anti-HIV-1 Antibodies in Ig Knockin Mice. *Cell* **166**, 1445-1458.e12 (2016).
75. McCoy, L. E. & Burton, D. R. Identification and specificity of broadly neutralizing antibodies against HIV. *Immunol. Rev.* **275**, 11–20 (2017).
76. Sun, Z. *et al.* Brief introduction of current technologies in isolation of broadly neutralizing HIV-1 antibodies. *Virus Res.* **243**, 75–82 (2018).
77. Mogus, A. T. *et al.* Virus-Like Particle Based Vaccines Elicit Neutralizing Antibodies against the HIV-1 Fusion Peptide. doi:10.3390/vaccines8040765
78. Köhler, G. & Milstein, C. Continuous cultures of fused cells secreting antibody of predefined specificity. *Nat. 1975 2565517* **256**, 495–497 (1975).
79. Wu, X. *et al.* Mechanism of human immunodeficiency virus type 1 resistance to monoclonal antibody B12 that effectively targets the site of CD4 attachment. *J. Virol.* **83**, 10892–10907 (2009).
80. McCoy, L. E. *et al.* Holes in the Glycan Shield of the Native HIV Envelope Are a Target of Trimer-Elicited Neutralizing Antibodies. *Cell Rep.* (2016). doi:10.1016/j.celrep.2016.07.074

81. Xu, K. *et al.* Epitope-based vaccine design yields fusion peptide-directed antibodies that neutralize diverse strains of HIV-1. *Nat. Med.* **24**, 857–867 (2018).
82. Scharf, L. *et al.* Antibody 8ANC195 Reveals a Site of Broad Vulnerability on the HIV-1 Envelope Spike. *CellReports* **7**, 785–795 (2014).
83. Falkowska, E. *et al.* Broadly Neutralizing HIV Antibodies Define a Glycan-Dependent Epitope on the Prefusion Conformation of gp41 on Cleaved Envelope Trimers. *Immunity* **40**, 657–668 (2014).
84. Lee, J. H. *et al.* Antibodies to a conformational epitope on gp41 neutralize HIV-1 by destabilizing the Env spike. *Nat. Commun.* **6**, 8167 (2015).
85. Cheng, C. *et al.* Consistent elicitation of cross-clade HIV-neutralizing responses achieved in guinea pigs after fusion peptide priming by repetitive envelope trimer boosting. *PLoS One* **14**, e0215163 (2019).
86. Lynch, R. M. *et al.* The Development of CD4 Binding Site Antibodies during HIV-1 Infection. *J. Virol.* **86**, 7588–7595 (2012).
87. Scheepers, C. *et al.* Ability to develop broadly neutralizing HIV-1 antibodies is not restricted by the germline Ig gene repertoire. *J. Immunol.* **194**, 4371–8 (2015).
88. Pushparaj, P. *et al.* Frequent use of IGHV3-30-3 in SARS-CoV-2 neutralizing antibody responses. *Front. Virol.* **3**, 5 (2023).
89. Masur, H. *et al.* An outbreak of community-acquired Pneumocystis carinii pneumonia: initial manifestation of cellular immune dysfunction. *N. Engl. J. Med.* **305**, 1431–8 (1981).
90. Cos, P. *et al.* Antiviral activity of Rwandan medicinal plants against human immunodeficiency virus type-1 (HIV-1). *Phytomedicine* **9**, 62–8 (2002).
91. Cos, P. *et al.* Plant substances as anti-HIV agents selected according to their putative mechanism of action. *J. Nat. Prod.* **67**, 284–93 (2004).
92. Barbaro, G. & Klatt, E. C. HIV infection and the cardiovascular system. *AIDS Rev.* **4**, 93–103 (2002).
93. Vermani, K. & Garg, S. Herbal medicines for sexually transmitted diseases and AIDS. *J. Ethnopharmacol.* **80**, 49–66 (2002).
94. Sierra, S., Kupfer, B. & Kaiser, R. Basics of the virology of HIV-1 and its replication. *J. Clin. Virol.* **34**, 233–44 (2005).
95. Chinen, J. & Shearer, W. T. Molecular virology and immunology of HIV infection.

J. Allergy Clin. Immunol. **110**, 189–98 (2002).

96. Chan, K.-W., Luo, C. C., Lu, H., Wu, X. & Kong, X.-P. A site of vulnerability at V3 crown defined by HIV-1 bNAb M4008_N1. *Nat. Commun.* **12**, 6464 (2021).
97. Derdeyn, C. A. *et al.* Envelope-constrained neutralization-sensitive HIV-1 after heterosexual transmission. *Science* **303**, 2019–22 (2004).
98. Keele, B. F. *et al.* Identification and characterization of transmitted and early founder virus envelopes in primary HIV-1 infection. *Proc. Natl. Acad. Sci. U. S. A.* **105**, 7552–7 (2008).
99. McCormack, S. *et al.* Pre-exposure prophylaxis to prevent the acquisition of HIV-1 infection (PROUD): effectiveness results from the pilot phase of a pragmatic open-label randomised trial. *Lancet (London, England)* **387**, 53–60 (2016).
100. Sharp, P. M. & Hahn, B. H. Origins of HIV and the AIDS pandemic. *Cold Spring Harb. Perspect. Med.* **1**, a006841 (2011).
101. Baeten, J. M. *et al.* Antiretroviral prophylaxis for HIV prevention in heterosexual men and women. *N. Engl. J. Med.* **367**, 399–410 (2012).
102. Anderson, P. L. *et al.* Emtricitabine-tenofovir concentrations and pre-exposure prophylaxis efficacy in men who have sex with men. *Sci. Transl. Med.* **4**, 151ra125 (2012).
103. Kashuba, A. D. M. *et al.* Genital Tenofovir Concentrations Correlate With Protection Against HIV Infection in the CAPRISA 004 Trial: Importance of Adherence for Microbicide Effectiveness. *J. Acquir. Immune Defic. Syndr.* **69**, 264–9 (2015).
104. Grant, R. M. *et al.* Preexposure Chemoprophylaxis for HIV Prevention in Men Who Have Sex with Men. *N. Engl. J. Med.* **363**, 2587–2599 (2010).
105. Choopanya, K. *et al.* Antiretroviral prophylaxis for HIV infection in injecting drug users in Bangkok, Thailand (the Bangkok Tenofovir Study): a randomised, double-blind, placebo-controlled phase 3 trial. *Lancet (London, England)* **381**, 2083–90 (2013).
106. Van Damme, L. *et al.* Preexposure Prophylaxis for HIV Infection among African Women. *N. Engl. J. Med.* **367**, 411–422 (2012).
107. Marrazzo, J. M. *et al.* Tenofovir-Based Preexposure Prophylaxis for HIV Infection among African Women. *N. Engl. J. Med.* **372**, 509–518 (2015).
108. Tsai, C. C. *et al.* Prevention of SIV infection in macaques by (R)-9-(2-

phosphonylmethoxypropyl)adenine. *Science* **270**, 1197–9 (1995).

109. Cardo, D. M. *et al.* A case-control study of HIV seroconversion in health care workers after percutaneous exposure. Centers for Disease Control and Prevention Needlestick Surveillance Group. *N. Engl. J. Med.* **337**, 1485–90 (1997).
110. Kuhar, D. T. *et al.* Updated US Public Health Service Guidelines for the Management of Occupational Exposures to Human Immunodeficiency Virus and Recommendations for. *Hosp. Epidemiol.* **34**, 875 (2013).
111. Sauter, D. *et al.* HIV-1 Group P is unable to antagonize human tetherin by Vpu, Env or Nef. *Retrovirology* **8**, 103 (2011).
112. Auvert, B. *et al.* Randomized, controlled intervention trial of male circumcision for reduction of HIV infection risk: the ANRS 1265 Trial. *PLoS Med.* **2**, e298 (2005).
113. Gray, R. H. *et al. Male circumcision for HIV prevention in men in Rakai, Uganda: a randomised trial*. *www.thelancet.com* **369**, (2007).
114. Bailey, R. C. *et al. Male circumcision for HIV prevention in young men in Kisumu, Kenya: a randomised controlled trial*. *www.thelancet.com* **369**, (2007).
115. Wawer, M. J. *et al. Circumcision in HIV-infected men and its effect on HIV transmission to female partners in Rakai, Uganda: a randomised controlled trial*. *www.thelancet.com* **374**, (2009).
116. Goodreau, S. M. *et al.* Can male circumcision have an impact on the HIV epidemic in men who have sex with men? *PLoS One* **9**, e102960 (2014).
117. Cafri, G., Sharbi-Yunger, A., Tzehoval, E. & Eisenbach, L. Production of LacZ inducible T cell hybridoma specific for human and mouse $gp100_{25-33}$ peptides. *PLoS One* **8**, (2013).
118. Buchacher, A. *et al.* Generation of human monoclonal antibodies against HIV-1 proteins; electrofusion and Epstein-Barr virus transformation for peripheral blood lymphocyte immortalization. *AIDS Res. Hum. Retroviruses* **10**, 359–69 (1994).
119. Duarte, J. N. *et al.* Generation of Immunity against Pathogens via Single-Domain Antibody-Antigen Constructs. *J. Immunol.* **197**, 4838–4847 (2016).
120. Graus, Y. F. *et al.* Selection of recombinant anti-HuD Fab fragments from a phage display antibody library of a lung cancer patient with paraneoplastic

encephalomyelitis. *J. Neuroimmunol.* **82**, 200–9 (1998).

121. Nduati, R. *et al.* Effect of breastfeeding and formula feeding on transmission of HIV-1: a randomized clinical trial. *JAMA* **283**, 1167–74 (2000).
122. Hemelaar, J., Gouws, E., Ghys, P. D., Osmanov, S. & WHO-UNAIDS Network for HIV Isolation and Characterisation. Global trends in molecular epidemiology of HIV-1 during 2000-2007. *AIDS* **25**, 679–89 (2011).
123. de Vincenzi, Isabelle, K. B. S. G. Triple antiretroviral compared with zidovudine and single-dose nevirapine prophylaxis during pregnancy and breastfeeding for prevention of mother-to-child transmission of HIV-1 (Kesho Bora study): a randomised controlled trial. *Lancet. Infect. Dis.* **11**, 171–80 (2011).
124. Baeten, J. M. *et al.* Safety, uptake, and use of a dapivirine vaginal ring for HIV-1 prevention in African women (HOPE): an open-label, extension study. *lancet. HIV* **8**, e87–e95 (2021).
125. Baeten, J. M. *et al.* Use of a Vaginal Ring Containing Dapivirine for HIV-1 Prevention in Women. *N. Engl. J. Med.* **375**, 2121–2132 (2016).
126. Nel, A. *et al.* Safety, Acceptability and Adherence of Dapivirine Vaginal Ring in a Microbicide Clinical Trial Conducted in Multiple Countries in Sub-Saharan Africa. *PLoS One* **11**, e0147743 (2016).
127. Hessell, A. J. *et al.* Fc receptor but not complement binding is important in antibody protection against HIV. **449**, 101–105 (2007).
128. Rerks-Ngarm, S. *et al.* Vaccination with ALVAC and AIDSVAX to prevent HIV-1 infection in Thailand. *N. Engl. J. Med.* **361**, 2209–20 (2009).
129. Gray, G. E. *et al.* Vaccine Efficacy of ALVAC-HIV and Bivalent Subtype C gp120-MF59 in Adults. *N. Engl. J. Med.* **384**, 1089–1100 (2021).
130. Barouch, D. H. *et al.* Evaluation of a mosaic HIV-1 vaccine in a multicentre, randomised, double-blind, placebo-controlled, phase 1/2a clinical trial (APPROACH) and in rhesus monkeys (NHP 13-19). *Lancet (London, England)* **392**, 232–243 (2018).
131. Feinberg, M. B., Russell, N. D., Shattock, R. J. & Youngdahl, K. B. The importance of partnerships in accelerating HIV vaccine research and development. *J. Int. AIDS Soc.* **24 Suppl 7**, e25824 (2021).
132. Leggat, D. J. *et al.* Vaccination induces HIV broadly neutralizing antibody precursors in humans. *Science (80-.).* **378**, (2022).
133. Bbosa, N., Kaleebu, P. & Ssemwanga, D. HIV subtype diversity worldwide. *Curr.*

Opin. HIV AIDS **14**, 153–160 (2019).

134. HW, S. & L, C. Structure and function of immunoglobulins. *J. Allergy Clin. Immunol.* **125**, (2010).
135. Chiu, M. L., Goulet, D. R., Teplyakov, A. & Gilliland, G. L. Antibody Structure and Function: The Basis for Engineering Therapeutics. *Antibodies 2019, Vol. 8, Page 55* **8**, 55 (2019).
136. Wagh, K. *et al.* Completeness of HIV-1 Envelope Glycan Shield at Transmission Determines Neutralization Breadth. *Cell Rep.* **25**, 893-908.e7 (2018).
137. Shen, C.-H. *et al.* VRC34-Antibody Lineage Development Reveals How a Required Rare Mutation Shapes the Maturation of a Broad HIV-Neutralizing Lineage. (2020). doi:10.1016/j.chom.2020.01.027
138. UNAIDS. UNAIDS_core-epidemiology-slides_en. 1–11 (2021).
139. Kharsany, A. B. M. *et al.* Community-based HIV prevalence in KwaZulu-Natal, South Africa: results of a cross-sectional household survey. *lancet. HIV* **5**, e427–e437 (2018).
140. Johnson, L. F. *et al.* The Effect of HIV Programs in South Africa on National HIV Incidence Trends, 2000–2019. *JAIDS J. Acquir. Immune Defic. Syndr.* **90**, 115–123 (2022).
141. Barnabas, S. L. *et al.* Converging epidemics of sexually transmitted infections and bacterial vaginosis in southern African female adolescents at risk of HIV. *Int. J. STD AIDS* **29**, 531–539 (2018).
142. Kong, R. *et al.* Antibody Lineages with Vaccine-Induced Antigen-Binding Hotspots Develop Broad HIV Neutralization. *Cell* **178**, 567-584.e19 (2019).
143. Loggerenberg, F. Van *et al.* Establishing a Cohort at High Risk of HIV Infection in South Africa : Challenges and Experiences of the CAPRISA 002 Acute Infection Study. **3**, 1–8 (2008).
144. Montefiori, D. C., Montefiori & C., D. Evaluating Neutralizing Antibodies Against HIV, SIV, and SHIV in Luciferase Reporter Gene Assays. in *Current Protocols in Immunology* 12.11.1-12.11.17 (John Wiley & Sons, Inc., 2005). doi:10.1002/0471142735.im1211s64
145. Zhang, J., Kobert, K., Flouri, T. & Stamatakis, A. PEAR: a fast and accurate Illumina Paired-End reAd mergeR. *Bioinformatics* **30**, 614–20 (2014).
146. Edgar, R. C. & Bateman, A. Search and clustering orders of magnitude faster than BLAST. *Bioinforma. Appl. NOTE* **26**, 2460–246110 (2010).

147. Schramm, C. A. *et al.* SONAR: A high-throughput Pipeline for Inferring Antibody ontogenies from Longitudinal sequencing of B Cell transcripts. **7**, (2016).
148. Stern, J. N. H. *et al.* B cells populating the multiple sclerosis brain mature in the draining cervical lymph nodes. *Sci. Transl. Med.* **6**, 248ra107-248ra107 (2014).
149. Zhou, T. *et al.* Multidonor analysis reveals structural elements, genetic determinants, and maturation pathway for HIV-1 neutralization by VRC01-class antibodies. *Immunity* **39**, 245–258 (2013).
150. Zhou, T. *et al.* Structural repertoire of HIV-1-neutralizing antibodies targeting the CD4 supersite in 14 donors. *Cell* (2015). doi:10.1016/j.cell.2015.05.007
151. Jardine, J. G. *et al.* Minimally mutated HIV-1 broadly neutralizing antibodies to guide reductionist vaccine design. *PLoS Pathog* **12**, e1005815 (2016).
152. Griffith, S. A. & McCoy, L. E. To bnAb or Not to bnAb: Defining Broadly Neutralising Antibodies Against HIV-1. *Front. Immunol.* **12**, 4339 (2021).
153. Moore, P. L. The Neutralizing Antibody Response to the HIV-1 Env Protein. *Curr. HIV Res.* **16**, 21–28 (2018).
154. Williams, W. B., Wiehe, K., Saunders, K. O. & Haynes, B. F. Strategies for induction of HIV-1 envelope-reactive broadly neutralizing antibodies. *J. Int. AIDS Soc.* **24 Suppl 7**, e25831 (2021).
155. Ditse, Z. *et al.* Hiv-1 Subtype C Infected Children With Exceptional Neutralization Breadth Exhibit Polyclonal Responses Targeting Known Epitopes. *J. Virol.* JVI.00878-18 (2018). doi:10.1128/JVI.00878-18
156. Walker, L. M. *et al.* Broad neutralization coverage of HIV by multiple highly potent antibodies. *Nature* **477**, 466–470 (2011).
157. Gautam, R. *et al.* A single injection of anti-HIV-1 antibodies protects against repeated SHIV challenges. *Nature* **533**, 105–109 (2016).
158. Liao, H.-X. *et al.* High-throughput isolation of immunoglobulin genes from single human B cells and expression as monoclonal antibodies. *J. Virol. Methods* **158**, 171–9 (2009).
159. Ye, J., Ma, N., Madden, T. L. & Ostell, J. M. IgBLAST: an immunoglobulin variable domain sequence analysis tool. *Nucleic Acids Res.* **41**, W34–W40 (2013).
160. Yuan, M. *et al.* Conformational Plasticity in the HIV-1 Fusion Peptide Facilitates Recognition by Broadly Neutralizing Antibodies. *Cell Host Microbe* **25**, 873–883 (2019).

161. Shingai, M. *et al.* Passive transfer of modest titers of potent and broadly neutralizing anti-HIV monoclonal antibodies block SHIV infection in macaques. *J. Exp. Med.* **211**, 2061–2074 (2014).
162. Walker, B. D. CMV, MHC-E, and the quest for an unconventional AIDS vaccine. *Sci. Immunol.* **6**, (2021).
163. Harrison, S. C. Viral membrane fusion. *Nat. Struct. Mol. Biol.* **15**, 690–698 (2008).
164. Wyatt, R. & Sodroski, J. The HIV-1 Envelope Glycoproteins: Fusogens, Antigens, and Immunogens. *Science (80-.).* **280**, 1884–1888 (1998).
165. Mogus, A. T. *et al.* Virus-Like Particle Based Vaccines Elicit Neutralizing Antibodies against the HIV-1 Fusion Peptide. *Vaccines* **8**, 765 (2020).
166. Binley, J. M. *et al.* Comprehensive cross-clade neutralization analysis of a panel of anti-human immunodeficiency virus type 1 monoclonal antibodies. *J. Virol.* **78**, 13232–52 (2004).
167. Gray, E. S. *et al.* Neutralizing Antibody Responses in Acute Human Immunodeficiency Virus Type 1 Subtype C Infection. *J. Virol.* **81**, 6187–6196 (2007).
168. Ng, C. T. *et al.* Passive neutralizing antibody controls SHIV viremia and enhances B cell responses in infant macaques. (2010). doi:10.1038/nm.2233
169. Lucier, A. *et al.* Frequent development of broadly neutralizing antibodies in early life in a large cohort of HIV-infected children. *bioRxiv* 2021.05.07.443081 (2021). doi:10.1101/2021.05.07.443081
170. Gupta, N. T. *et al.* Change-O: a toolkit for analyzing large-scale B cell immunoglobulin repertoire sequencing data. *Bioinformatics* **31**, 3356–8 (2015).
171. Li, S. *et al.* IMGT/HighV QUEST paradigm for T cell receptor IMGT clonotype diversity and next generation repertoire immunoprofiling. *Nat. Commun.* **4**, 2333 (2013).
172. Csardi, G., InterJournal, T. N.-, systems, complex & 2006, undefined. The igraph software package for complex network research. *researchgate.net*
173. Kondo, H. X. *et al.* Effects of a remote mutation from the contact paratope on the structure of CDR-H3 in the anti-HIV neutralizing antibody PG16. *Sci. Rep.* **9**, 19840 (2019).
174. Sacks, D. *et al.* Somatic hypermutation to counter a globally rare viral immunotype drove off-track antibodies in the CAP256-VRC26 HIV-1 V2-directed

bNAb lineage. *PLOS Pathog.* **15**, e1008005 (2019).

175. Wiehe, K. *et al.* Functional Relevance of Improbable Antibody Mutations for HIV Broadly Neutralizing Antibody Development. *Cell Host Microbe* **23**, 759-765.e6 (2018).
176. Zhu, P. *et al.* Electron tomography analysis of envelope glycoprotein trimers on HIV and simian immunodeficiency virus virions. *Proc Natl Acad Sci USA* **100**, 15812–15817 (2003).
177. Behrens, A. J. *et al.* Composition and Antigenic Effects of Individual Glycan Sites of a Trimeric HIV-1 Envelope Glycoprotein. *Cell Rep.* (2016). doi:10.1016/j.celrep.2016.02.058
178. Ward, A. B. & Wilson, I. A. Insights into the trimeric HIV-1 envelope glycoprotein structure. *Trends Biochem Sci* **40**, 101–107 (2015).
179. Moore, P. L. & al., et. Nature of nonfunctional envelope proteins on the surface of human immunodeficiency virus type 1. *J. Virol.* **80**, 2515–2528 (2006).
180. Harrison, S. C. Viral membrane fusion. *Virology* **479**–**480**, 498–507 (2015).
181. Guttman, M. *et al.* CD4-Induced Activation in a Soluble HIV-1 Env Trimer. *Structure* **22**, 974–984 (2014).
182. Pierson, T. C. & Doms, R. W. HIV-1 entry and its inhibition. *Curr. Top. Microbiol. Immunol.* **281**, 1–27 (2003).
183. Lee, J. H. & Crotty, S. HIV vaccinology: 2021 update. *Semin. Immunol.* **51**, 101470 (2021).
184. Chuang, G.-Y. *et al.* Development of a 3Mut-Apex-Stabilized Envelope Trimer That Expands HIV-1 Neutralization Breadth When Used To Boost Fusion Peptide-Directed Vaccine-Elicited Responses. *J. Virol.* **94**, (2020).
185. Landais, E. *et al.* Broadly neutralizing antibody responses in a large longitudinal sub-Saharan HIV primary infection cohort. *PLoS Pathog* **12**, e1005369 (2016).
186. Piantadosi, A. *et al.* Breadth of Neutralizing Antibody Response to Human Immunodeficiency Virus Type 1 Is Affected by Factors Early in Infection but Does Not Influence Disease Progression. *J. Virol.* **83**, 10269–10274 (2009).
187. Sather, D. N. *et al.* Factors associated with the development of cross-reactive neutralizing antibodies during human immunodeficiency virus type 1 infection. *J. Virol.* **83**, 757–69 (2009).
188. Seaman, M. S. *et al.* Tiered categorization of a diverse panel of HIV-1 Env pseudoviruses for assessment of neutralizing antibodies. *J. Virol.* **84**, 1439–52

(2010).

189. Mikell, I. Characteristics of the earliest cross-neutralizing antibody response to HIV-1. *PLoS Pathog.* **7**, e1001251 (2011).
190. Goo, L., Chohan, V., Nduati, R. & Overbaugh, J. Early development of broadly neutralizing antibodies in HIV-1-infected infants. *Nat Med* **20**, 655–658 (2014).
191. Simonich, C. A. A. *et al.* HIV-1 Neutralizing Antibodies with Limited Hypermutation from an Infant. *Cell* (2016). doi:10.1016/j.cell.2016.05.055
192. Roider, J. M., Muenchhoff, M. & Goulder, P. J. R. Immune activation and paediatric HIV-1 disease outcome. *Curr Opin HIV AIDS* **11**, 146–155 (2016).
193. Doria-Rose, N. Breadth of human-immunodeficiency-virus-specific neutralizing activity in sera: clustering analysis and association with clinical variables. *J. Virol.* **84**, 1631–1636 (2010).
194. Deruaz, M. *et al.* Protection of Humanized Mice From Repeated Intravaginal HIV Challenge by Passive Immunization: A Model for Studying the Efficacy of Neutralizing Antibodies In Vivo. (2016). doi:10.1093/infdis/jiw203
195. Hua, C. K. & Ackerman, M. E. Increasing the Clinical Potential and Applications of Anti-HIV Antibodies. *Front. Immunol.* **8**, 1–19 (2017).
196. Tortora, G.J., Funke, B.R. and Case, C.L. (2010) Microbiology: An Introduction. 10th Edition, Pearson Benjamin Cummings, San Francisco.
197. Lever, M., L. (2009). HIV: the virus. Medicine, **37**(7), 313-316.
198. Grulich AE, Bavinton BR, Jin F, Prestage G, Zablostka IB, Grinsztejn G, et al. HIV transmission in male serodiscordant couples in Australia, Thailand and Brazil [Poster Number 1019LB]. 22nd Conference on Retroviruses and Opportunistic Infections; Seattle, USA, (2015).
199. Baeten, J.M., Palanee-Phillips, T., Mgodi, N., Ramjee, G., Gati, B., Mhlanga, F., Hunidzarira, P., Mansoor, L., Siva, S., Govender, V. and Makanani, B., (2019), July. High adherence and sustained impact on HIV-1 incidence: final results of an open-label extension trial of the dapivirine vaginal ring. In JOURNAL OF THE INTERNATIONAL AIDS SOCIETY **22**, 29-29. The atrium, southern gate, chichester po19 8sq, w sussex, england: john wiley & sons ltd.
200. Straub C, Zubler RH. Immortalization of EBV-infected B cells is not influenced by exogenous signals acting on B cell proliferation. Effects of mutant EL-4 thymoma cells and transforming growth factor-beta. *J Immunol*;**142**(1):87-93, (1989). PMID: 2535862.